Seismic performance of a semi-active MR damper improved by fuzzy control system

Keyhan Faraji

A Thesis in

The Department of Building, Civil & Environmental Engineering

Presented in Partial Fulfillment of the Requirements

for the Degree of Master of Applied Science (Civil Engineering) at

Concordia University

Montreal, Quebec, Canada

June 2018

CONCORDIA UNIVERSITY

School of Graduate Studies

This is to certify that the thesis prepared

By: Keyhan Faraji

Entitled: Seismic performance of a semi-active MR damper improved by fuzzy control system

and submitted in partial fulfillment of the requirements for the degree of

Master of Applied Science

Complies with the regulations of the University and meets the accepted standards with respect to originality and quality.

Signed by the final Examining Committee:

_____ Chair
Lucia Tirca

_____ Examiner
Ramin Sedaghati

_____ Examiner
Anjan Bhowmick

_____ Supervisor
Ashutosh Bagchi

Approved by _____
Chair of Department or Graduate Program Director

_____
Dean of Faculty

Date _____

Abstract

Seismic performance of a semi-active MR damper improved by fuzzy control system

Control systems play a crucial role in the operation of airplanes, robots and the new generation of smart automobiles to improve their performance, safety and robustness. Considering the ability of control systems to optimize the functionality of damping devices, such controllable devices can effectively dissipate the seismic vibrations of structures in which they are installed. Although dampers are utilized in many structures, the main issue is that most of such devices function in passive mode without control systems. In some cases, such passive damping systems may perform inefficiently and cause detrimental effects which may endanger the safety of the structures. Magnetorheological (MR) damper is a type of semi-active damper that produces variable resistant force according to the intensity of the magnetic field which is induced by a direct electricity current (DC). Since direct current can be supplied by batteries, this type of damper is functional and serviceable in harsh conditions in which the power supply may be interrupted. Therefore, the capability of variable force production demanding less energy is the major advantage of MR dampers. In this research, seismic response of a 2D single-story structure which is equipped with an adaptive MR damper is investigated and a fuzzy control system is added to the damper to smartly control and adjust its performance in real time. The fuzzy controlled system adjusts the applied electric current to the damper according to the displacement response of the structure caused by an earthquake. Therefore, it makes the resisting damper force proportional and adaptive to the magnitude of the earthquake forces. The analytical results illustrate that such controllable damping system can effectively dissipate the seismic vibration of the structure subjected to two sets of far-field and near-field (pulse- like) earthquake records. In this way the average of the maximum seismic demands in the dynamic model including wave energy, acceleration, velocity and displacement decrease by 38%,40%,36% and 83% for far-field records and by 40%,43%,40% and 82% for near-field (pulse-like) records respectively.

Keywords: MR damper, fuzzy logic, mamdani system, seismic loads, energy dissipation

Table of Contents

Contents

List of Figures

List of Tables xviii

Chapter 1

Introduction

1-1- The use of energy dissipating systems in Hazard mitigation

The statistics published by the United Nations in June 2017 indicate that the current world population is 7.6 billion and it is expected to reach 8.6 billion in 2030, 9.8 billion in 2050 and 11.2 billion in 2100 (UNITED NATIONS 2018), With roughly 83 million people being added to the world's population every year, the upward trend in population size is expected to continue and arise dramatic demands for new buildings, infrastructures and facilities. The construction of such structures needs billions of dollars. On the other hand, the existing structures account for an immense portfolio of public and private capital in every country. Therefore, it is crucially important to build more resilient new structures and strengthen current buildings against natural devastating phenomena such as earthquake, tsunami and tornado, which often happen in many areas of our world resulting in loss of lives, human properties and national capitals.

Among all destructive natural phenomena, earthquakes have claimed a huge number of human lives and property loss in many countries throughout the human history.

Table 1-1 presents some of catastrophic earthquakes which have happened in different countries in the last 10 years illustrating the magnitude of the earthquake waves and the number of victims (BBC www.bbc.com, June 2018) .

It should be noticed that not only does earthquake cause direct damage and destruction such as collapse of structures, but also it may lead to indirect, secondary damages and losses including fires, rupture of water and gas mains, interruption of electricity supplies, loss of businesses, etc. This indicates that a comprehensive long-term strategy including economic, technical and cultural aspects with an immediate attempt is required to reduce the catastrophic effects and consequences of earthquakes. To do so, it is notably important to design and construct new structures based on new methods and updated seismic provisions.

On the other hand, based on the new seismic codes, many of existing buildings and infrastructures are unsafe and vulnerable to failure under seismic loads. For instance, inspections after the 1994 Northridge and 1995 Kobe earthquakes illustrated that sever brittle fractures occurred in some structures that were designed to perform well during earthquakes, in some cases the damage was so critical and led to failure (Mahin 1998).

Table 1-1: 21 catastrophic earthquakes which have happened in different countries in the last 10 years

Date	Place	Magnitude(Mw)	Number of the Killed People
September 17, 2017	Mexico city-Mexico	7.1	200
September 7, 2017	southern Mexico & Guatemala	8.1	65
August 24, 2016	Central Italy	6	298
April 16, 2016	Ecuador	7.8	650
October 26, 2015	North -Eastern of Afghanistan-Pakistan	7.5	400
April 25, 2015	Nepal	7.8	8000
August 3, 2014	China -Yunnan	6.1	600
October 15, 2013	Philippines	7.2	200
September 25, 2013	Pakistan	7.7	300
April 20, 2013	China -south-western Sichuan	6.6	160
August 11, 2012	Iran-Ahar (varzaghan)	6.4	250
October 23, 2011	south-eastern Turkey	7.2	200
March 11, 2011	Japan (Tsunami)	8.9	> 18000
February 22, 2011	NewZeland	6.3	160
April 14, 2010	China-Quinghai	6.9	400
February 27, 2010	Chile	8.8	700
January 12, 2010	Haiti	7	230000
September 30, 2009	Indonesia-Sumatra	7.6	1000
April 6, 2009	Italy -Aquila	6.3	309
May 12, 2008	China-Sichuan	7.8	87000
August 15, 2007	Peru	7.9	519

Although the inefficiency of the design codes and provisions which were used at that time were the most important reason of such failures, the aging, deterioration, imperfection in production process of structural elements and changes in building performance objective were the other reasons that took part in that disaster (Kurata et al. 2011). The official reports indicated the devastation of Northridge earthquake caused 20 billion dollars of property loss (Bruneau et al. 1998). This illustrates that many structures such as buildings, hospitals, bridges and power plants which are constructed in the past decades are susceptible to severe damage and even collapse in the regions which are prone to harsh earthquakes, therefore, they need to be strengthened and seismically retrofitted or even rebuilt according to updated seismic codes and technics.

Considering financial and budget limitations and the fact that it is not possible to rebuild thousands of buildings and infrastructures which are in service, it is obvious that these structures should be seismically updated with efficient retrofit methods.

It means that in each city there are many buildings in service, rendering highly valued services such as health, commercial activities and administrative services. Since any decision on reconstruction of such buildings will fundamentally disrupt such services for the cities and also considering the high cost of reconstruction; cost-effective, practical and quick rehabilitation methods are usually more advantageous than reconstruction.

One of the most economic and quick methods that is used in both new construction and rehabilitation to improve the seismic resilience of the structures is the application of energy dissipating systems.

A damping device or damper as defined in the standard of Federal Emergency Management Agency standard FEMA 450 (2003), is a flexible structural element that dissipates energy due to the relative motion of each end of the device. Damping devices should be connected to other structural elements of the main structure such as bracing and beams. Such devices may be classified as either displacement-dependent or velocity dependent, or a combination of them and may be configured to act in either a linear or nonlinear manner (FEMA 2003).

Although in the past 20 years some special structures such as high-rise building and bridges have been equipped with dampers, today the competitive pricing policies of damper manufacturing companies and the approval of well performance of such systems, are going to make the use of dampers a practical approach in construction and renovation of ordinary buildings.

Since the technology is developing, new controllable and adaptive dampers are going to replace the conventional passive dampers and be more widely used. The most efficient part of the new generation of dampers is the control system that commands their function. Control systems play a crucial role in the operation of airplanes, robots and the new generation of smart automobiles, in order to make such dynamic systems more practical and improve their performance, safety and robust serviceability. Therefore, it is important to investigate and study the control system for using them in civil engineering structures.

One of the most advanced and high-tech damping systems, which is proposed in recent years, is the magnetorheological (MR) damper.

By exposing the MR fluid used in this damper to a magnetic field, its viscosity changes leading the damper to produce variable resistant force. The induced magnetic field can be produced by a small direct electricity current (DC) provided by batteries.

A well-designed control system such as fuzzy control systems, can monitor, correct and adjust the performance of the MR damper and provide the structure in which the damper is installed with a high level of safety demand.

In this research different types of damping system are discussed and the performance of a large-scale MR damper which is controlled by a fuzzy controller and the seismic response of the structure, in which the damper is installed, is investigated.

1-2- The objective of this research

MR dampers are the recently presented type of dampers that can be used as extra damping components of structures to increase the resilience of structures against earthquakes and decrease their seismic risks.

The objectives of the research are as follows:

- To define a fuzzy control system that can properly adjust the performance of the MR damper according to the magnitude and pattern of applied earthquake
- To study the effectiveness of MR dampers in controlling the seismic demand of buildings with the developed fuzzy control system
- To investigate the behavior of buildings under far-field and near field pulse-like earthquakes

1-3- Organization of the thesis

This thesis is organized into six chapters and two appendices.

In Chapter1, the introduction and objective of the research are presented

In Chapter 2, different control technics and energy dissipating devices, including their advantages and disadvantages, are discussed. In addition, the characteristic of magnetorheological fluid and the different phenomenological models of MR damper are investigated.

In Chapter 3, different control operations including open-loop and closed loop systems, the model dependent and model independent control systems are discussed then the principal concepts of fuzzy logic, fuzzy control systems and their functionality are delved.

In Chapter4, the methodology, the strategy for doing this research and the utilized earthquake records considering their characteristic are investigated.

In Chapter5, the modeling, analytical models and analyses are proposed, and the resulted figures and graphs are discussed.

In Chapter 6, the summary and conclusion are explained, and the scope of future research are discussed.

In the appendix I the tables of the analytical results are proposed and in the appendix II the design procedure of a moment resisting frame is explained.

Chapter 2

Literature Review

Finding the best way to control the vibration of the structures has been a great challenge for civil engineers.In this way different strategies,methodes and technics of vibration control in civil engineering structures are proposed, investigated and developed to improve the resilience of the structures against vibrations.

Since most of destructive vibrations in the structures are caused by earthquakes,the damping system must be able to dissipate the effects of seismic excitations in the structures properly and improve the seismic demand of them.

The application of energy dissipating systems in civil engineering structures started more than fifty years ago (Soong et al. 2014) and the use of such systems that can mitigate the seismic hazard in structures are rapidly growing and engineers try to design more advanced energy dissipating systems and devices that can provide civil engineering structures with higher safety levels.

Today, a wide vriety of damping devices are designed and manufatured by many companies with competitiive prices and the different types of damper are being utilized in many buildings and infrastructures as an important element of the structural system of such structures .Therefore, it is so important for engineers to select the most efficient ,reliable and practical vibration damping system for the structures considering the technical and economical concerns.

In this chapter different strategies of vibration control are discussed ,then different damping devices which are currently used in civil engineering structure ,considering the advatages and the disadvantages of each damper are investigated.

Furthurmore, the charactristic, modelling and behavior of magnethoreoloical damper as the newest semi-active and controllable damper,are discussed.

2-1- Different types of vibration control and energy dissipating systems

The different strategies of energy dissipating systems which are currently utilized can be classified into the following four major categories: Active damping Systems, Passive damping systems, Semi-active damping systems, and Hybrid damping systems

2-2- Active damping System:

Active energy dissipating systems are made of three main components including force producing devices such as electromotors or actuators, sensors and control unit.

In this system by utilizing different sensors which are installed in the structure, the detailed data related to structural demand such as displacements, base shears, accelerations and drifts can be monitored. The gathered data are processed to determine the control instruction and appropriate order is sent to the force producing devices such as actuators and electro motors that work with external source of power such as public electricity; these devices produce the force that is ordered by the control unit and apply it to the structure in order to neutralize or decrease the effect of external applied forces and keep the structure in the safe zone (Figure 2-1).

It should be noted that the control unit, by using feedback of the dynamic system, adjusts the amount and pattern of the resistant forces which are produced by the dampers according to the magnitudes and patterns of the applied external loads and monitors the structural demands and conditions of the structure in real-time.

In the control unit, proper algorithms, logical rules and feedback control methods should be utilized to make this active system properly practical under dynamic loads such as earthquakes. Although this active control system has important advantages such as quick response in real-time and the capability of producing and applying variable force based on the magnitude, direction and pattern of the applied external forces, it needs expensive and highly technical routine maintenance and services to prevent the active system malfunctioning that may cause applying undesired force to the main structure that may cause detrimental effects such as instability.

The other issue that can negatively affect this system is dependence of it on the external power source that may fail in harsh conditions such as earthquake. The schematic diagram of active controlling of the structures is shown in Figure 2-1.

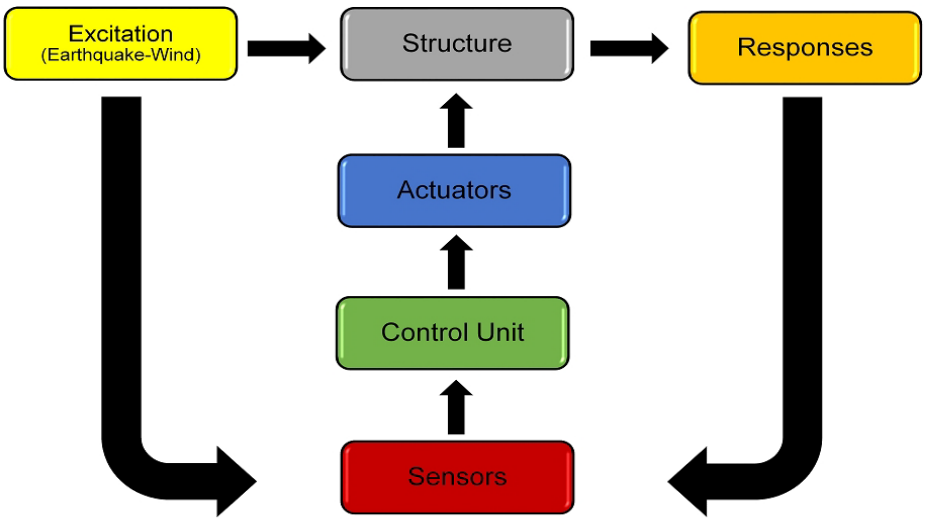

Figure 2-1 : The schematic diagram of a structure which is equipped with an active control system

Although in some cases such as wind turbines, air traffic control towers and some industrial structures where a structure continuously sustains huge vibrations, the application of active energy dissipating systems are well accepted, this type of energy damping systems may not be economically feasible for regular structures.

Common active dampers can be in the form of the following equipment (Yang et al. 2017) (Casciati et al. 2006).

- Active tendons with Hydraulic
- Active mass dampers

2-2-1- Active tendons:

The first generation of the system was proposed by Freyssinet more than five decades ago in around 1960, since then calculation and experimental research has confirmed the good behavior of the structures equipped with this system, confronting dynamic loads (Soong et al. 2014).

This system which works with alternating electricity current (AC) can actively apply variable forces to the structure according to the magnitude and direction of the applied external dynamic forces such as seismic loads (Soong et al. 2014).

The active tendon systems contain a set of components including the following items:

- Actuators such as pre-stressed tendons
- Sensors
- Control unit
- External power sources such as electro -hydraulic system

In this system, the control system runs the electro-hydraulic mechanism and produces active forces to pull the tendons in a way that can properly reduce the effect of applied vibrations. It is done based on the data such as displacements, velocities, accelerations and drift ratios, which are collected by the sensors installed in the structure.

One of the important advantages of this system is that it can easily replace the bracing system of many existing low and medium height structures in retrofitting process to strengthen them against seismic loads.

2-2-2- Active mass dampers:

Active mass damper (AMD) is a type of common active control system mostly installed in tall building and towers which are exposed to earthquakes and strong winds. This system can efficiently protect high rise building and towers against strong vibrations and provide residence with a good comfort.

Because of the convenient performance of the system, it is installed in many high-rise buildings and air traffic control towers all around the world ; for example, this system is installed in more than 50 important high-rise buildings in Japan (Yamamoto et al. 2014) .

The AMD system does not need so much space to be installed, therefore, it is an ideal vibration control system for ATC towers in which there is space limitation due to many sensitive devices and machines which are installed tightly (Figure 2-2).

This system consists of an AC actuator, a mass attached to the actuator with ball screw mechanism, a control unit, some displacement measuring sensors and some accelerometer sensors

In this system the acceleration of the structure is measured and used as the feedback in a closed-loop algorithm. This feedback is utilized in the control unit to command the actuator and make it apply controlled forces to adjust the position of the mass to reduce the story motion caused by vibration (Yang et al. 2017).

Figure 2-2 : AMD (Active Mass Damper) for Incheon International Airport Apron ATC Tower, after installation (www.tesolution.com)

In active mass dampers, the necessary feedback is just the acceleration of the structure and the stroke displacement of the AMD is used to regard the internal function of the AMD device (Yamamoto et al. 2014).

2-3- Passive damping systems:

passive system is the simplest energy dissipating system which operates without any control unit and external power source. Passive dampers can modify the stiffness and damping of the structure in which they are installed and improve its seismic demands. Since this type of damper is very simple and economic, a large variety of passive dampers are manufactured and installed in many structures, considering the design concerns and availability.
This behavior of passive dampers can be simulated by a spring or a spring and dashpot model.

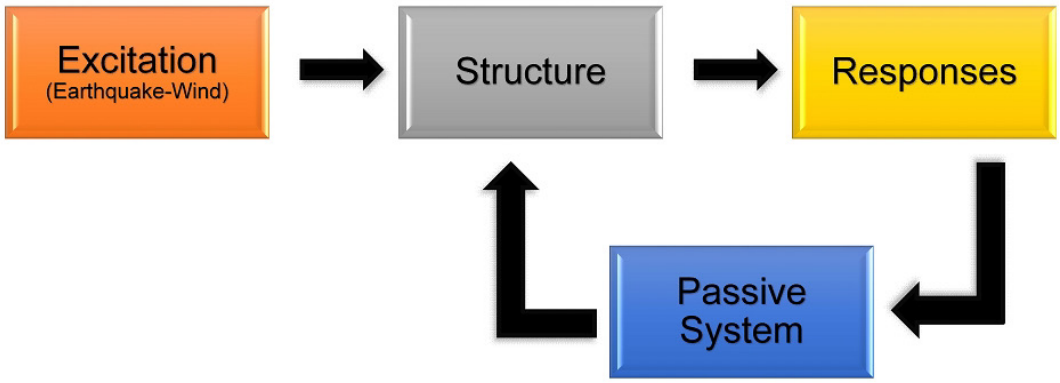

Figure 2-3 : The schematic diagram of a structure which is equipped with a passive control system

Passive dampers have the following advantages:

- Simple, inexpensive and economic
- No need to power source
- Inherently stable

The most ordinary passive damping systems are named as following:

- Frictional dampers (straight and rotational)
- Tuned mass dampers

- Viscous dampers
- Metal yielding dampers

2-3-1- Straight friction dampers:

This type of damper (Figure 2-4) is installed in bracing systems of the structures. The friction dampers translate the energy of vibration to heat by friction and dissipate the effects of lateral dynamic force loads such as earthquakes, indicating high energy-dissipation capacity and stable cyclic behavior. The friction dampers can be considered in initial design of the new structures or it can be easily and quickly installed in existing structures to seismically retrofit and strengthen them.

Although frictional dampers have the mentioned considerable advantages, they also have some disadvantages, as listed below, which may decrease the effectiveness of this type of damper.

- Frictional interfaces in this type of dampers are mostly made of steel plates which are vulnerable to corrosions, especially in humid weather conditions that can form rust patched on the steel plates of the dampers, in addition dust particle can cover the steel plates. These two negative factors can reduce the functionality and reliability of this type of dampers.
- Another problem arises due to the process of rubbing caused by dynamic lateral loads which leads to abrasion in the friction surface of steel plates in the damper, this phenomenon decreases the capability of the dampers.
- Deformation in the shape and geometry of this type of dampers due to temperature change or applied lateral loads and also small imperfections that may be caused in installation may lead to malfunction in frictional dampers.
- Stick-Slip in friction surfaces may cause an undesired behavior in this kind of dampers. This phenomenon is caused by the difference in static and kinetic coefficients in friction surfaces because the static friction coefficient between two surfaces is larger than the kinetic friction coefficient, therefore, If an applied force is large enough to overcome the static friction, then the reduction of the friction to the kinetic friction can cause a sudden jump in the velocity of the movement in the damper. This jump can be transferred to the structure in which the damper is installed.

Figure 2-4 : Straight frictional dampers installed in the bracing system of a building- Torre Cuarzo-Mexico D.F-Mexico (QUAKETEK www.quaketek.com, June 2018)

It should be considered that the above mentioned probable disadvantages of straight friction dampers can be notably decreased by using high quality material in the manufacturing process, exact and accurate installation, regular inspections and maintenance.

2-3-2- Rotational friction damper:

This type of passive damper is another type of frictional dampers which can be installed easily and requires less space compared to ordinary frictional dampers. This type of damper which is installed between the beam and bracing elements is designed and manufactured in different shapes (Figure 2-5).

This is how this type of damper works: while the structure which is equipped with this type of damper is exposed to earthquake, the lateral component of earthquake loads pushes the structure.

By moving the structure and the beam in which the damper is installed, the damper moves with the structure; then the central plate of the damper rotates around its hinge in the opposite direction of the motion, and because of the tensile forces in the bracing elements, the horizontal plates rotate in opposite direction to the structure. In this device the friction surfaces of the plates rub against each other and dissipate the earthquake energy by changing it into heat energy. When the direction of earthquake loads changes, this process reverses.

The negative point of this dampers is that they are just functional in small to medium displacements while straight friction dampers are functional confronting small to large displacements.

Figure 2-5 : Rotational friction damper installed in a building –Tehran-Iran (Damptech www.damptech.com, June 2018)

2-3-3- Tuned Mass Damper (TMD):

This kind of passive damper which consists of a mass, a spring and a dissipater is installed on top of the many high-rise buildings and bridges all over the world to mitigate the seismic and wind vibrations (Figure 2-6 and Figure 2-7). Since the first mode of the vibration in the structures is usually the most effective and dominant mode in seismic responses; these dampers are mostly set and tuned for the first frequency and mode. On the other hand, the structure might be exposed to other dynamic loads that can excite the structure in other frequencies and cause the other vibration modes to be dominant. Therefore, Tuned Mass Damper may be less effective and operative. For example, wind load can vibrate structures in their second frequency and make their second mode dominant.

In order to overcome this limitation, a solution is to utilize multiple TMDs adjusted and tuned in a frequency band around the natural frequency of the structure. That is a method used to dissipate the vibration in bridges. (Li 2000, Esteki et al. 2015). It should be considered that in ordinary tall buildings, the TMD ‘s are mostly limited to 1.5-2 % of the main structure’s mass (Esteki et al. 2015)

Figure 2-6: A pendulum type 150 ton TMD designed and manufactured by TESolution company for a residential tower -Taichung- South Korea (TESoulution www.tesolution.com, June 2018)

Figure 2-7: Jindo suspended bridge which is equipped with a TMD by TESolution company - South Korea (TESoulution www.tesolution.com, June 2018)

TMD dampers are also installed in bridges to limit the vibration of the bridge deck which may be caused by earthquake and winds (Figure 2-7 and Figure 2-8). It should be considered that bridges are mostly vulnerable to winds rather than earthquakes and this problem is more significant in

long–span and suspended bridges. As an acceptable solution for this problem many important bridges are equipped with a series of TMD that can efficiently reduce the vibrations caused by strong winds.

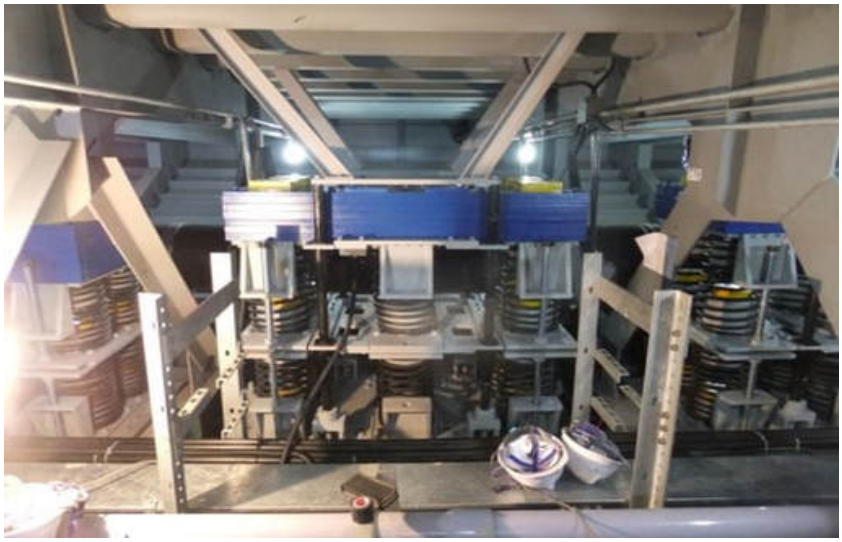

Figure 2-8 : Tuned Mass Damper(TMD) installed under the bridge deck at Jindo bridge - South Korea (TESoulution www.tesolution.com, June 2018)

2-3-4- Viscous dampers:

Viscous dampers are velocity-dependent passive energy dissipating devices which can be installed in bracing systems in order to form an energy dissipation system in the structures.

This device is made up of a piston and a cylindrical container that is partially filled with a highly viscous liquid such as silicon, oil, etc.

As the lateral forces are applied to the damper, the movement of the piston pushes the fluid through orifices which are around and through the piston head; the fluid flow which is passing the orifices has a very high velocity, and therefore, the compression energy of the fluid changes to the form of kinetic energy, then while the fluid volume is transferred to the other side of piston it cannot continue flowing ahead and loses its velocity because the other side of the container is closed (Figure 2-9) .

Because the kinetic energy has a direct relation with the velocity, some perturbations, which are called turbulence, happen in the fluid volume due to the loss of the velocity. This phenomenon causes the pressure of the fluid to be so low in this area compared with the fluid pressure in the other side of the piston head. The difference of the pressure between the two sides of the piston head produces a resistant force in the opposite direction of the piston movement, reducing the

applied external force. In addition, the friction between the fluid flow and the internal surface of the cylindrical container and the orifices dissipate a little part of the applied load to the form of heat. The mentioned process indicates how the viscous dampers dissipate the energy of applied loads such as earthquake.

The damping law of viscous dampers is given as follows:

$$F=CV^{N} \qquad \textbf{(2-1)}$$

Where, F is the damper force; C is an arbitrary constant (C remains constant over the full range of velocities); V is velocity; N is an exponent that can range from 0.3 to 1.95 (N remains constant over the full range of velocities).

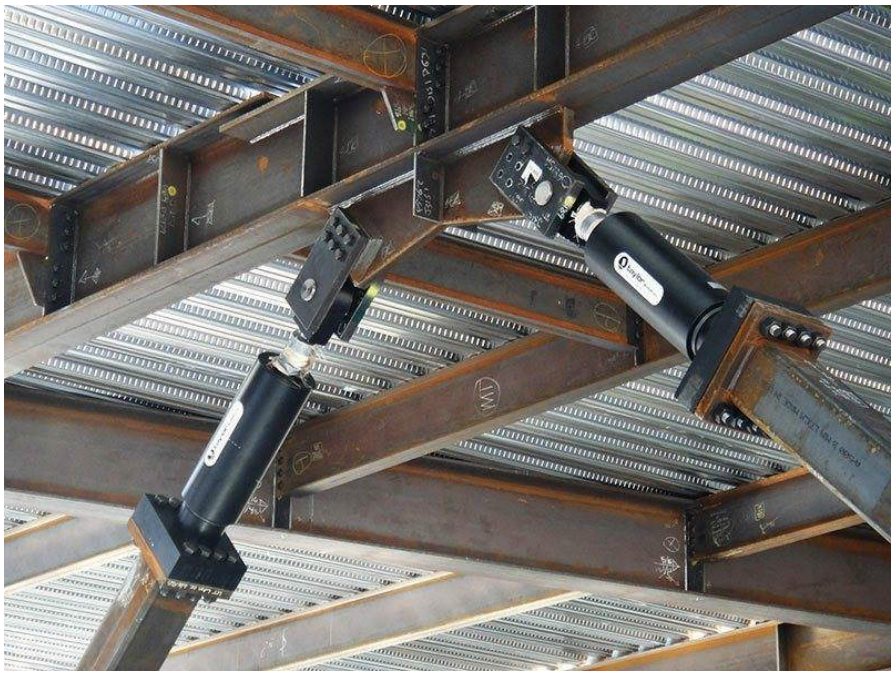

Figure 2-9 : Two viscous dampers used in bracing system of a steel structure (Robinson Seismic www.rslir.com, June 2018)

The equation (2-2) indicates that the in vicous dampers, the resistant force varies only with velocity changes .In this damper for a given velocity, the damper force will be the same at any point in the stroke; therefore, the damper provide no restoring force and the structure itself must resist all static lateral loads (Lee et al. 2001) .

Although viscous dampers can absorb a great part of the applied dynamic lateral force to the structure in which they are installed, there are some issues that can reduce the reliability and functionality of viscous dampers which are explained in the following:

- This damping system needs periodic maintenance and inspection to check the amount and quality of the viscous liquid that may reduce due to leakage and chemical reactions.
- Similar to other passive systems this kind of dampers have constant properties, therefore, they can produce resistant viscous passive force which can dissipate a limited range and pattern of dynamic forces, As a result, if the structure equipped with such dampers sustains a dynamic load such as an earthquake which has seismic characteristics different from those considered in the initial design, the viscous dampers may be ineffective. (Lee et al. 2001).

2-3-5- Material yielding dampers:

Material yielding energy dissipating systems such as added damping and stiffness (ADAS) and triangular added damping and stiffness (TADAS) are passive energy dissipating devices that can be used in buildings in order to dissipate seismic vibrations (Tena-Colunga 1997).

The mechanism of these systems, which are shown in Figure 2-10 and Figure 2-11 is plastic deformation of metallic materials such as steel alloys that dissipates the dynamic energy by changing the energy into internal work and heat.

Some disadvantages of this system are as follows:

- Random cyclic loads such as the shakings caused by heavy vehicles and wind may weaken the capacity of energy absorbing characteristic of these dampers due to fatigue by time, and, as a result, the amount of the capacity fall cannot be estimated.
- After a large earthquake this kind of dampers will lose a big part of their capacity or even may yield, and the structure in which the dampers are installed will not have a proper protection against lateral loads, therefore, the aftershocks that usually happen in the days after the primary earthquake can critically jeopardize the structure.
- The procedure which is utilized to analyze and design of this type of dampers is not common knowledge, and also these energy damping devices are protected by patent, therefore the structures designed with such dampers will be expensive (Tena-Colunga 1997).

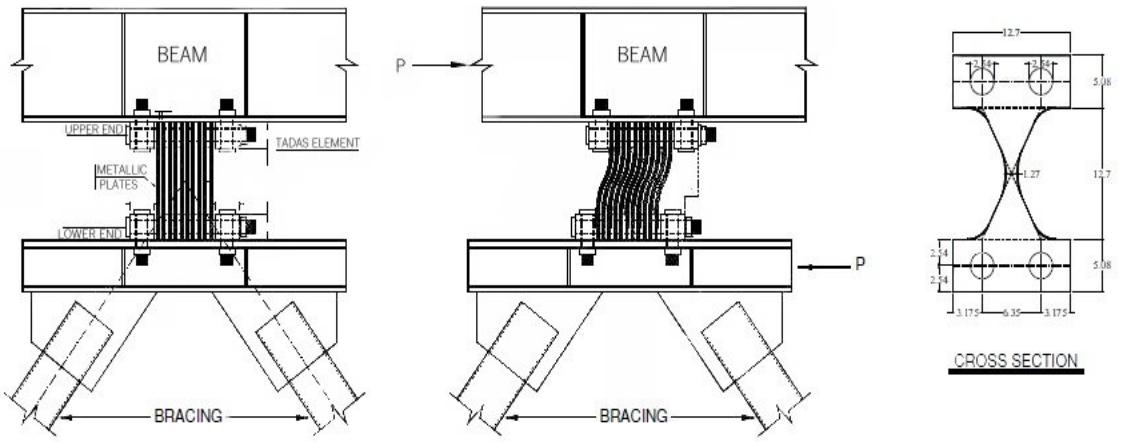

Figure 2-10 : The drawing of ADAS dampers with its details(Tena-Colunga 1997)

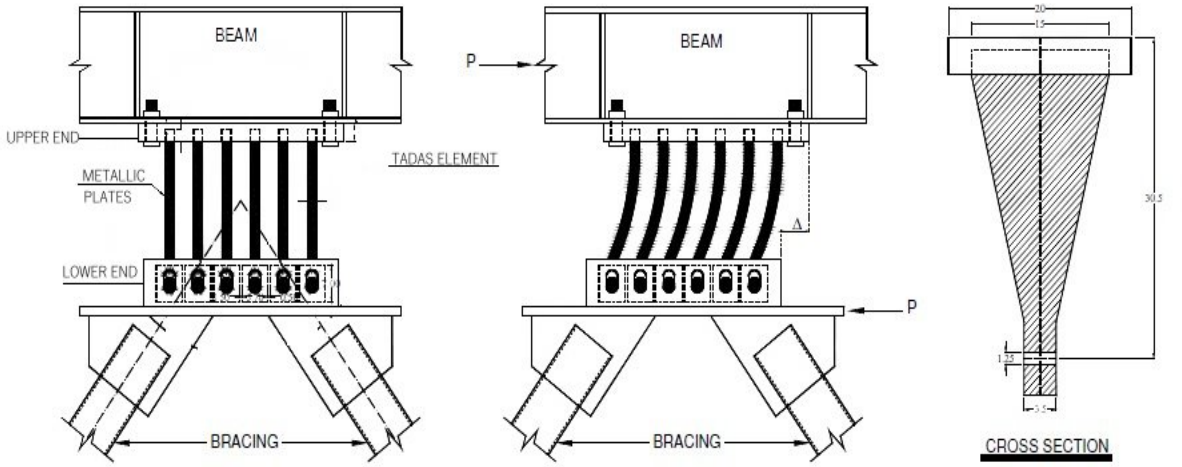

Figure 2-11 : The drawing of TADAS dampers with its details(Somerville et al. 1997, Tena-Colunga 1997)

2-3-6- Base Isolators

This system is one of the well accepted passive methods that can protect buildings and bridges against earthquakes. (Naeim et al. 1999, Lu et al. 2013). In this system some isolators are put underneath the main structure. When earthquake occurs, the isolators behave as a unit isolated layer and separate the structure from its sub structure. The base isolators absorb the energy of ground motion and protect the main structure during earthquakes (Figure 2-12). The isolators are made of energy absorbing material such as, slider bearing (SB), elastomeric bearings (EB), lead rubber bearings (LRB), Lead Extrusion Damper (LED), and friction pendulum system (FPS) which

are produced in different shapes. In bridges the isolators should be placed between the deck and piles to prevent transferring of the ground motion to force to the deck (Figure 2-12).

Figure 2-12 : Base isolators (LRB) installed between columns and foundation – Taiwan (Robinson Seismic www.rslir.com, June 2018)

Figure 2-13 : Base isolators installed between the deck and pies of a bridge – Roudshour -Saveh –Iran (Robinson Seismic www.rslir.com, June 2018)

2-4- Semi –Active energy dissipating System:

This system is designed based on variable mechanical properties which make it more worthwhile rather than passive systems. The idea of the utilizing this system is to have the advantages of active and passive systems simultaneously. In semi-active energy dissipating devices which are also called semi-active dampers, a small amount of energy that is mostly provided by batteries is used just to change the mechanical properties of the dampers and quickly adjust them proportional to the applied external dynamic forces such as seismic loads which should be reduced by the dampers. It also should be noted that the semi-active dampers inherit the characteristics and advantages of the passive device group that they belong to; in other words, they are the improved passive dampers that can produce variable resistant force.

Compared to active dampers, semi-active dampers have a safer performance; potential errors in control units of active damping system may lead to applying undesired active force to the structure which may cause instability and detrimental behavior in the structure, while semi-active dampers do not add any active force to the structure and do not cause any instability.

On the other hand, since there is no control in passive systems, they might become ineffective under some conditions and cause unwanted behavior in the structure; in the following the range of effectiveness and ineffectiveness of passive dampers in a single degree of freedom (SDOF) dynamic model is discussed.

Figure 2-14 illustrates the ratio of the force transmitted to the base to the exciting force in a SDOF dynamic system for a range of damping between 0 to 100%. The graph in Figure 2-14 show when the β, which is the ratio of the excitation frequency to the natural frequency of the system ,is between 0 and $\sqrt{2}$; by increasing the damping ratio (ξ) , the transmissibility (β) of the system decrease, It means that in this range of β, passive damper can function efficiently and dissipate the vibrations increasing the damping coefficient of the structure; but for the β bigger than $\sqrt{2}$, which means that the applied dynamic load has the vibration frequencies more than 1.414 times the natural frequency of the structure including the passive damper, the passive damper becomes ineffective. While by replacing the passive damper with a semi-active damper, the semi-active damper can be adjusted to change the natural frequency of the system in a proper way and effectively dissipate the vibration (Casciati et al. 2006, Pinkaew et al. 2001).

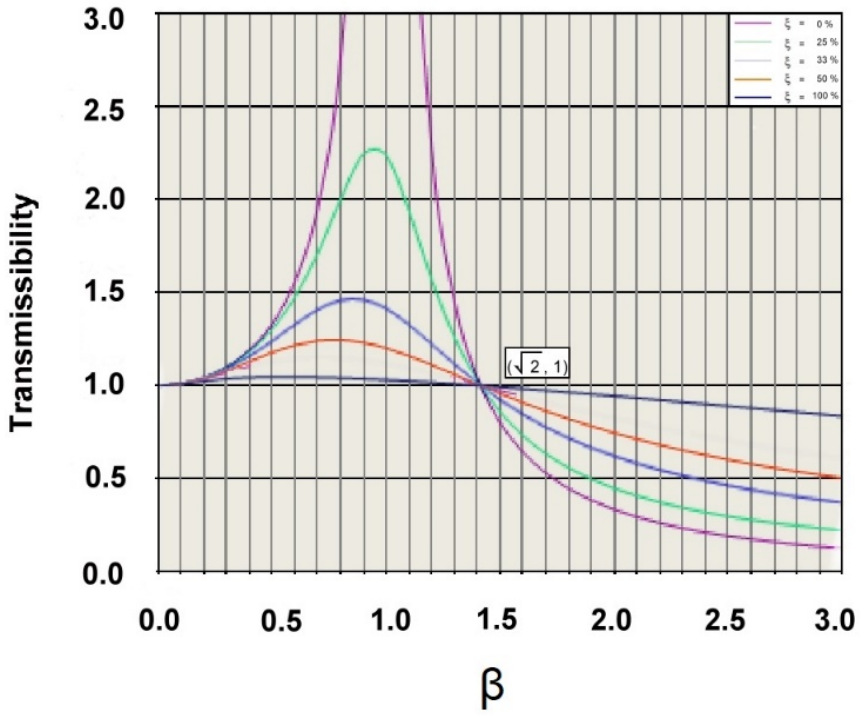

Figure 2-14 : Transmissibility of a SDOF system for several values of supplemental damping (Casciati et al. 2006)

Some of the semi-active dampers are named as following:

- Variable Viscous Devices (variable orifice)
- Variable Stiffness Devices
- Controllable Frictional Dampers
- Magneto Rheological Dampers (MR)

2-4-1- Variable Viscous Dampers (variable orifice)

These dampers are an improved type of viscous dampers, in which the diameter of the orifices can change by a small electrical servo-valve. This device has a variable damping coefficient that can change in a range between two numbers.

$$F_{damper} = C_{adaptive}(V - V_0) \qquad \textbf{(2-3)}$$

Where; C is viscous damping coefficient, $C_{min} \ll C_{adaptive} \ll C_{max}$; C_{min} and C_{max} are related to the minimum and maximum diameter of the orifice opening. The amount $V - V_0$ is the difference between the velocities at two ends of the device

2-4-2- Variable Stiffness Dampers

This type of damper is made of a spring whose stiffness can be adjusted by changing its length using a small electrical actuator.

This damper can be installed in the bracing of structures and it operates using a control system that adjusts its stiffness between two upper and lower values of K_{max} and K_{min}.

The simplest type is controlled by an on-off control system; in the Off mode the damper is ineffective and in the On mode the damper is effective (Casciati et al. 2006).

This equation indicates how this device works:

$$F_{damper} = K_{adaptive}(X - X_0) \quad \textbf{(2-4)}$$

Where; K is stiffness; $K_{min} \ll K_{adaptive} \ll K_{max}$; $(X - X_0)$ is the difference between positions at two ends of the device

2-4-3- Controllable Frictional dampers

In this device the friction between the sliding surfaces of the damper be adjusted by changing the pressure between the two sliding surfaces, this pressure can be changed by two actuators installed in the frictional surfaces (Feng et al. 1993, Sato et al. 2004).

$$F_{damper} = \mu (P_0 + P) \quad \textbf{(2-5)}$$

Where; F_{damper} is the friction force; μ is the friction coefficient; P_0 is the initial pressure, and P is the actuator variable pressure.

2-4-4- Magnetorheological dampers

This type of damper is proposed in recent years and researchers have been investigating about the performance of this damper under seismic loads. In order to explain the characteristic of such dampers, the characteristic of Magnetorheological fluid should first be explained.

2-4-4-1- MR fluids:

In early 1950's Jacob Rainbow observed the magnetorheological characteristic of MR fluids (Henrie et al. 2002). It is a class of smart materials which consists of micro-scale (3-8 μm), magnetically polarizable ferrous particles, suspended in a carrier liquid such as mineral oil, synthetic oil, silicon and glycerol. A typical MR fluid consists of 20-40% by volume of relatively pure iron particles in the carrier liquid (Henrie et al. 2002).

The rheological properties of MR fluids can rapidly vary by applying a magnetic field; when this fluid is exposed to a magnetic field the suspended particles polarize and interact to form a columnar structure parallel to applied magnetic field; therefore, the viscosity of the fluid increases and it can resist larger amounts of shear force (Figure 2-15).

It should be noted that just a small electricity charge is needed to provide such a magnetic field that can properly activate the MR fluid. This phenomenon is in proportion to the magnitude of the magnetic field applied and is immediately reversible. When there is no magnetic field, MR fluid indicates the behavior of a Newtonian fluid but while it is exposed to a magnetic field it characteristic changes to a semi-solid material and can be modeled as a Bingham plastic model; and its shear resistance can be formulated as follows:

$$\tau_{total} = \tau_y(\mathrm{H}) + \eta_p \dot{\gamma} \qquad \textbf{(2-6)}$$

where $\boldsymbol{\tau_{total}}$ is the total shear stress of the material, $\boldsymbol{\tau_y}$ Is the yield stress as a function of the magnetic field, H is the magnetic field strength, $\boldsymbol{\eta_p}$ is the plastic viscosity or post yield viscosity, and y is the shear strain rate in the fluid (Henrie et al. 2002, Casciati et al. 2006, Yang et al. 2002).

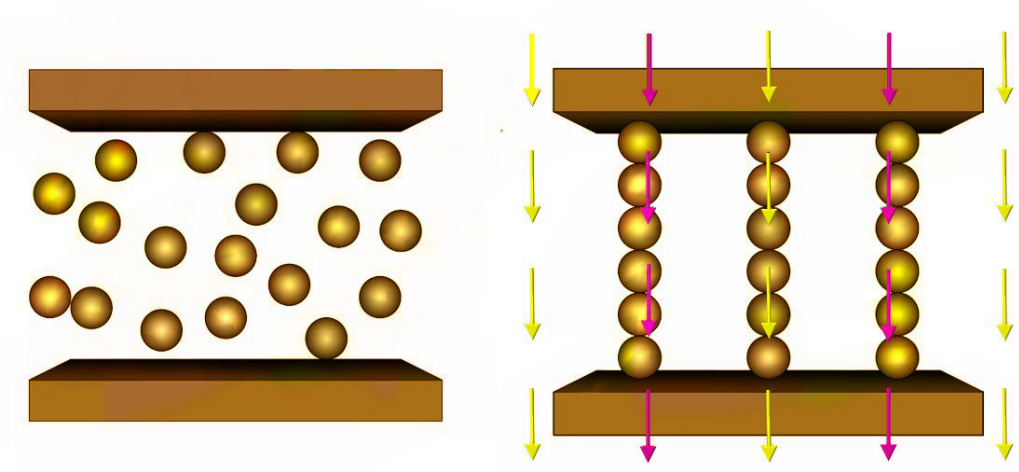

Figure 2-15 : The left picture shows MR fluid not exposed to any magnetic field and the right picture shows columnar structure of magnetized particles in MR fluid due to a magnetic field(Casciati et al. 2006).

The characteristic of MR fluid that its viscosity can change immediately, exposed to a magnetic field, made it an ideal material in designing a new generation of semi-active dampers named MR dampers. In the recent years many researchers have been interested to study and test the performance of MR dampers in structures. The largest MR damper which has been used in some

seismic tests, can produce up to 20 ton resistant force. This large-scale MR damper is designed and produced in LORD company by the model name Rheonetic MRD-900 Seismic Damper (Figure 2-16).

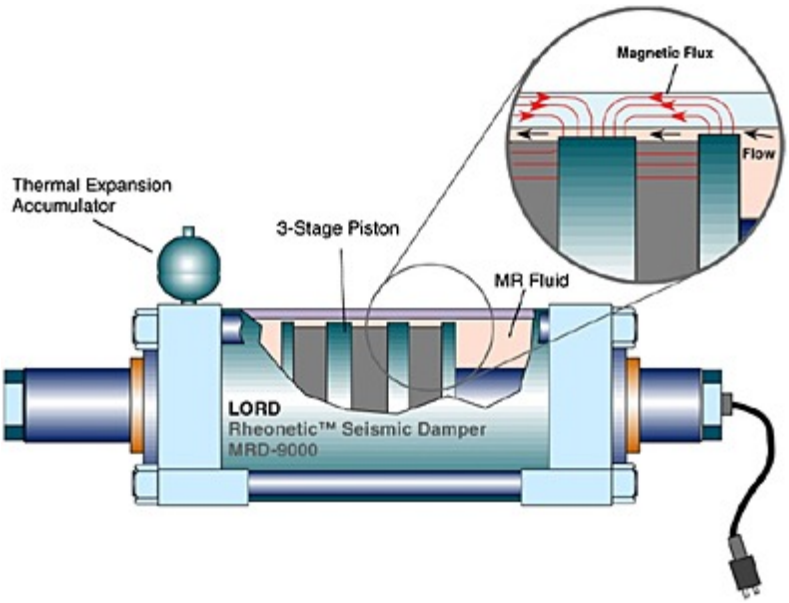

Figure 2-16 : The large scale 20 tom MR damper (Rheonetic MRD-900) made by Lord company (Yang et al. 2002, LORD www.lord.com, June 2018)

The MR damper is made of a piston placed in a cylindrical tube full of magnetorheological fluid. The piston can move fore and back inside the cylindrical body and the MR fluids flows through the space between the piston and the body. An electric coil is twisted around the cylindrical body of the damper and by applying a DC electricity current which can be provided by batteries, an electromagnetic field is induced around the damper (Figure 2-17).

Based on the characteristic of the MR fluid that is mentioned above, the viscosity of the MR fluid inside the damper increases and the damper produce bigger resistant force which can be transferred to the structure from the stroke of the piston (Yang et al. 2002).

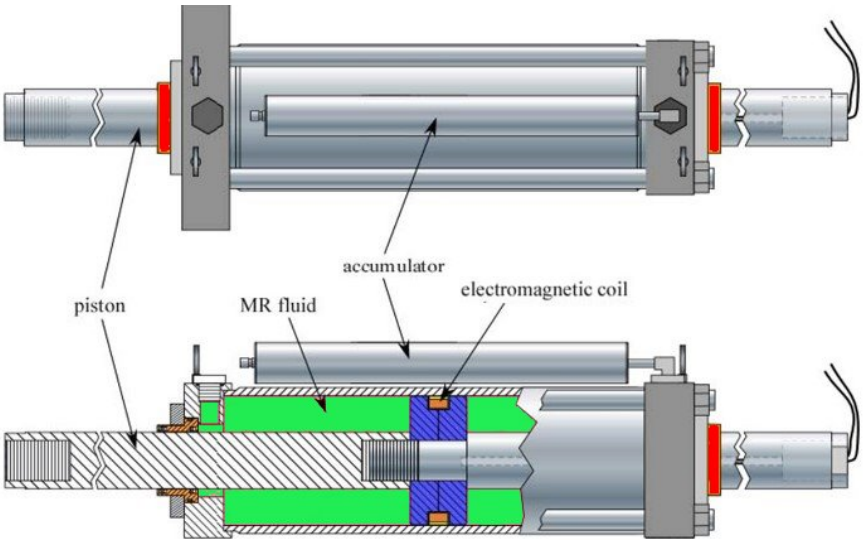

Figure 2-17 : The different component of an MR damper - (LORD www.lord.com, June 2018)

In 1996, for the first time, Dyke et al. tested a controlled model of an MR damper in the laboratory and showed the controlled semi-active damper is able to mitigate seismic force efficiently requiring a small amount of electricity power (Dyke et al. 1996). Since then, researchers have conducted studies on the performance of MR dampers (Yang et al. 2002, Yoshioka et al. 2002, Villarreal et al. 2004).

2-5- Hybrid systems:

The Hybrid system as its name implies is a combined system, this system consists of at least two types of dampers (Figure 2-18). Many of hybrid dampers are designed by using active and passive or semi-active and passive devices. For example, a series of frictional or viscous dampers as the bracings of a building in addition to an AMD which is attached on top of the building form a hybrid system. The concept of designing hybrid systems is to decrease the limitations of each system and use the advantages of all used systems.

In this system as shown in Figure 2-18 , a passive damper can be added to an active or semi - active system to form a combined damping system that needs less external power to function compared with the power required by an active system with the same capacity. In addition, since the hybrid system applies less active force, the risk of instability in the structure will decrease.

The other notable advantage of such hybrid systems is that in harsh conditions that the active damper may lose its functionality due to the failure of external power source, the structure has at least a passive or semi-active damping system that can dissipate the applied dynamic force to some extent; and it provides the main structure with some protection. Furthermore, in this system the active or semi-active dampers that can produce controllable and variable force utilize the passive system in a proper way and can compensate the lack of adjustment of properties in passive dampers efficiently, eliminating the undesired behavior that may cause by the passive dampers.

It also should be concerned that there are a variety of hybrid systems that the structural designers consider as the availability and economic concerns which can be utilized in the construction of new structures or rehabilitation of current structures.

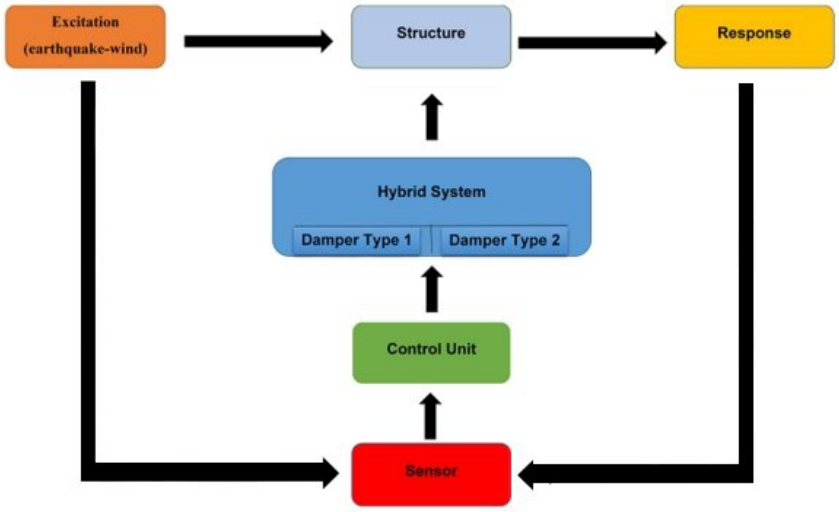

Figure 2-18 : The schematic diagram of a structure which is equipped with a Hybrid control system

The most important hybrid system is called hybrid mass damper (HMD) which is made of an AMD and a TMD system. The advantage of such systems is that the TMD dissipates the vertical vibrations and the AMD dissipates the horizontal vibration. Such systems are mostly used in sky-scrapers and airport traffic control towers and they are able protect structures against harsh earthquake and strong winds.

Figure 2-19 shows a modern Hybrid mass damper with 50 ton moving mass. This Hybrid which is manufactured by TE solution company is installed in a 54-story building (Technomart) with the height of 189 m to mitigate the building vibration.

Figure 2-19 : Technomart Hybrid Mass Damper with 50 ton moving mass at TESolution structural lab-South Korea (TESoulution www.tesolution.com, June 2018)

2-5-1- Modelling of Magnetorheological (MR) dampers:

It is worth mentioning that to investigate the performance of MR damper in structures, it is important to use a well-defined model that can properly illustrate the behavior of MR dampers. Previous research and tests illustrate that phenomenological models, obtained from experiments, can simulate the behavior of MR dampers properly (Spencer Jr et al. 1997, Sapiński et al. 2003) .

In the following common phenomenological models that are used to present and model the behavior of MR dampers, are presented:

2-5-2- Bingham Model

The Bingham model which was proposed in 1985, is one of the simplest models that is commonly used to identify the behavior of MR dampers with a reasonable approximation, despite the complex behavior of MR damper. This visco-elastic-plastic model has a variable yield strength ($\tau_y(field)$), that varies according to the magnitude of the applied magnetic field. In this model when the shear stress τ is less than $\tau_y(field)$ the model indicates visco-elastic behavior which is defined by the equation:

τ =G γ $\qquad\qquad$ $\tau \leq \tau_y(field)$ **(2-7)**

When the shear stress becomes more than the yield shear stress, the model shows plastic behavior that can be presented by the following formula:

$$\tau = \tau_y(field) + \eta\,\dot{\gamma} \qquad \tau > \tau_y(field) \qquad \textbf{(2-8)}$$

where, τ is applied shear stress to the modeled damper; $\tau_y(field)$ is yield strength of the damper which varies according to the magnitude of the induced magnetic field; G is complex modulus; η is viscosity of the MR fluid; and γ is shear strain. This Bingham model consists of a coulomb friction and a viscous damper which are in parallel together (Figure 2-20).

The damping force of a MR damper which is modelled by a Bingham model can be proposed by the following simplified and idealized equation:

$$F_{Damper} = f_c \operatorname{sgn} x' + c_0 x' + f_0 \qquad \textbf{(2-9)}$$

where, f_c is frictional force; c_0 is viscous damping parameter; f_0 is a component that is defined to account for the non-zero mean that is observed in the measured force and caused by the presence of the accumulator (Dyke et al., 1996). This last simplification in the model results from the assumption that the elasticity which is replaced the accumulator activity, has a low stiffness and linear characteristics (Sapiński et al. 2003) .In the following the extensions of Bingham model are discussed.

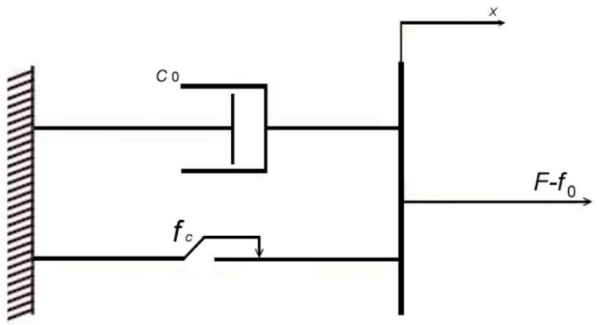

Figure 2-20 : The Bingham model of MR damper (Spencer Jr et al. 1997)

2-5-3- Bingham body model

The Bingham body model, which is shown in Figure 2-21 is an improved Bingham model in which a spring, with the stiffness k, (an elastic body) is added to Bingham model. This model indicates

a two-phased behavior, in the first phase the model confronts a shear force below or equal to a certain amount, which is the frictional force (f_c) of damper, then it presents elastic behavior and only the spring deforms and becomes active, when the shear force exceeds the frictional force (f_c) of damper, the two other components friction and dashpot elongate and become active and the model enters to the second phase in which it has visco-plastic behavior.

This model presents the damping force as:

$$F_{Damper} = f_c \operatorname{sgn} \dot{x} + c_0 \dot{x} + f_0 \qquad \text{for } |F| > f_c \qquad \textbf{(2-10)}$$

$$F_{Damper} = k\,(x_2 - x_1) + f_0 \qquad \text{for } |F| \leq f_c \qquad \textbf{(2-11)}$$

where, the parameters c_0 , f_c, and f_0 have the same meaning as in equation **(2-12),** *k* represents the stiffness of the added spring as the elastic part (Sapiński et al. 2003).

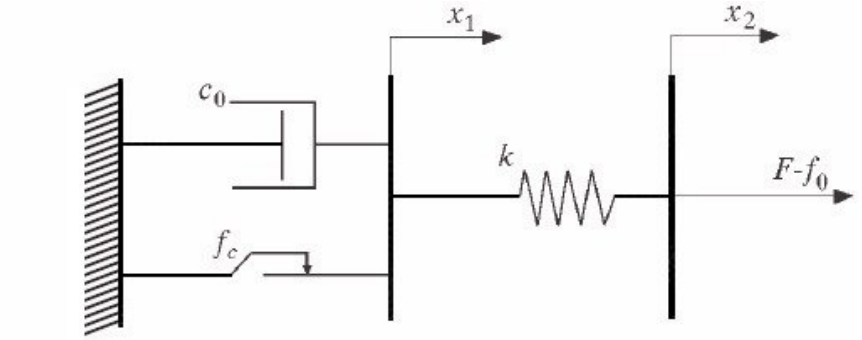

Figure 2-21 : The Bingham body model of MR damper (Spencer Jr et al. 1997)

2-5-4- Gamota - Filisko Model

Another improved type of Bingham model that has visco-elastic-plastic behavior was presented in 1991 by Gamota and Filisko (Spencer Jr et al. 1997). This model, which is illustrated in Figure 2-22, consists of three parts which are set in series. The first part is a Bingham model, the second part consists of a spring in parallel with a dashpot and the last part includes just a spring. Although this model was designed to indicate the performance of Electrorheological dampers, the later experiments indicated that this model can illustrate the behavior of Magnetorheological damper

well (Spencer Jr et al. 1997). This model has a two-phased performance and produces force which is formulated as the following equation:

$F_d = k_1(x_2\text{-}x_1)+c_1\dot{x}_2 + f_0 = k_2\,(x_3 - x_2) + f_0$ for $|F| \le f_c$ **(2-13)**

$F_d = k1\,(x_2 - x_1) + c_1\,(\dot{x}_2 - \dot{x}_1)+f_0 = c_0\dot{x}_1 + f_c sgn\,(\dot{x}_1)+ f_0$ for $|F| > f_c$ **(2-14)**

$= k_2\,(x_3 - x_2) + f_0$

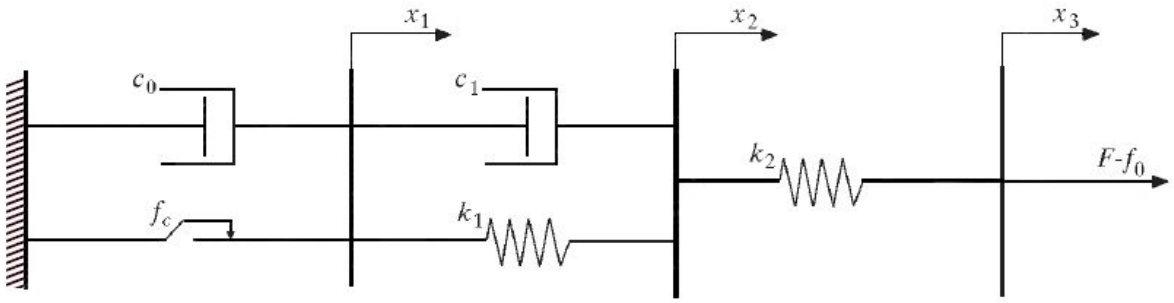

Figure 2-22 : The Gamato –Filisco model of MR damper (Spencer Jr et al. 1997)

Where,c_0, c_1 are viscous damping; f_0 , f_c are force due to the presence of the accumulator and frictional force respectively; and k_1, k_2 are stiffness of the springs

2-5-5- Bouc - Wen model:

The behavior Bouc-Wen model is another phenomenological model that can simulate the behavior of MR dampers very well. As it is shown in Figure 2-23, this model contains a dashpot, a spring and a hysteresis. This model can present the force-displacement and force-velocity behavior of a real damper very well (Kwok et al. 2007).

The damping force F in this model is:

$F=c_0\dot{x}(x - x_0)+ \alpha z$ **(2-15)**

The z can be defined as:

$\dot{Z}= \gamma|\dot{x}|z|z|^{n-1}\text{-}\beta\dot{x}|z|^n+A\dot{x}$ **(2-16)**

where, α is a scaling factor for hysteresis n, γ, β and A are parameters which control the linearity during unloading and the smoothness of the transition from the pre-yield to post-yield region; k_0 is stiffness of the spring; c_0, c_1 are viscous damping parameter of dashpot; x_0 is the initial displacement of the spring; Z is the hysteretic variable .

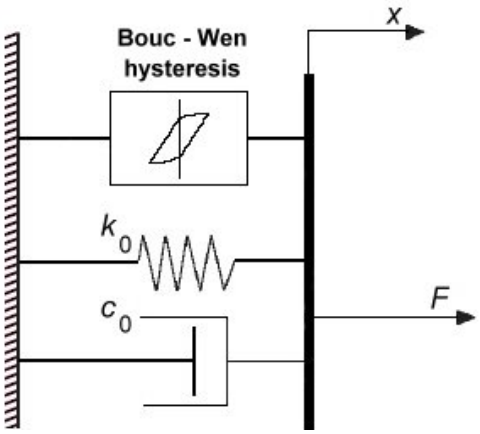

Figure 2-23 : The Bouc-Wen model of MR damper(Spencer Jr et al. 1997)

2-5-6- Spencer Model:

Spencer et al. (1997) proposed an improved model based on Bouc–Wen model that could capture the force roll-off in the low velocity regions which are observed in experimental data (Spencer Jr et al. 1997, Yang et al. 2002).

In this model, a dashpot and a spring are added to Bouc-Wen model (Figure 2-24).

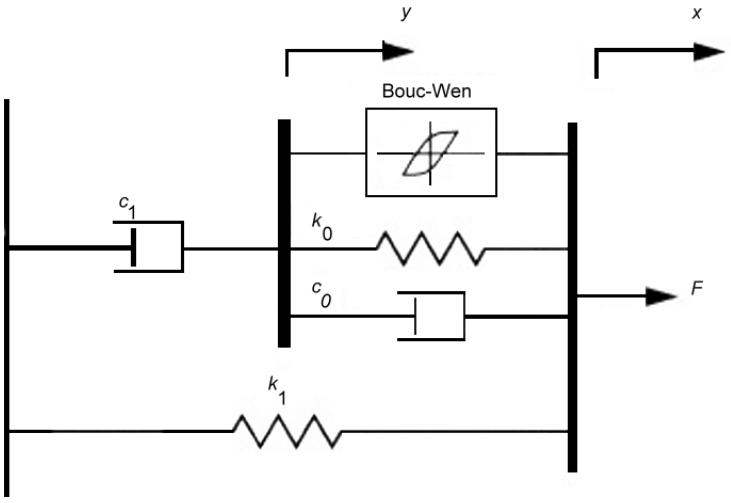

Figure 2-24 : The spencer model of MR damper(Spencer Jr et al. 1997)

$$F=\alpha z+c_0(\dot{x} - \dot{y}) + k_0(x - y)+ k_1(x - x_0)= c_1\dot{y}+k_1(x - x_0) \quad \textbf{(2-17)}$$

where, z and y is governed by:

$$\dot{z}= - \gamma |\dot{x} - \dot{y}|z|z|^{n-1}-\beta(\dot{x}-\dot{y}) |z|^n+A (\dot{x} - \dot{y}) \quad \textbf{(2-18)}$$

$$\dot{y}=\frac{1}{c_0+c_1}(\alpha z+c_0 \dot{x} + k_0(x - y)) \quad \textbf{(2-19)}$$

where, k_1 is accumulator stiffness; c_0 is viscous damping at large velocities; c_1 is viscous damping for force roll-off at low velocities; k_0 is stiffness at large velocities; x_0 is the initial displacement of spring k1; and c_0, and c_1 are also functions of the input current

Since the Spencer model can predict the behavior of MR dampers well, many researchers have used this model for the numerical simulation of structures with MR dampers. It was also used to model the first generation large-scale MR damper manufactured by Lord Corporation (Yang et al. 2002).

There are also some other models that are less used such as Li model and Dahl Model (Sapiński et al. 2003, Casciati et al. 2006).

2-6- Summary

It is observed that semi active energy dissipating systems are efficient are reliable, effective and economic systems that can be installed in civil engineering structures to mitigate the destructive effects of dynamic loads such as earthquake. An MR damper that is a modern semi-active energy dissipating device is an innovative damping system, which has been considered in recent years, and can be improved by a control system to be efficiently utilized in structures. This adaptive damper can dissipate the seismic vibration of the structures demanding a small power source.

Chapter 3

Control Systems

Control systems currently play a crucial role in many important systems and devices. The main reason that we apply a controller in a dynamic system is to command the performance of the system and get the desired output based on the pre-defined references. In order to reach this goal, the control unit should continuously monitor the performance of the system and adjust its input in such a way that the system works desirably and produces correct outputs.

The more important, valuable and complicated the system is, the higher demand for control systems is required to guaranty the function of the system, for instance; advanced systems such as airplanes, power plants and high-rise buildings, that continuously confront different patterns of dynamic loads and excitations, need reliable control units; which are able to work under different conditions including harsh conditions and emergency situations accurately, while malfunction of such systems may lead to catastrophic consequences that can jeopardize the people' lives and capital. The other advantage of utilizing control units in systems is that they can improve and optimize the performance of the systems using less energy.

The previous investigations have shown that controllable dampers have considerably better performance in dissipating vibrations. Since an MR damper has the capability of producing variable forces, a reliable and effective control system can improve and optimize its functionality. By installing such controllable MR dampers that can produce adaptive resistant force according to the magnitude and pattern of applied seismic load, we can effectively dissipate the seismic vibrations of the structure where it is installed.

In this chapter the major configurations of control systems are discussed; then the state-space control theory and model-dependent and model-independent control systems are investigated and finally the fuzzy control system applied to design the control unit of the adaptive MR damper is explained.

3-1- Major configurations of control systems:

Control systems are categorized in two forms of open-loop and closed loop. Open loop systems, which are called no feedback systems, operate based on the input of the main system and the output has no effect on their operation; while closed loop systems, which are called feedback systems, utilize both input and output of the main system.

In the following the operation of both open loop and closed loop systems will be discussed.

3-1-1- Open-loop systems:

An open-loop control system adjusts the function of the main system by using just the input data, while the output data has no effect on its operation. In other words, it cannot balance and correct the errors and disturbances which may affect the performance of the main system. Therefore, open loop control systems cannot command and adjust the performance of sophisticated dynamic systems which continuously confront disturbances (Nise 2011).

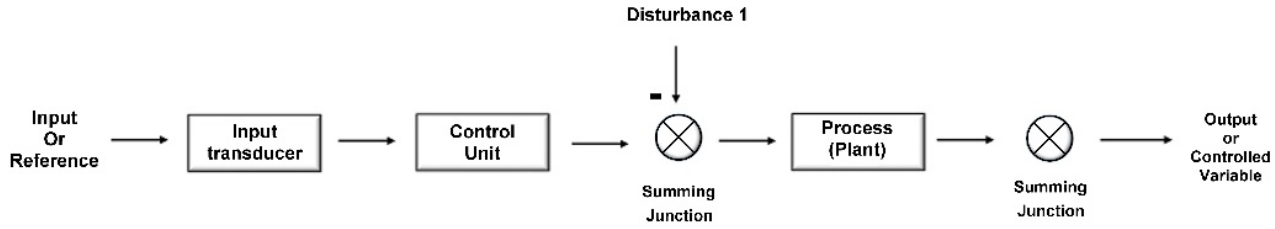

Figure 3-1 : Open-loop Control System (Nise 2011)

3-1-2- Closed loop systems:

A closed-loop control system operates based on both input and output data of the main system. This control system is a practical solution that can be utilized in complicated dynamic systems. In this type of control system, the output data of the main system are measured and fed back to the controller. Then the controller decides how to adjust the system input in order to reduce the disturbance errors and improve the system performance.

In this closed loop process, the transducers transfer the input and output data to summing junction unit simultaneously. The difference between the input of system, which plays the role of set point, and the output determined from the control system indicates the number of errors that is due to disturbance, then it is minimized by an appropriate algorithm in the control system.

Then the output of controller commands the operation of the main system. In a dynamic system, this closed loop process including input adjustment and error correction should be continuously done to guarantee the well performance of the system (Nise 2011, Lilly 2011). It should be noted that as the control unit is responsible for minimizing and correcting the errors, the selection of a reliable and practical controller is crucial. Figure 3-2 illustrates the process of the closed-loop control system.

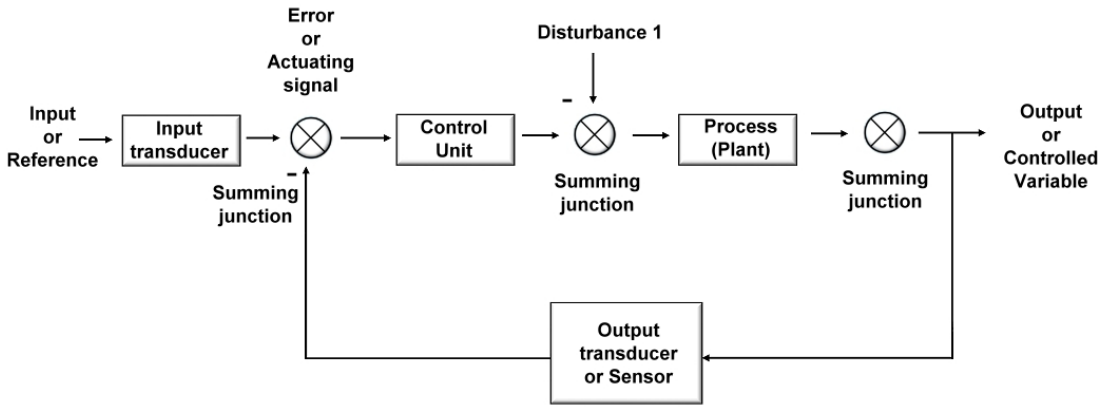

Figure 3-2 : Closed-loop Control System (Nise 2011)

3-1-3- State-Space Control Theory

One of the most applicable modern control approaches that can properly meet the requirements of complex dynamic systems including linear and non-linear, time variant and time invariant is the state space method, which also covers both time-domain and frequency-domain approaches. This method can solve the dynamic equations of sophisticated dynamic systems. Meanwhile conventional methods have many limitations in solving the complicated partial differential equations (PDE). It should be noted that utilizing modern computers have made the solving of PDEs, which are used in the state space method, quite fast. (Franklin et al. 1994, Ogata 1999).

3-1-4- Model based and model independent control systems in the structural engineering

A reliable control system has a pivotal role in improving the efficiency of semi-active dampers. In other words, if we install a resilient and economic control device which can perfectly adjust the operation of the MR dampers installed on the structures, such system not only does optimize the performance of the dampers, but also reduces the number of dampers required in the seismic design of the structure. It means with fewer dampers, we can get an acceptable structural response. Furthermore, as the economic principles are matters of importance in construction, it can strongly justify using smartly controlled dampers in structures (Lagaros et al. 2012)

There are two kinds of control algorithms which are utilized in closed-loop control systems: model-dependent and model-independent.

The model-dependent control algorithms which are commonly utilized in designing the control systems in the structures are linear quadratic regulator, linear quadratic Gaussian, H∞, etc. (Tan et al. 2009, Narasimhan et al. 2006, Lagaros et al. 2012).

The control systems which utilize model-dependent algorithms are called model-dependent or model free control systems, and they are designed based on the mathematical model of the main dynamic system whose performance they should adjust. Therefore, the model-dependent controllers malfunction and may fail due to the lack of accurate mathematical model of the main system.

The control systems which utilize the model-independent algorithms are called model-independent or model-free control systems. The mentioned model-free control systems are extensively designed based on the frame works such as fuzzy logic theory and neutral network algorithms.

The main advantage of the model-free control systems is that they can adjust and control the operation of nonlinear complex dynamic systems whose mathematical models are not accurately known (Lagaros et al. 2012, Lilly 2011).

A structure equipped with an MR damper, which has nonlinear behavior, forms a complicated system. When this complicated system is exposed to seismic loads, it becomes even more complicated. Therefore, a model-free control system is required to adjust the MR damper behavior in this complex dynamic system.

By utilizing the fuzzy logic as a famous model-free algorithm in the structures equipped with an MR damper, we will have a smart control system in the structure that can efficiently control the performance of the damper and improve the seismic response of the structure in a proper way.

3-1-5- Fuzzy Logic

In 1965, Lotfi A Zadeh introduced the fuzzy logic for the first time and Zadeh and other researchers developed this method (Lilly 2011). Japanese industries were this first to be interested to use this logic in designing the control systems of their products in early 80s, although this method was not accepted by many other countries at that time due to some unexplored mathematical concepts related to it.

The wide use of control systems working based on fuzzy logic in Japanese industries from the production of simple electrical appliances such as washing machine to huge infrastructures such as Sendai Subway Namboku Line, which was developed by Hitachi, led to numerous success.

This achievement motivated the other countries such as the US, to rapidly start utilizing this method in their industries in the late 80s. The fuzzy systems are developed in such a way that now a day many complicated devices are working with fuzzy controllers.

One of the most important characteristic of human is to solve complicated problems and complex processes based on past experience and heuristic knowledge, which means that people solve many technical issues based on expert knowledge without the aid of any model. Since fuzzy logic is similar to the human thinking and reasoning way, it operates based on the expert knowledge and simplify many complicated cases in control of systems. This outstanding characteristic makes fuzzy systems eligible to easily and correctly control such complex systems that it is too difficult to control them with model-dependent control systems (Lilly 2011).

3-1-5-1- Mamdani fuzzy Control System:

Mamdani's fuzzy inference method, which is proposed in 1975 by Ebrahim Mamdani (Mamdani et al. 1981), is one of the most commonly used fuzzy method and it was among the first control systems built using fuzzy set theory. Takagi and Sugeno is also another useful approach which is defined based on the fuzzy method.

Similar to any other fuzzy control systems, Mamdani fuzzy control system consists of three stages which are fuzzification, inference mechanism and defuzzification as below:

Fuzzification:

In this stage the data of measured quantities derived from the system are converted to fuzzy sets through fuzzification process and these sets are utilized by inference stage.

Inference:

In the inference stage, the fuzzified values are processed to determine the fuzzy output based on a set of fuzzy rules that are built upon expert's knowledge, the output of this stage is fuzzy sets indicating the recommended rules considering their firing degree. In this stage the input fuzzy sets are characterized by membership function and for each crisp input a particular rule is fired to the extent of membership function. The extent of membership function is between 0 and 1.

Defuzzification:

In this stage, by using the centroid defuzzification method which are center of gravity (COG) or center average (CA) methods, the weighted average of the recommended rules is calculated. Then the crisp output is calculated from the weighted average of all fuzzy rules involved in finding

the fuzzy output and the defuzzified output is used for commanding the system which should be controlled by the controller.

Advantages of the Mamdani Method

- It is intuitive.
- It has widespread acceptance.
- It is well suited to human input.

3-2- Summary:

Considering the reliable and successful performance of fuzzy control systems in adjusting and controlling complex dynamic systems during the recent years, it is perfectly reasonable to apply them in modern civil engineering structures. These control systems can operate in tandem with MR damper and adjust them in a way to properly react to applied earthquake loads and mitigate their effects. The fuzzy system applied in this research is defined and designed based on Mamdani method which is widely used in fuzzy control systems.

Chapter 4

Methodology of research

4-1- Methodology

In this research two single-story structures with the same features and properties are modeled under two conditions; first without damper and second with smart MR damper; and two sets of earthquakes including far-field and near-field records are applied to each structure. The seismic responses of both structures are analyzed and compared to illustrate the efficiency of the smart damper. This procedure is performed by utilizing MATLAB and SIMILINK software. Since the dynamic systems of the models are complicated, the state-space method is utilized to facilitate the analyses. The output of the analyses in terms of displacement, velocity and acceleration are compared to indicate the seismic behavior of the structures.

In the model which is equipped with the smart damper, a closed-loop path is designed to transfer the analytical output to the fuzzy control unit in real time. Based on the received feedback, the fuzzy control system adjusts the driven electricity current to the damper to make it produce the resistant force according to the magnitude and directions of the applied earthquake.

The MR damper utilized in this research is simulated based on spencer phenomenological model which is the most efficient model to represent the behavior of an MR damper. It should be mentioned that the phenomenological models are mostly obtained from experiments, while the mechanical models are maintained from calculational methods.

The experimental equation of spencer model shows that the relation between the input electricity current, and the output damper force is highly nonlinear. Therefore, the dynamic model of the structure with the damper is nonlinear. As, the applied earthquake loads increase the complexity of the system. The only way to properly control such a complicated nonlinear dynamic system is to utilize a model-independent control system. Therefore, the Mamdani fuzzy system which is one of the commonly used model -independent control systems, is utilized to adjust the performance of the MR damper. The analytical results in terms of seismic demand of structures and probability curves are derived and compared.

4-2- Case Study structure

In this research, to investigate the seismic response of a structure which is upgraded with a controllable MR damper and to determine the performance of the damper, a simplified dynamic

system which contains a 2D single story structure equipped with a controllable 200 KN large-scale MR damper is modeled then two sets of earthquake records, which are explained in part 4-3, are applied to the structural model. In this research the seismic performance of a 200 KN large -scale MR damper is investigated and there should be a technical coordination between the ultimate damper force and the dynamic properties of the modeled structures.

The ultimate capacity of the selected MR damper is assumed to be 5% of the magnitude of the force exerted of the structure mass .Therefore, the magnitude of the structure mass (M) must be $4 \times 10^5\ kg$ and the two other dynamic properties which are stiffness and structure inherent damping ratio, are considered as K= $1.5 \times 10^8\ N/m$; and $C = 1.55 \times 10^5\ N.s/m$ $(\xi = 0.01)$ respectively. (Lagaros et al. 2012, Yang et al. 2002, Yang et al. 2004) .

The period of the modeled structure is 0.33 s calculated using the following formula:

$\mathrm{T} = 2\pi\sqrt{\mathrm{M/K}}$=$2\pi\sqrt{4 \times 10^5/1.5 \times 10^8}$ = 0.33 s

The design procedure for a moment resting frame is discussed in appendix II.

The simulation of the modeled system is performed by the MATLAB and SIMULINK software.

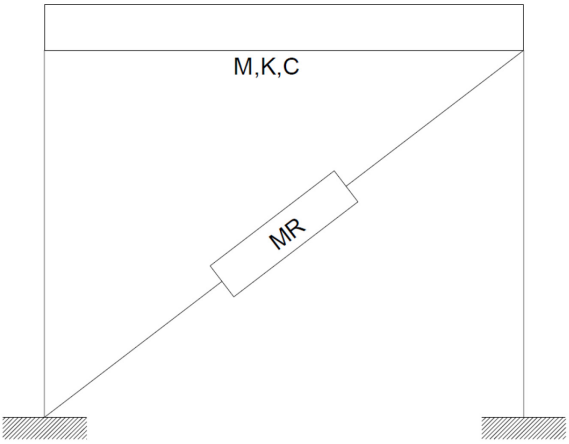

Figure 4-1: The schematic illustration of the modeled structure.

4-2-1- State-Space realization for a one-story structure:

In the following the process of state-space realization for the modeled structure with damper and without damper is discussed; in this case the applied earthquake force is considered as an external factor in the equations. (Ogata 1999, Chopra 2001).

4-2-1-1- General dynamic equation

Dynamic equation based on which the system acts is as follows:

$$M\ddot{X} + C\dot{X} + KX = M\ddot{X}_g - f_d \quad \textbf{(4-1)}$$

Where, X, $\dot{X}$, and $\ddot{X}$ are relative displacement, relative velocity and relative acceleration, respectively. In this equation, M, C and K are Mass, Inherent damping and Stiffness of the model respectively. The factors $\ddot{X}_g$ and f_d illustrate the earthquake acceleration and damper force respectively. In the following, the dynamic system is represented in the state space form by the following equations.

$$\begin{cases} \dot{q} = Aq + Bu \\ X = Cq + Du \end{cases} \quad \textbf{(4-2)}$$

Where, A is the state matrix, B is the input matrix, C is the output matrix, D is the direct transmission matrix and U = $\begin{bmatrix} \ddot{X}_g \\ f_d \end{bmatrix}$ is the external factor matrix

The relation between state variables q_1, q_2 and their derivatives are shown as:

$$q = \begin{bmatrix} q_1 \\ q_2 \end{bmatrix} = \begin{bmatrix} X \\ \dot{X} \end{bmatrix} \quad \textbf{(4-3)}$$

Where q is the matrix of state variables

This equation results in:

$$\dot{q} = \begin{bmatrix} \dot{q}_1 \\ \dot{q}_2 \end{bmatrix} = \begin{bmatrix} \dot{X} \\ \ddot{X} \end{bmatrix} = \begin{bmatrix} q_2 \\ \ddot{X} \end{bmatrix} \quad \textbf{(4-4)}$$

The output is:

$$Y = \begin{bmatrix} y_1 \\ y_2 \\ y_3 \end{bmatrix} = \begin{bmatrix} X \\ \dot{X} \\ \ddot{X} \end{bmatrix} \quad \textbf{(4-5)}$$

It is concluded that:

$$\ddot{X} = -M^{-1} C\, q_2 - M^{-1} k_s q_1 - U \quad \textbf{(4-6)}$$

Then

$\dot{q}_2$= $\ddot{X}$ = $-\ M^{-1}\ C\ q_2 - M^{-1}\ k_s q_1$- U **(4-7)**

Which yields:

$$\dot{q} = \begin{bmatrix}\dot{q}_1\\ \dot{q}_2\end{bmatrix} = \begin{bmatrix} q_2 \\ -M^{-1}\ C\ q_2 - M^{-1}\ k_s q_1 - U\end{bmatrix} \quad \textbf{(4-8)}$$

This equation is simplified as:

$$\dot{q} = \begin{bmatrix} 0 * q_1 + q_2 \\ - M^{-1}\ k_s q_1 - M^{-1} C\ q_2\end{bmatrix} + \begin{bmatrix}0\\ -1\end{bmatrix}\ U \quad \textbf{(4-9)}$$

Which can be rewritten as:

$$\dot{q} = \begin{bmatrix} 0 & 1 \\ - M^{-1}\ k_s & -M^{-1} C\end{bmatrix} \begin{bmatrix}q_1\\ q_2\end{bmatrix} + \begin{bmatrix}0\\ -1\end{bmatrix}\ U \quad \textbf{(4-10)}$$

4-2-1-2- State-space equations of the system without Damper:

In the following the state-space equation of the system without damper is written. Since in this system there is no damper, the component f_d ,which presents the damper force component in the external factor matrix, is equal to zero. Therefore, the only component of the external factor is the earthquake acceleration $\ddot{X}_g$.

In this system

f_d=0, U= $\ddot{X}_g$

$$Y = \begin{bmatrix}y_1\\ y_2\\ y_3\end{bmatrix} = \begin{bmatrix}X\\ \dot{X}\\ \ddot{X}\end{bmatrix} = \begin{bmatrix} q_1 \\ q_2 \\ -M^{-1} C\ q_2 - M^{-1}\ k_s q_1 - u\end{bmatrix} \quad \textbf{(4-11)}$$

Then:

$$Y = \begin{bmatrix} 1 & 0 \\ 0 & 1 \\ - M^{-1}\ k_s & -M^{-1} C\end{bmatrix} \begin{bmatrix}q_1\\ q_2\end{bmatrix} + \begin{bmatrix}0\\ 0\\ -1\end{bmatrix}\ u \quad \textbf{(4-12)}$$

4-2-1-3- State-space equation of the system improved with MR damper:

In the following the state-space equation of the system with the damper is illustrated. In this system the external factor matrix U consists of the components f_d and $\ddot{X}_g$ that present the damper force and earthquake acceleration, respectively.

In this system:

$$U = \begin{bmatrix} \ddot{X}_g \\ f_d \end{bmatrix} \quad \textbf{(4-13)}$$

$$q = \begin{bmatrix} q_1 \\ q_2 \end{bmatrix} = \begin{bmatrix} X \\ \dot{X} \end{bmatrix} \quad \textbf{(4-14)}$$

$$\dot{q} = \begin{bmatrix} \dot{q}_1 \\ \dot{q}_2 \end{bmatrix} = \begin{bmatrix} \dot{X} \\ \ddot{X} \end{bmatrix} = \begin{bmatrix} q_2 \\ \ddot{X} \end{bmatrix} = \begin{bmatrix} q_2 \\ -M^{-1}C\, q_2 - M^{-1} k_s q_1 - M^{-1} f_d - \ddot{X}_g \end{bmatrix} \quad \textbf{(4-15)}$$

Which results:

$$\dot{q} = \begin{bmatrix} q_2 \\ -M^{-1}C\, q_2 - M^{-1} k_s q_1 \end{bmatrix} + \begin{bmatrix} 0 \\ -M^{-1} f_d - \ddot{X}_g \end{bmatrix} \quad \textbf{(4-16)}$$

The equation is rewritten as:

$$\dot{q} = \begin{bmatrix} 0 & 1 \\ -M^{-1} k_s & -M^{-1}C \end{bmatrix} \begin{bmatrix} q_1 \\ q_2 \end{bmatrix} + \begin{bmatrix} 0 \\ -M^{-1} f_d - \ddot{X}_g \end{bmatrix} \quad \textbf{(4-17)}$$

Then:

$$\dot{q} = \begin{bmatrix} 0 * q_1 + q_2 \\ -M^{-1}C\, q_2 - M^{-1} k_s q_1 \end{bmatrix} + \begin{bmatrix} 0 & 0 \\ -1 & -M^{-1} \end{bmatrix} \begin{bmatrix} \ddot{X}_g \\ f_d \end{bmatrix} \quad \textbf{(4-18)}$$

The equation is simplified as:

$$\dot{q} = \begin{bmatrix} 0 & 1 \\ -M^{-1} k_s & -M^{-1}C \end{bmatrix} \begin{bmatrix} q_1 \\ q_2 \end{bmatrix} + \begin{bmatrix} 0 & 0 \\ -1 & -M^{-1} \end{bmatrix} \begin{bmatrix} \ddot{X}_g \\ f_d \end{bmatrix} \quad \textbf{(4-19)}$$

The output is :

$$Y = \begin{bmatrix} y_1 \\ y_2 \\ y_3 \end{bmatrix} = \begin{bmatrix} X \\ \dot{X} \\ \ddot{X} \end{bmatrix} = \begin{bmatrix} q_1 \\ q_2 \\ -M^{-1} k_s q_1 - M^{-1}C\, q_2 - M^{-1} f_d - \ddot{X}_g \end{bmatrix} \quad \textbf{(4-20)}$$

4-3- Selected ground motion records

In this research the seismic response of the modeled structure with the damper and without the damper, exposed to two major types of earthquakes, far-field and near-field pulse-like with different characteristic, are investigated.

The characteristics of the far-field earthquakes are well known, therefore in most seismic and hazard assessments such as collapse assessment these types of earthquakes are utilized as the main records, while the near-field earthquake records are used as the supplemental records due to the lack of sufficient information about their characteristics (FEMA 2009). The near-field earthquakes are divided to two sub sets which are named pulse-like and non-pulse-like categories.

The pulse-like ground motion may be caused by a fault rupturing whereby, the ground motion has more critical effects in the direction of rupture than the other directions on the site; this phenomenon is called “Directivity Effect” (Somerville et al. 1997, Baker 2007).

The Northridge 1994 strong earthquake is the example of an earthquake that indicated the directivity effect. Such pulse-like earthquakes which are contained of strong velocity pulses (Baker 2007), may cause severe seismic demands that are not completely predictable by usual measures such as using response spectra (Bertero et al. 1978, Baker 2007). Therefore, the investigation of the effects of such ground motions is a step forward to help the researchers knowing the characteristic of such earthquakes. In this research, two sets of far-field and near-field (pulse-like) earthquakes are applied to the modeled structure. Then, considering the performance of the fuzzy controlled MR damper, the seismic response of the modeled structure with and without the damper in terms of displacement, acceleration, velocity and energy is compared. In the selection of these two sets of earthquake records, some technical criterion as are mentioned in the following are concerned.

4-3-1- Far-Field earthquakes

By considering the information and concepts provided by the provision “FEMA P695”, a set of 44 earthquake records, are applied to the case study. The selected ground motions include 22 record pairs from sites located greater than or equal to 10 km from fault rupture, referred to as the “Far-Field” record set. These record sets include twenty-two records (44 individual components) selected from the “PEER NGA” database.

For each record, Table 4-1 summarizes the magnitude, year, and name of the event, as well as the name and owner of the station. The twenty-two records are chosen from 14 earthquakes that

happened between the year 1971 and 1999. Of the 14 earthquakes, eight took place in California earthquakes and the other six in five different foreign countries. Event magnitudes range from M6.5 to M7.6 with an average magnitude of M =7.0 for the Far-Field record set (FEMA 2009).

Table 4-1 The magnitude, year, name of the event, as well as the name of the station of 22 far-field record pairs suggested in FEMA P695 (FEMA 2009, PEER https://ngawest2.berkeley.edu, June 2018).

ID No.	PEER-NGA Record Information				Recorded Motions	
	Record	Lowest	File Names - Horizontal Records		*PGA Max*	*PGV Max*
	Seq. No.	Freq (Hz.)	Component 1	Component 2	*(g)*	(cm/s)
1	953	0.25	NORTHR/MUL009	NORTHR/MUL279	0.52	63
2	960	0.13	NORTHR/LOS000	NORTHR/LOS270	0.48	45
3	1602	0.06	DUZCE/BOL000	DUZCE/BOL090	0.82	62
4	1787	0.04	HECTOR/HEC000	HECTOR/HEC090	0.34	42
5	169	0.06	IMPVALL/H-DLT262	IMPVALL/H-DLT352	0.35	33
6	174	0.25	IMPVALL/H-E11140	IMPVALL/H-E11230	0.38	42
7	1111	0.13	KOBE/NIS000	KOBE/NIS090	0.51	37
8	1116	0.13	KOBE/SHI000	KOBE/SHI090	0.24	38
9	1158	0.24	KOCAELI/DZC180	KOCAELI/DZC270	0.36	59
10	1148	0.09	KOCAELI/ARC000	KOCAELI/ARC090	0.22	40
11	900	0.07	LANDERS/YER270	LANDERS/YER360	0.24	52
12	848	0.13	LANDERS/CLW-LN	LANDERS/CLW-TR	0.42	42
13	752	0.13	LOMAP/CAP000	LOMAP/CAP090	0.53	35
14	767	0.13	LOMAP/G03000	LOMAP/G03090	0.56	45
15	1633	0.13	MANJIL/ABBAR--L	MANJIL/ABBAR--T	0.51	54
16	721	0.13	SUPERST/B-ICC000	SUPERST/B-ICC090	0.36	46
17	725	0.25	SUPERST/B-POE270	SUPERST/B-POE360	0.45	36
18	829	0.07	CAPEMEND/RIO270	CAPEMEND/RIO360	0.55	44
19	1244	0.05	CHICHI/CHY101-E	CHICHI/CHY101-N	0.44	115
20	1485	0.05	CHICHI/TCU045-E	CHICHI/TCU045-N	0.51	39
21	68	0.25	SFERN/PEL090	SFERN/PEL180	0.21	19
22	125	0.13	FRIULI/A-TMZ000	FRIULI/A-TMZ270	0.35	31

4-3-2- Near-Field pulse-like earthquakes

In the second part of the analysis in this research, a set of 91 pulse-like earthquake records which are selected by Baker Research Group are applied to the modeled structures (Table 4-2).
Since the near-field pulse-like earthquakes include a strong velocity pulse and are able to critically affect the seismic demands of structures (Baker 2007), a part of this research is assigned to investigate the effects of such earthquakes on the performance of the controllable adaptive MR damper. These records are chosen based on wavelet analysis considering the following factors:

Peak Ground velocity (PGV):

Peak Ground velocity of the records should be equal or greater than 30 cm/s because the records with the PGV of less than this threshold have a low amplitude. Therefore they are not able to damage the conventional structures (Baker 2007).

Cumulative squared velocity $\mathbf{CSV(t)}$:

The seismologists believe that in a near-field earthquakes including pulse–like earthquake, if the pulses arrives early, they are likely to be caused by the directivity effect (Baker 2007). The cumulative squared velocity $CSV(t)$ is a factor that is utilized to separate the pulse-like records than the other type of ground motions.

$$CSV(t) = \int_0^t v^2(u)du \qquad \textbf{(4-21)}$$

Where, $v(u)$ is the velocity of the earthquake wave.

In pulse-like nearfield earthquakes the $CSV(t)$ of $t_{10\%,pulse}$ is bigger than $CSV(t)$ of $t_{20\%,original}$.

Pulse indicator value (PI):

This factor is another filter that can select the ground motion records of pulse-like earthquakes, this factor ranges between 0 and 1. The records that have pulse indicator bigger than 0.85 are pulse-like and the ones whose their pulse indicator is smaller than 0.15 are non-pulse-like waves (Baker 2007).

$$\text{PI}=\frac{1}{1+e^{-23.3+14.6(PGV\ ratio)+20.5(energy\ ratio)}} \qquad \textbf{(4-22)}$$

where:

$$PGV\ ratio = \frac{PGV\ residual\ Wave}{PGV\ Original\ Wave} \quad \textbf{(4-23)}$$

$$energy\ ratio = \frac{CSV(t)\ residual\ Wave}{CSV(t) Original\ Wave} \quad \textbf{(4-24)}$$

It should be noticed that in the wavelet technique, by excluding the pulse component, the remaining component is a residual signal. In Figure 4-2 the near–field pulse-like velocity record of Imperial Valley earthquake and its pulse and residual components of are illustrated, respectively.

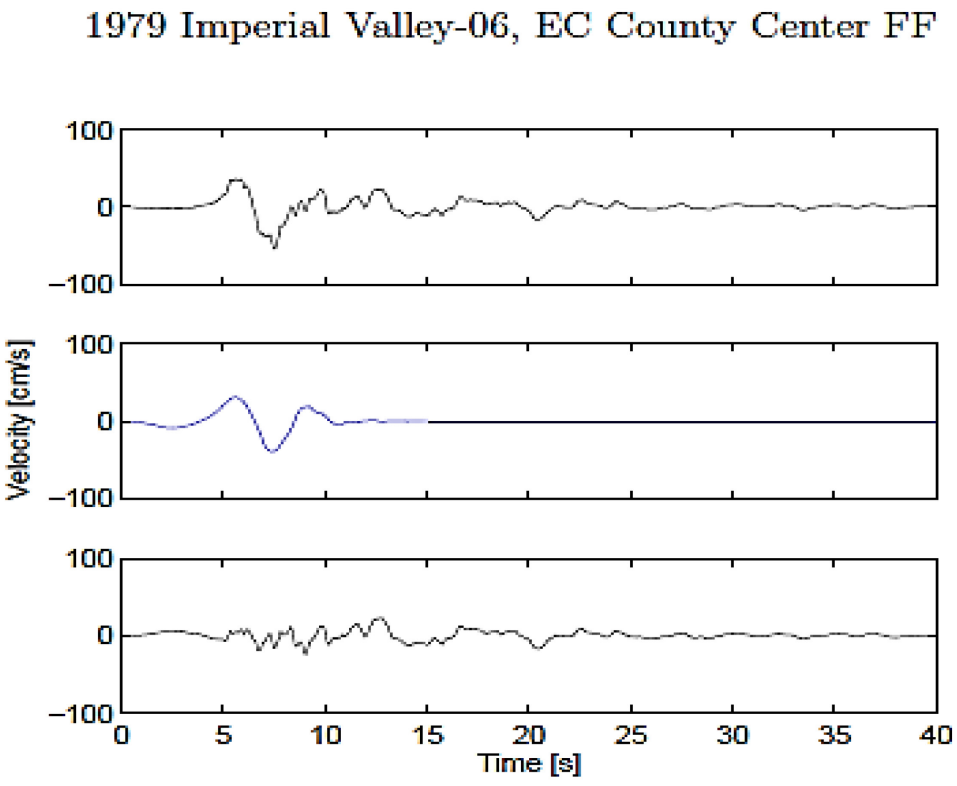

Figure 4-2: Illustration of the pulse portion of a ground motion (the fault-normal component of the 1979 Imperial Valley) extracted by decomposition procedure (Baker 2007)

Table 4-2 The magnitude, year, and name of the event, as well as the name and owner of the station of 91 near-field pulse-like records suggested by Baker Reserch Group(Baker 2007, PEER https://ngawest2.berkeley.edu, June 2018)

ID No.	Event	Year	Station	PGV (cm/s)	Mw	Closest D (Km)	Epi.D (Km)
1	San Fernando	1971	Pacoima Dam (upper left abut)	116.4756	6.61	1.81	11.86
2	Coyote Lake	1979	Gilroy Array #6	51.54825	5.74	3.11	4.37
3	Imperial Valley-06	1979	Aeropuerto Mexicali	44.32454	6.53	0.34	2.47
4	Imperial Valley-06	1979	Agrarias	54.38436	6.53	0.65	2.62
5	Imperial Valley-06	1979	Brawley Airport	36.11781	6.53	10.42	43.15
6	Imperial Valley-06	1979	EC County Center FF	54.48569	6.53	7.31	29.07
7	Imperial Valley-06	1979	EC Meloland Overpass FF	115.0394	6.53	0.07	19.44
8	Imperial Valley-06	1979	El Centro Array #10	46.92101	6.53	6.17	26.31
9	Imperial Valley-06	1979	El Centro Array #11	41.10419	6.53	12.45	29.44
10	Imperial Valley-06	1979	El Centro Array #3	41.10381	6.53	12.85	28.65
11	Imperial Valley-06	1979	El Centro Array #4	77.92506	6.53	7.05	27.13
12	Imperial Valley-06	1979	El Centro Array #5	91.48135	6.53	3.95	27.8
13	Imperial Valley-06	1979	El Centro Array #6	111.8723	6.53	1.35	27.47
14	Imperial Valley-06	1979	El Centro Array #7	108.8192	6.53	0.56	27.64
15	Imperial Valley-06	1979	El Centro Array #8	48.55419	6.53	3.86	28.09
16	Imperial Valley-06	1979	El Centro Differential Array	59.60526	6.53	5.09	27.23
17	Imperial Valley-06	1979	Holtville Post Office	55.14696	6.53	7.65	19.81
18	Mammoth Lakes-06	1980	Long Valley Dam (Upr L Abut)	33.09608	5.94	n/a	14.04
19	Irpinia, Italy-01	1980	Sturno	41.49513	6.9	10.84	30.35
20	Westmorland	1981	Parachute Test Site	35.84779	5.9	16.66	20.47
21	Coalinga-05	1983	Oil City	41.19912	5.77	n/a	4.6
22	Coalinga-05	1983	Transmitter Hill	46.05597	5.77	n/a	5.99
23	Coalinga-07	1983	Coalinga-14th & Elm (Old CHP)	36.12878	5.21	n/a	9.57
24	Morgan Hill	1984	Coyote Lake Dam (SW Abut)	62.3035	6.19	0.53	24.55
25	Morgan Hill	1984	Gilroy Array #6	35.3851	6.19	9.86	36.34
26	Taiwan SMART1(40)	1986	SMART1 C00	31.20015	6.32	n/a	68.18
27	Taiwan SMART1(40)	1986	SMART1 M07	36.11846	6.32	n/a	67.16
28	N. Palm Springs	1986	North Palm Springs	73.63034	6.06	4.04	10.57
29	San Salvador	1986	Geotech Investig Center	62.25574	5.8	6.3	7.93
30	Whittier Narrows-01	1987	Downey - Co Maint Bldg	30.40388	5.99	20.82	16.04

ID No.	Event	Year	Station	PGV	Mw	Closest D (Km)	Epi. D (Km)
31	Whittier Narrows-01	1987	LB - Orange Ave	32.88396	5.99	24.54	20.68
32	Superstition Hills-02	1987	Parachute Test Site	106.7548	6.54	0.95	15.99
33	Loma Prieta	1989	Alameda Naval Air Stn Hanger	32.15925	6.93	71	90.77
34	Loma Prieta	1989	Gilroy Array #2	45.67426	6.93	11.07	29.77
35	Loma Prieta	1989	Oakland - Outer Harbor Wharf	49.20977	6.93	74.26	94
36	Loma Prieta	1989	Saratoga - Aloha Ave	55.58054	6.93	8.5	27.23
37	Erzincan, Turkey	1992	Erzincan	95.41539	6.69	4.38	8.97
38	Cape Mendocino	1992	Petrolia	82.10093	7.01	8.18	4.51
39	Landers	1992	Barstow	30.41219	7.28	34.86	94.77
40	Landers	1992	Lucerne	140.2697	7.28	2.19	44.02
41	Landers	1992	Yermo Fire Station	53.22633	7.28	23.62	85.99
42	Northridge-01	1994	Jensen Filter Plant	67.42525	6.69	5.43	12.97
43	Northridge-01	1994	Jensen Filter Plant Generator	67.37772	6.69	5.43	13
44	Northridge-01	1994	LA - Wadsworth VA Hospital North	32.38256	6.69	23.6	19.55
45	Northridge-01	1994	LA Dam	77.10767	6.69	5.92	11.79
46	Northridge-01	1994	Newhall - W Pico Canyon Rd.	87.75178	6.69	5.48	21.55
47	Northridge-01	1994	Pacoima Dam (downstr)	50.39736	6.69	7.01	20.36
48	Northridge-01	1994	Pacoima Dam (upper left)	107.0704	6.69	7.01	20.36
49	Northridge-01	1994	Rinaldi Receiving Sta	167.2024	6.69	6.5	10.91
50	Northridge-01	1994	Sylmar - Converter Sta	130.2724	6.69	5.35	13.11
51	Northridge-01	1994	Sylmar - Converter Sta East	116.564	6.69	5.19	13.6
52	Northridge-01	1994	Sylmar - Olive View Med FF	122.7227	6.69	5.3	16.77
53	Kobe, Japan	1995	Takarazuka	72.6463	6.9	0.27	38.6
54	Kobe, Japan	1995	Takatori	169.606	6.9	1.47	13.12
55	Kocaeli, Turkey	1999	Gebze	51.9609	7.51	10.92	47.03
56	Chi-Chi, Taiwan	1999	CHY006	64.71363	7.62	9.77	40.47
57	Chi-Chi, Taiwan	1999	CHY035	42.04828	7.62	12.65	43.9
58	Chi-Chi, Taiwan	1999	CHY101	85.44828	7.62	9.96	31.96
59	Chi-Chi, Taiwan	1999	TAP003	33.02368	7.62	102.39	151.65
60	Chi-Chi, Taiwan	1999	TCU029	62.34353	7.62	28.05	79.2

ID No.	Event	Year	Station	PGV (cm/s)	Mw	Closest D (Km)	Epi. D (Km)
61	Chi-Chi, Taiwan	1999	TCU031	59.86109	7.62	30.18	80.09
62	Chi-Chi, Taiwan	1999	TCU034	42.76516	7.62	35.69	87.88
63	Chi-Chi, Taiwan	1999	TCU036	62.42965	7.62	19.84	67.81
64	Chi-Chi, Taiwan	1999	TCU038	50.85595	7.62	25.44	73.11
65	Chi-Chi, Taiwan	1999	TCU040	52.99257	7.62	22.08	69.04
66	Chi-Chi, Taiwan	1999	TCU042	47.34435	7.62	26.32	78.37
67	Chi-Chi, Taiwan	1999	TCU046	43.95766	7.62	16.74	68.89
68	Chi-Chi, Taiwan	1999	TCU049	44.81769	7.62	3.78	38.91
69	Chi-Chi, Taiwan	1999	TCU053	41.89629	7.62	5.97	41.2
70	Chi-Chi, Taiwan	1999	TCU054	60.91842	7.62	5.3	37.64
71	Chi-Chi, Taiwan	1999	TCU056	43.53243	7.62	10.5	39.73
72	Chi-Chi, Taiwan	1999	TCU060	33.69667	7.62	8.53	45.37
73	Chi-Chi, Taiwan	1999	TCU065	127.6757	7.62	0.59	26.67
74	Chi-Chi, Taiwan	1999	TCU068	191.149	7.62	0.32	47.86
75	Chi-Chi, Taiwan	1999	TCU075	88.4351	7.62	0.91	20.67
76	Chi-Chi, Taiwan	1999	TCU076	63.73335	7.62	2.76	16.03
77	Chi-Chi, Taiwan	1999	TCU082	56.11555	7.62	5.18	36.2
78	Chi-Chi, Taiwan	1999	TCU087	53.66615	7.62	7	55.64
79	Chi-Chi, Taiwan	1999	TCU098	32.74007	7.62	47.67	99.73
80	Chi-Chi, Taiwan	1999	TCU101	68.39302	7.62	2.13	45.05
81	Chi-Chi, Taiwan	1999	TCU102	106.5746	7.62	1.51	45.56
82	Chi-Chi, Taiwan	1999	TCU103	62.17803	7.62	6.1	52.43
83	Chi-Chi, Taiwan	1999	TCU104	31.4297	7.62	12.89	49.28
84	Chi-Chi, Taiwan	1999	TCU128	78.66183	7.62	13.15	63.29
85	Chi-Chi, Taiwan	1999	TCU136	51.81756	7.62	8.29	48.75
86	Northwest China-03	1997	Jiashi	36.99188	6.1	n/a	19.11
87	Yountville	2000	Napa Fire Station #3	42.953	5	n/a	9.89
88	Chi-Chi, Taiwan-03	1999	CHY024	33.09321	6.2	19.65	25.52
89	Chi-Chi, Taiwan-03	1999	CHY080	69.93326	6.2	22.37	29.48
90	Chi-Chi, Taiwan-03	1999	TCU076	59.35209	6.2	14.66	20.8
91	Chi-Chi, Taiwan-06	1999	CHY101	36.25917	6.3	35.97	49.98

4-4- The proposed fuzzy control system:

In MR dampers, the relation between the driven current and the produced resistant force is non-linear. Therefore, by adding the MR damper on the modeled structure the whole system becomes nonlinear. In addition, by applying seismic loads to this dynamic system, it becomes more complicated. To control such non-linear complicated system making the damper behave in an efficient way and improve the seismic response of the modeled structure, a control system based on Mamdani fuzzy technique is used in the model.

In this proposed fuzzy control system, the displacement of the modeled structure is converted to fuzzy sets through the fuzzification process; and then in fuzzy inference system processes the fuzzified displacement values to determine the fuzzy output based on a set of fuzzy rules that are built upon expert's knowledge. Finally, the fuzzy output is converted to crisp values via defuzzification process. Using centroid defuzzification method, the crisp output is calculated from the weighted average of all fuzzy rules involved in finding the fuzzy output. The defuzzified output is the magnitude of the electrical current used for driving the MR damper to produce the resistant force (Lilly 2011, Nise 2011). It means that the fuzzy controller receives the displacement of the structure as a feedback of the system in very short intervals (0.1 μs), and based on the feedback, it adjusts the performance of the system continuously. This closed-loop process is demonstrated in the following block diagram (Figure 4-3).

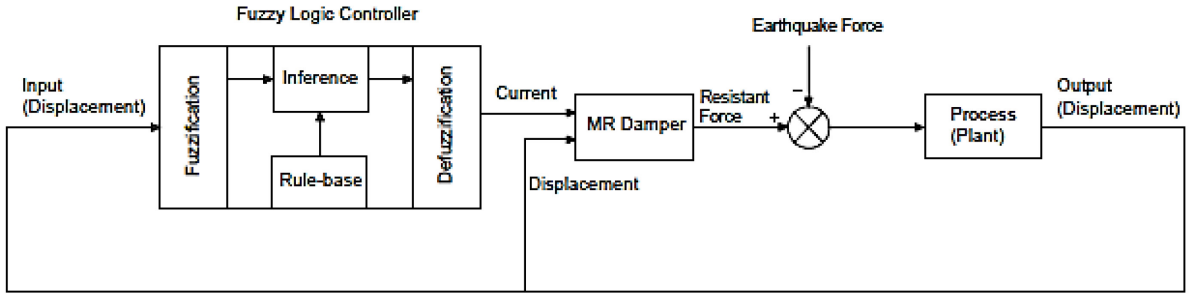

Figure 4-3: Block diagram of the closed – loop system with fuzzy control

4-4-1- Fuzzy sets and Membership functions:

In this part, the different stages of the fuzzy systems including fuzzification, inference and defuzzification for the used Mamdani system are discussed.

4-4-1-1- Fuzzification stage of the proposed Mamdani fuzzy control unit:

In the first part of the analysis as mentioned before, two sets of earthquake records including 44 far-field and 91 near-field pulse-like earthquake records are applied to the structure with the damper. The input displacement data are transferred to the fuzzy control system and in the fuzzification stage, the controller converts the data to fuzzy sets. In this way, as the average of maximum displacement of the structure for these two sets of earthquake records are calculated to be about 0.35 m and 0.31 m, respectively. The average maximum displacement is rounded to 0.04 m and the effective universe of discourse for the variable displacement is defined between 0 and 0.04 m.

By considering equal bases, two fuzzy sets with a trapezoidal–shaped membership function and five fuzzy sets with a triangular-shaped membership function for displacements are identified; it also should also be noted that the displacements bigger than 0.04 m are covered with the seventh set (Figure 4-4). Then these fuzzy sets which are defined below are sent to the inference stage.

i) mf1 (0-0.001) m

ii) mf2 (0.005-0.015) m

iii) mf3 (0.01-0.02) m

iv) mf4 (0.015-0.25) m

v) mf5 (0.02-0.03) m

vi) mf6 (0.025-0.035) m

vii) mf7 (0.03-0.04) and displacement >0.04 m

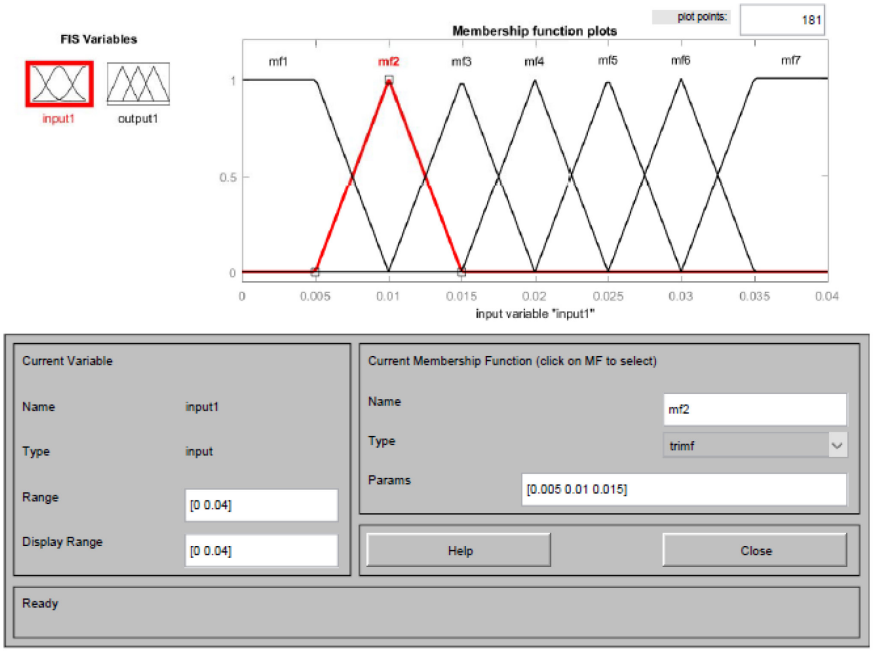

Figure 4-4: The defined input membership functions (Displacement) in MATLAB software

4-4-1-2- Inference stage of the proposed Mamdani fuzzy control unit:

In this stage regarding the technical properties of the utilized 200KN Rheonetic MRD-900(LORD) MR damper, the effective universe of discourse for the variable driven electricity current to the damper, is defined between 0 and 2.4 ampere (A).

By dividing the range to four equal subranges with the same base four fuzzy sets (Figure 4-5) with a triangular-shaped membership function for the electricity current are identified as below:

i) current 1 (0-0.6) A

ii) current 2 (0.3-0.9) A

iii) current 3 (0.6-1.2) A

iv) current 4 (0.9-1.5) A

v) current 5 (1.2-1.8) A

vi) current 6 (1.5-2.1) A

vii) current 7 (2.1-2.4) A

The fuzzy sets for currents in addition to all the defined rule base including seven rules as follows are sent to the next stage which is defuzzification stage.

i) If input displacement is mf1 then output current 1.

ii) If input displacement is mf2 then output current 2.

iii) If input displacement is mf3 then output current 3.

iv) If input displacement is mf4 then output current 4.

v) If input displacement is mf5 then output current 5.

vi) If input displacement is mf6 then output current 6.

vii) If input displacement is mf7 then output current 7.

These rules are defined based on the magnitude of the displacements and their distribution.

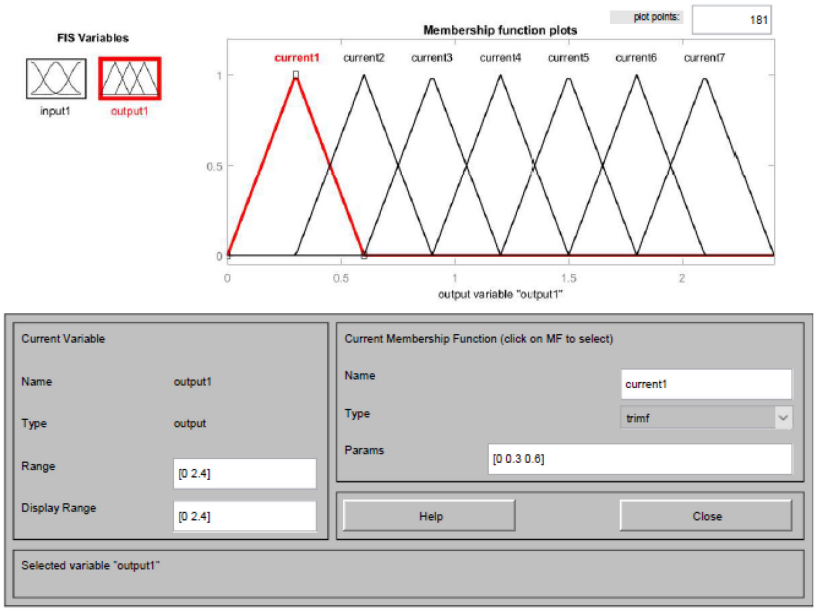

Figure 4-5: The defined output membership functions (Current) in MATLAB software

4-4-1-3- Defuzzification stage of the proposed Mamdani fuzzy control unit:

In this stage the collection of the recommended rules and membership functions of the driven currents are combined by taking the weighted average of them with the center of gravity method (COG) and the final output is the driven electricity current to the damper.

This process is done in a closed-loop in the very minute intervals equal to 0.1 μs continuously during the earthquake, monitoring the displacement of the system and adjusting the driven electricity current to apply proper resistant force and reduce the displacement of the structure efficiently. In this controller, in order to decrease the time of magnetic induction in damper and prevent the structure to be shocked by the applied earthquakes another rule is added to the control system. This rule is that, as soon as the earthquake starts, the controller drives a minimum of 0.3 A current to the damper to set the damper and prevent structure from immediate shocks and high displacements. Furthermore, this initial current minimizes the response time of the damper which is due to the response time of the MR fluid inside the damper to the induced magnetic field and this helps the damper to reach its required performance quickly.

4-4-2- Modelling of the system with software:

In this research all the modeling of the systems is designed and simulated by MATLAB and Simulink software. Simulink software has powerful toolbox and block library and can accurately simulate and analyze a dynamic variable model, in addition, MATLAB software, which is one of the most powerful software in engineering, is well adapted and compatible with Simulink software and these two software can interact and work together very well. They can easily display and illustrate the input and output data in the form of different types of graphs with a wide variety of styles and colors, the analytical results can be visually identified and compared very well.

In this research the structure is modeled by MATLAB software where its properties such as stiffness, mass, and damping are defined with the MATLAB codes in the form of matrices. The MR damper is modeled in a closed loop subsystem based on the Spencer (modified Bouc-Wen) model utilizing the Simulink library blocks which are connected by logical paths. Then this subsystem is added to a collection of Simulink library block connected by logical paths in a closed loop to form the whole dynamic system including a damper, structure and the external excitation. This system is designed in a way to simultaneously give the seismic response of the structure with and without damper. In this case the external excitation factor is the earthquake acceleration records applied to the system.

The earthquakes are inputted from text files which are connected to the Simulink software using MATLAB Software. In order to get the accurate results and monitor the performance of the system continually, the system is designed to work based on Runge-Kutta numerical method with the fixed steps of very high precision of 0.0001, that can cover all the steps of the earthquake records available in the PEER database. The Figure 4-6 and Figure 4-7 illustrate the Simulink models of

the whole system and the subsystem representing the simulated MR damper, respectively. The different elements of the system are defined by the blocks of Simulink and these blocks are connected together by paths that form a closed loop.

The matrices of the properties of the system defined in MATLAB codes are linked to the Simulink program.

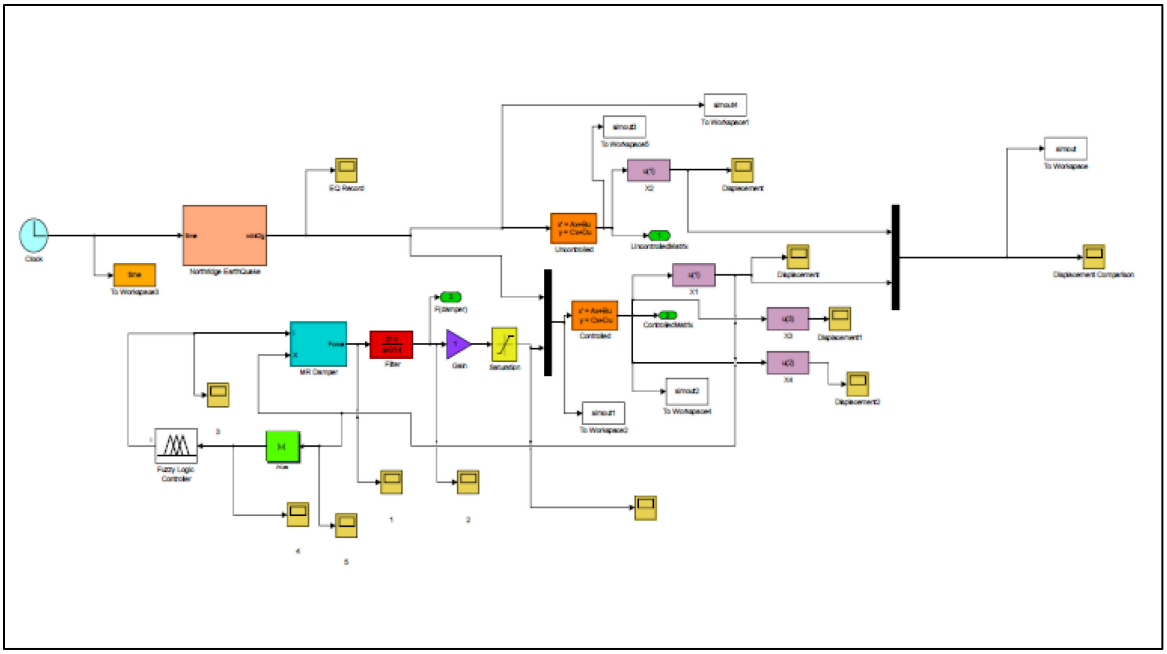

Figure 4-6: The Simulink Blocks of the Dynamic System including Fuzzy Control Unit and The MR Damper Subsystem

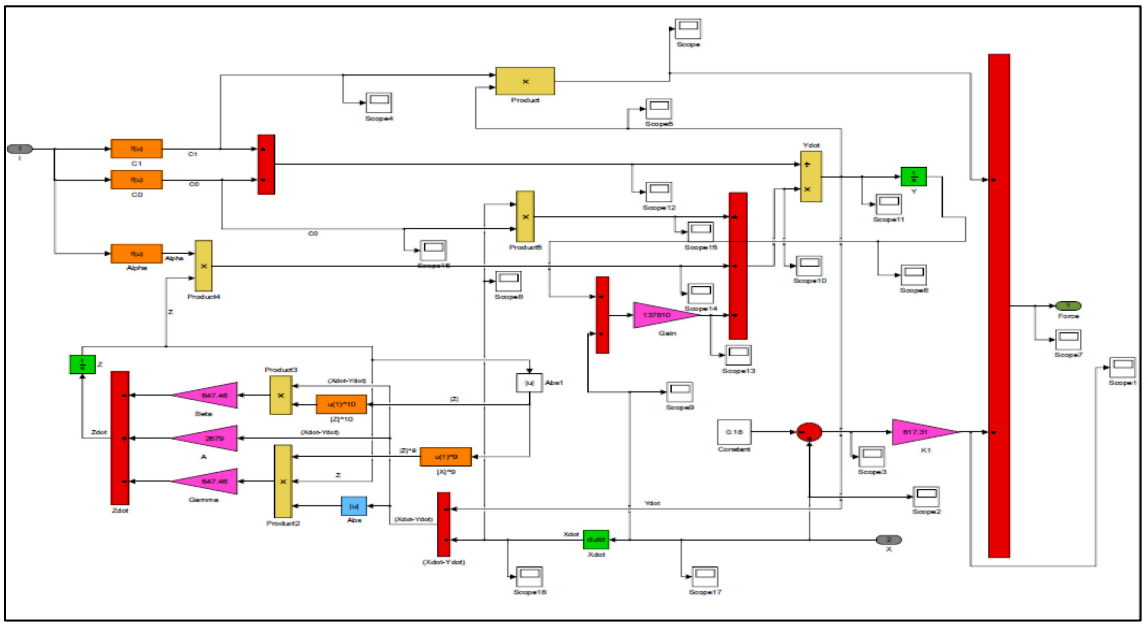

Figure 4-7: The Simulink Blocks of MR Damper (Villarreal et al. 2004)

4-5- Summary:

In this chapter the selected earthquakes including 44 far-field and 91 near-field pulse-like records are studied. A fuzzy control system based on Mamdani method is designed using MATLAB software. Then the dynamic system including the modeled structure, fuzzy control unit, MR damper and the applied earthquake loads were simulated by SIMULINK software.

In the next chapter the extracted analytical results which are the output of the simulation process will be discussed. The output data include the seismic response of the modeled structure with and without damper. Then the results will be compared to illustrate the efficiency of the fuzzy controlled MR damper.

Chapter 5

Analyses

To determine the performance of the proposed control system and illustrate the behavior of the modeled structure equipped with the MR damper against seismic loads, the analytical results of two far-field and two near-field pulse like earthquakes are shown and discussed. In the following, the different seismic demands of the structure including displacement, velocity and acceleration due to two 44 far-field and 91 near-field pulse like earthquakes in two conditions with the damper and without the damper are illustrated in the forms of graphs, bar charts and tables and the results are compared. Furthermore, the probability curve of the displacement for the two applied sets of far-field and near-field records are drawn. Moreover, as the final stage of the analyses, the efficiency of the designed fuzzy control is determined by comparing the performance of the damper adjusted by the proposed fuzzy control system and an on/off control system using the same amount of electricity.

5-1- Northridge 1994 (Far-Field Record):

This earthquake happened on January 17, 1994 with a moment magnitude of 6.7 in San Fernando Valley region of Los Angeles- the US. Figure 5-1 to Figure 5-4, indicate the seismic demands of the modeled structure subjected to the far-field record of this earthquake. From the graphs illustrated in Figure 5-1 to Figure 5-4 , it is observed that in the model equipped with the controllable MR damper, when the earthquake starts the fuzzy controller, based on the defined rules, applies a 0.3 A electricity current to the MR damper. It is observed that in the period between 4 and 9 s when the acceleration of the earthquake reaches to its highest magnitudes, and the damper applies larger magnitudes of the electric current to increase the damper force to control and reduce the increasing displacements, velocity and accelerations of the structure. The graphs show that as the earthquake continues, the acceleration of the earthquake reduces, and it causes smaller displacements in the structure. Therefore, the control unit decreases the driven current to 0.3 A, controlling the seismic demands of the structure up to the end of the earthquake.

The results in Table AI-3 to Table AI-5 , indicate that the vibration in the structure is dissipated and the maximum amounts of displacement, velocity and acceleration in the structure equipped with the controlled MR damper are about 37% ,40% and 37% smaller than the maximum seismic demands in the same structure without damper.

Furthermore, the seismic demand’s peaks of the structure with and without damper will occur in different times. It is demonstrated that the peaks corresponding to the same time of the maximum seismic demands (displacement, velocity and acceleration) of a system with the damper has been reduced by 50%, 55% and 43% respectively (Table AI-11 to Table AI-13).

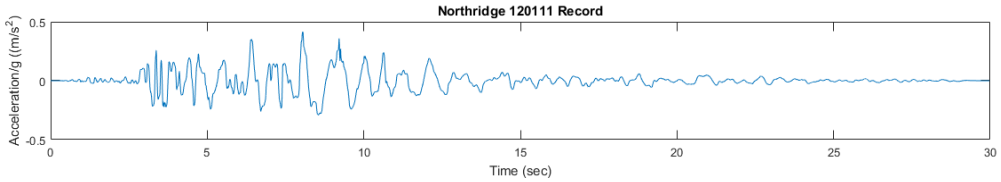

Figure 5-1: The acceleration record of Northridge (120111) 1994, far-field earthquake

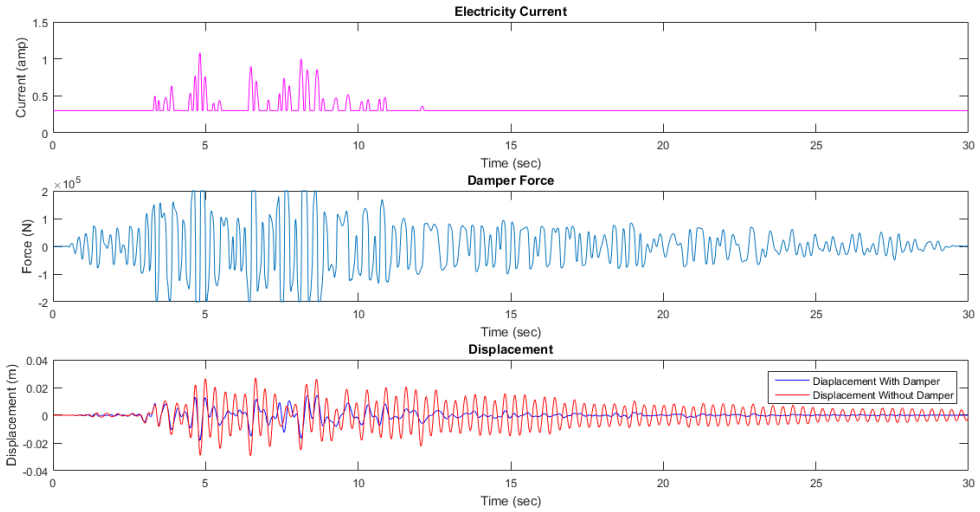

Figure 5-2: These graphs indicate the driven current to the damper by fuzzy controller, damper resistant force and the displacement of the modeled structure vs Time, subjected to Northridge (120111) 1994, far-field earthquake record

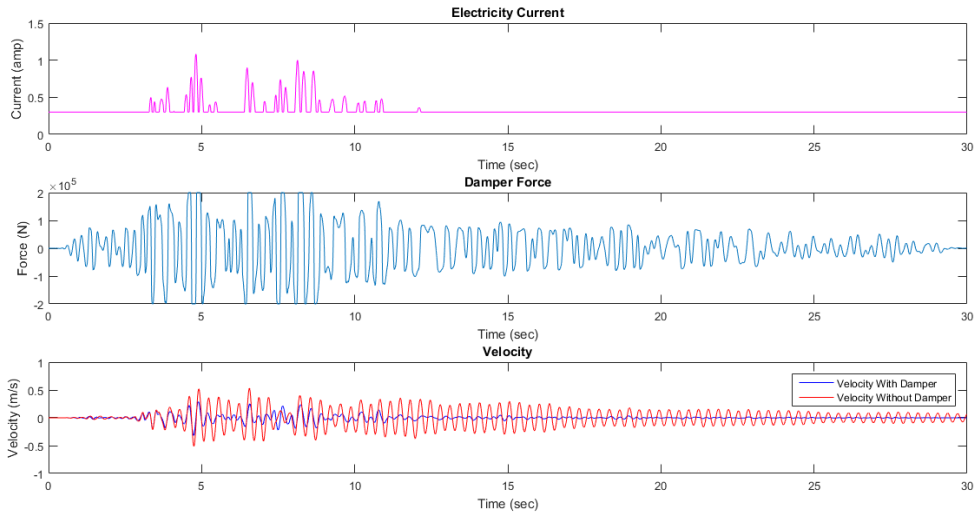

Figure 5-3: These graphs indicate the driven current to the damper by fuzzy controller, damper resistant force and the velocity of the modeled structure vs Time, subjected to Northridge (120111) 1994 ,far-field earthquake record

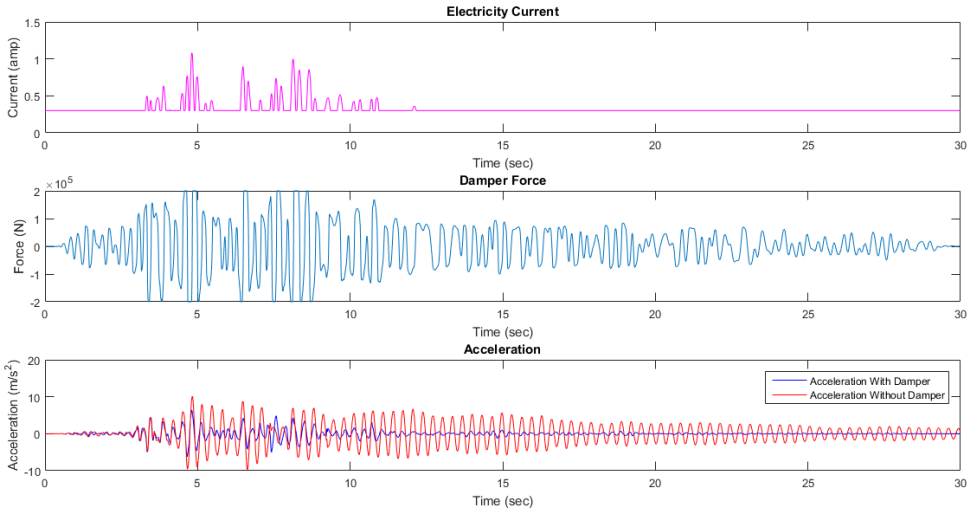

Figure 5-4: These graphs indicate the driven current to the damper by fuzzy controller, damper resistant force and the acceleration of the modeled structure vs Time, subjected to Northridge (120111) 1994 - far-field earthquake record

5-2- Manjil 1990 (Far-Field Record):

This earthquake happened on June 21 1990 in Rudbar and Manjil region in northern Iran and had a moment magnitude of 7.4 and prolonged 53.52 seconds. In the model the control unit has a similar performance to the above mentioned process and as it is shown in Figure 5-6 to Figure 5-8, in the seconds between 6 and 15, the fuzzy controller causes some jumps in the magnitude of the electricity current to make the damper produce a higher resistant force, adapted to the displacement of the structure. After this period the current levels out at 0.5A up to about the second 33 due to low amplitude of the ground motion. In the second 33 the magnitude of the ground motion increases; therefore, the fuzzy controller immediately increases the output electricity current to reduce the effects of the high acceleration. With the decrease in the earthquake acceleration, the controller decreases the current to 0.5A and keeps it stable up to the end when the displacement, velocity and acceleration are reduced efficiently.

The numerical analysis results in Table AI-3 to Table AI-5 indicate that by applying the far-field record of Manjil earthquake, the structure with the adaptive damper has the maximum amounts of displacement, velocity and acceleration of about 28%, 20% and 18% smaller than the maximum amount of the same seismic demands in the structure without the damper. As it is mentioned, the peaks of the structure with and without the damper will happen at different times. The results in Table AI-11 to Table AI-13, illustrate that the damper has decreased the peaks corresponding to

the same time of the maximum displacement, velocity and acceleration of the system without the damper by 31%,28% and 61% respectively.

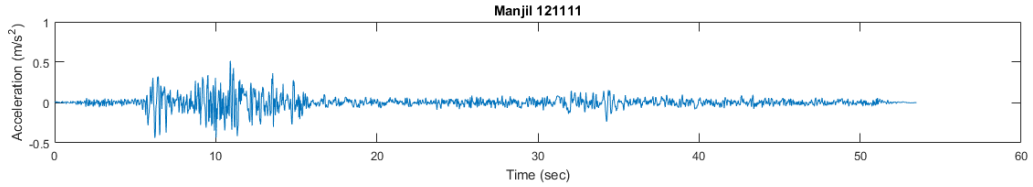

Figure 5-5: The acceleration record of Manjil (121111) 1994, far-field earthquake

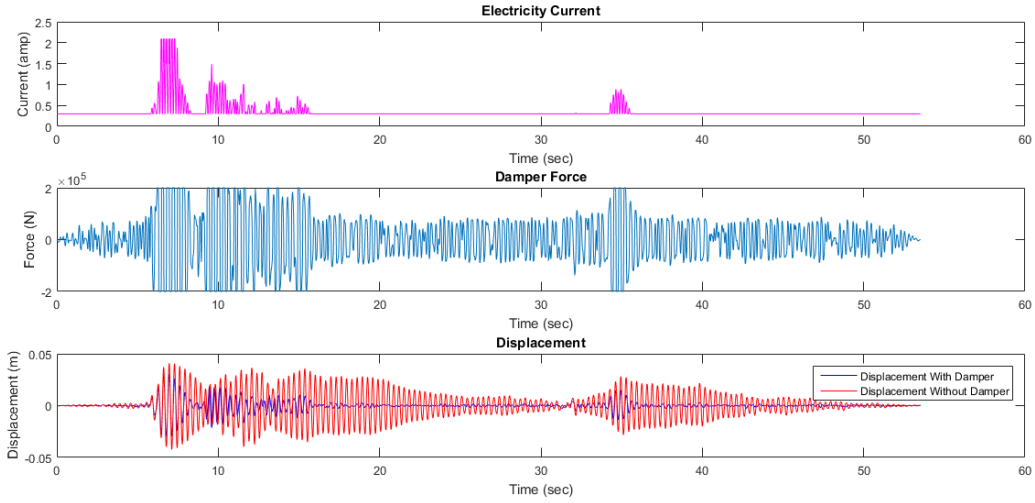

Figure 5-6: These graphs indicate the driven current to the damper by fuzzy controller, damper resistant force and the displacement of the modeled structure vs Time, subjected to Manjil (121111) 1990,far-field earthquake record

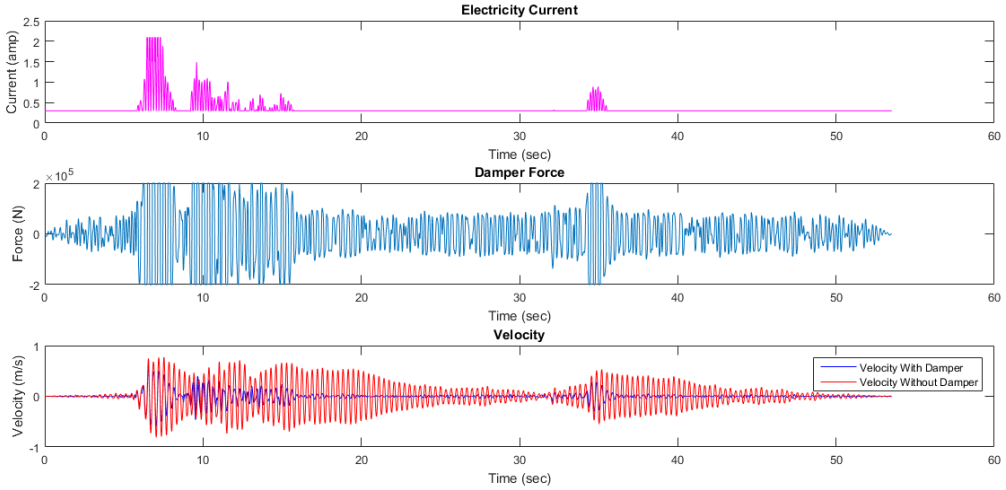

Figure 5-7: These graphs indicate the driven current to the damper by fuzzy controller, damper resistant force and the Velocity of the modeled structure vs Time, subjected to Manjil (121111) 1990, far-field earthquake record

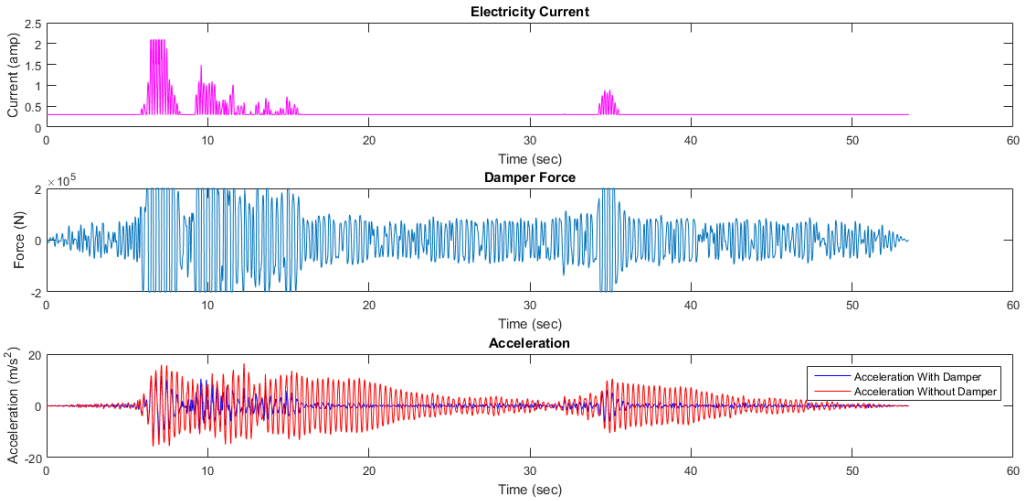

Figure 5-8: These graphs indicate the driven current to the damper by fuzzy controller, damper resistant force and the acceleration of the modeled structure vs Time, subjected to Manjil (121111) 1990, far-field earthquake record

5-3- Super Stition Hills –Parachute Test Site 1987 (Near-Field Pulse Like Record):

The earthquake occurred on November 24, 1987 with the moment magnitude of 6.5 and lasted about 22.3 seconds.

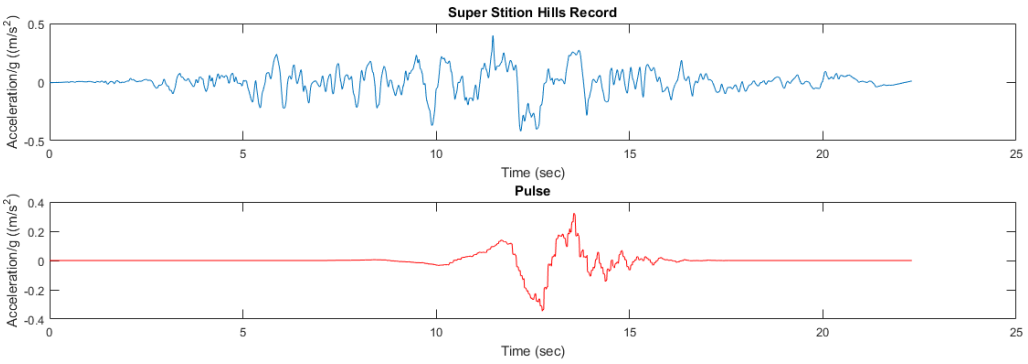

Figure 5-9: The graph up indicated the acceleration record of Super Stition Hills – Parachute Test Center 1997 earthquake and the graph below shows the acceleration record of its major pulse extracted by decomposition procedure

From the Figure 5-9 to Figure 5-12, it is observed that when the near-field pulse like earthquake record is applied to the structure, the fuzzy control unit function starts with driving a 0.3 A electricity current to the damper. The first significant jumps in the magnitude of the applied current to the

damper, occurred in steps between 6 and 8 seconds where the earthquake acceleration is moderately large. But the maximum increase in the current is observed in the steps approximately between the seconds 12 and 13, when the major pulse of this earthquake record happens. In the structure without the damper, the maximum displacement is produced in the pulse period in the second 12.59.

The results indicate the good performance of the fuzzy controller and the MR damper dissipating the effect of pulse in the structure. The analytical results in Table AI-7 to Table AI-9 confirm that the proposed fuzzy control unit can adjust the performance of the MR damper in such a way that the maximum of the displacement, velocity and acceleration of the modeled structure, subjected to this near-field earthquake record are about 33%, 46% and 50% smaller, comparing the highest amounts of displacement, velocity and acceleration in the structure without the damper. The results in Table AI-14 to Table AI-16, show that the damper has decreased the peaks corresponding to the same time of the maximum displacement, velocity and acceleration of the system without the damper by 42%, 65% and 74% respectively.

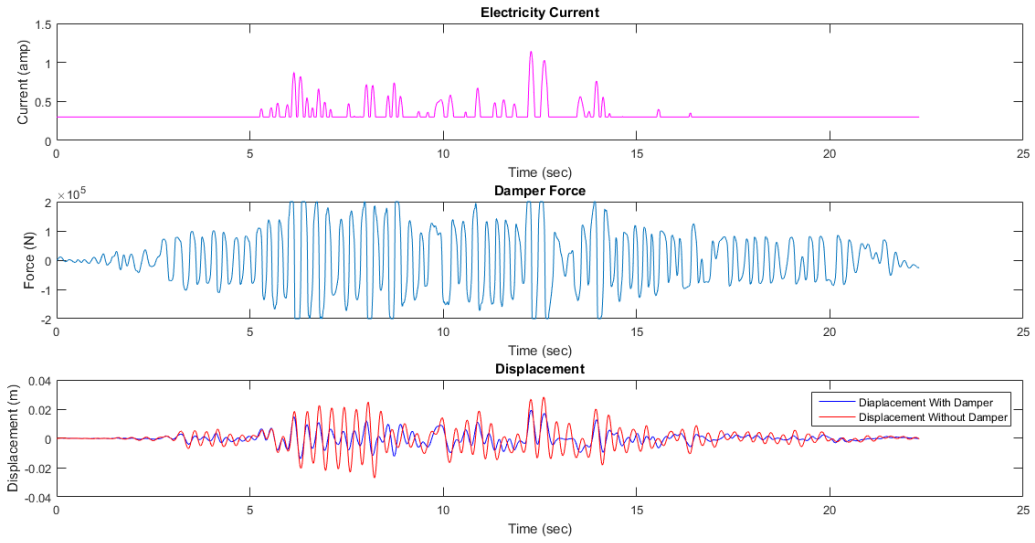

Figure 5-10: These graphs indicate the driven current to the damper by fuzzy controller, damper resistant force and the displacement of the modeled structure vs Time, subjected to Super Stition Hills-Parachute Test Site 1987,near-field earthquake record

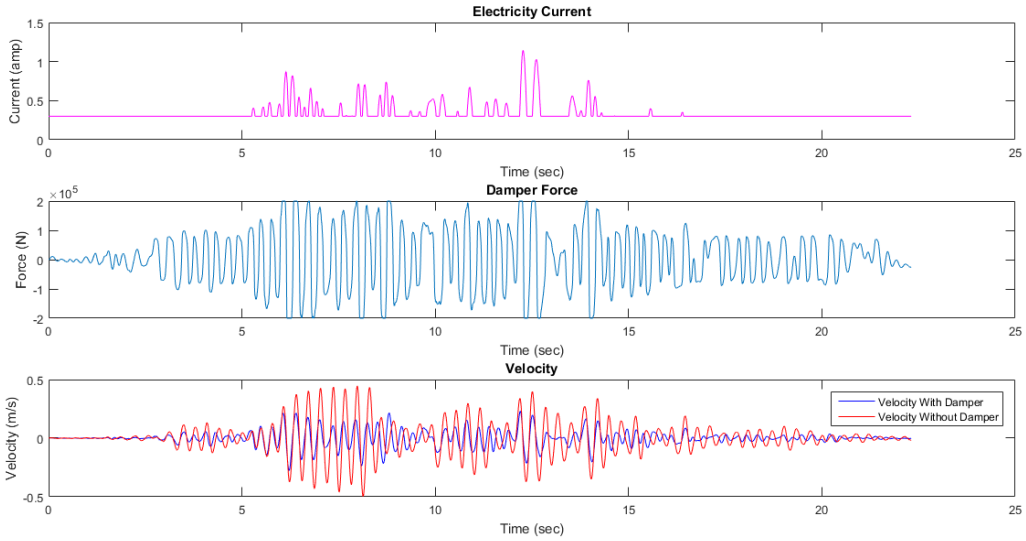

Figure 5-11: These graphs indicate the driven current to the damper by fuzzy controller, damper resistant force and the velocity of the modeled structure vs Time, subjected to Super Stition Hills-Parachute Test Site 1987, near-field earthquake record

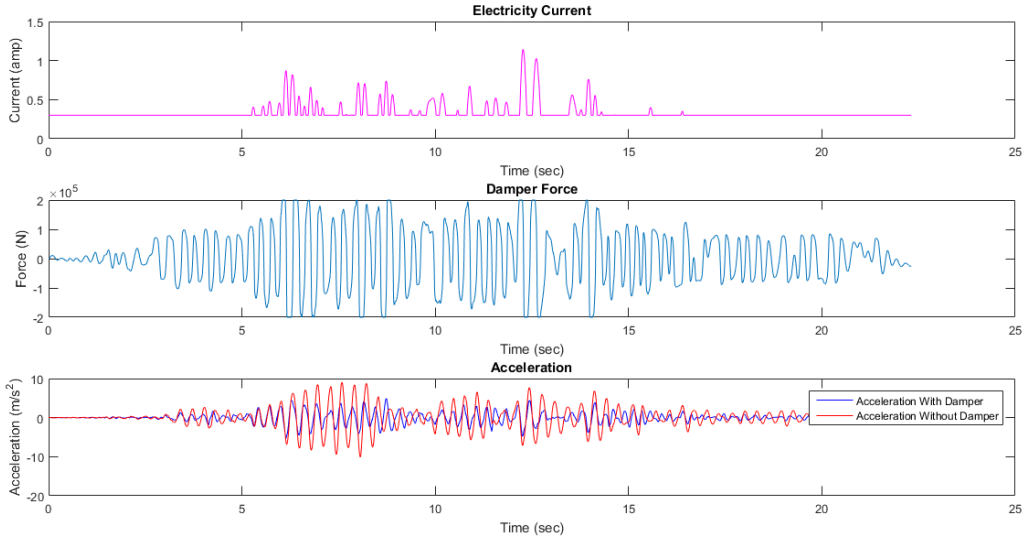

Figure 5-12: These graphs indicate the driven current to the damper by fuzzy controller, damper resistant force and the acceleration of the modeled structure vs Time, subjected to Super Stition Hills-Parachute Test Site 1987, near-field earthquake record

5-4- Erzincan 1992 (Near-Field Pulse Like Record):

This earthquake struck Erzincan in eastern Turkey with a moment magnitude of 6.7 on 13 March 1992.

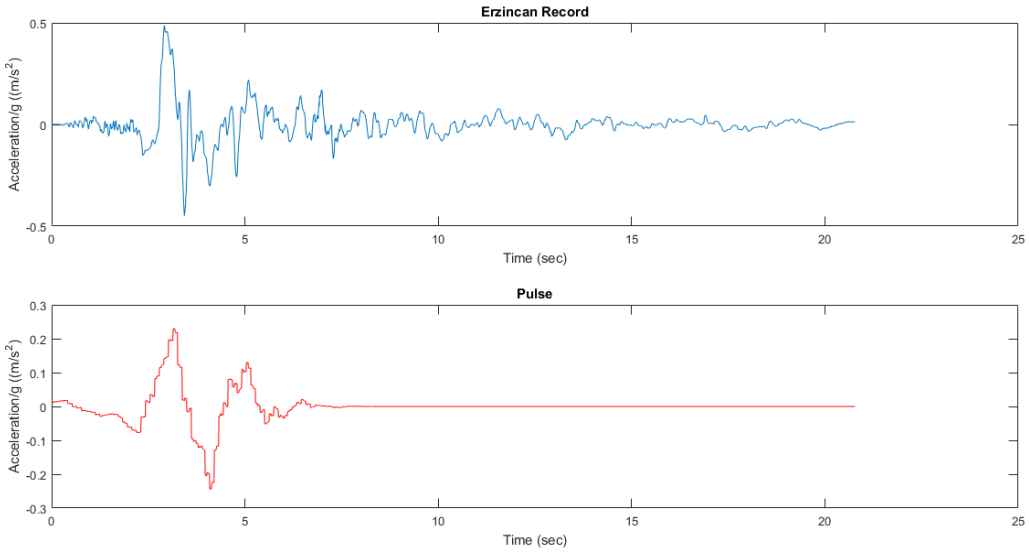

Figure 5-13: The graph up indicated the acceleration record of Erzincan 1992 earthquake and the graph below shows the acceleration record of its major pulse extracted by decomposition procedure

The near-field pulse like record of the Erzincan–Turkey 1992 earthquake (Figure 5-13) was applied to the modeled structure. The graphs in Figure 5-14 to Figure 5-16 indicate that by applying this record, the controller applies the highest adaptive electricity current (1.1 A) in the pulse period of Erzincan near-field earthquake. From the graphs it is observed that the major pulse is in the period between 3 and 5 seconds, when it causes the maximum displacement, velocity and acceleration in the structure. The analyses show that the maximum seismic displacement, velocity and acceleration are decreased about 43%, 46% and 35% (Table AI-7 to Table AI-9).

Furthermore, it is also observed that in the structure equipped with the fuzzy controlled MR damper the peaks corresponding to the same time of the displacement, velocity and acceleration of a system without damper are reduced by about 35%, 47% and 52% respectively (Table AI-14 to Table AI-16).

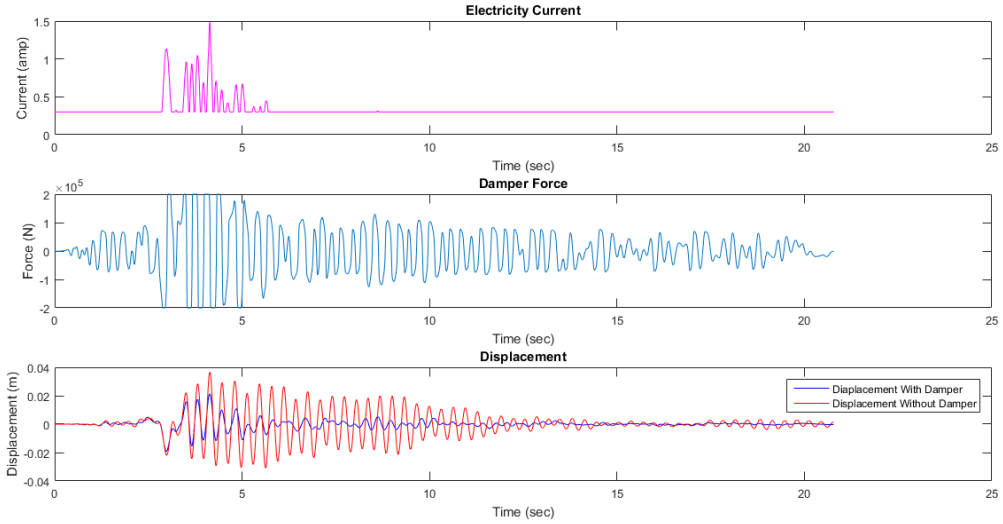

Figure 5-14: These graphs indicate the driven current to the damper by fuzzy controller, damper resistant force and the displacement of the modeled structure vs Time, subjected to Erzincan 1992, near-field earthquake record

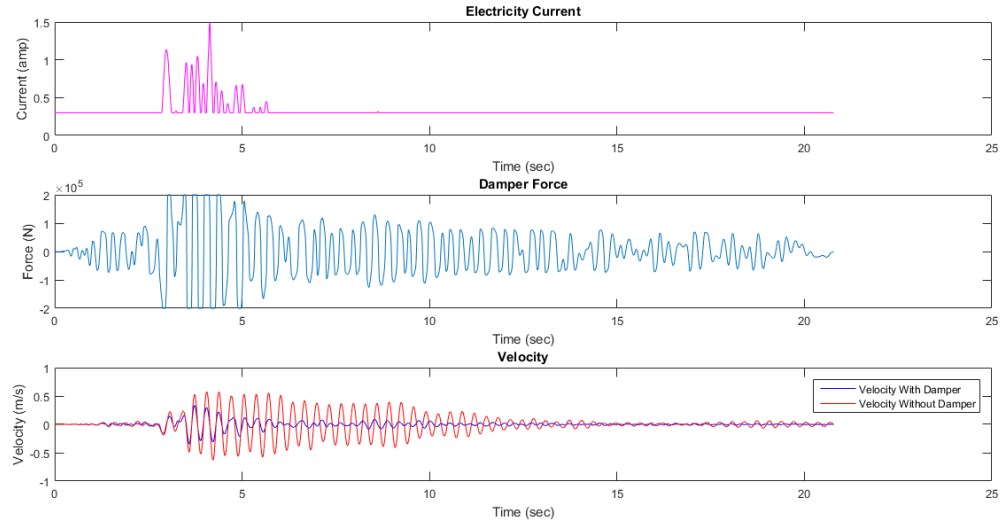

Figure 5-15: These graphs indicate the driven current to the damper by fuzzy controller, damper resistant force and the velocity of the modeled structure vs Time, subjected to Erzican 1992, near-field earthquake record

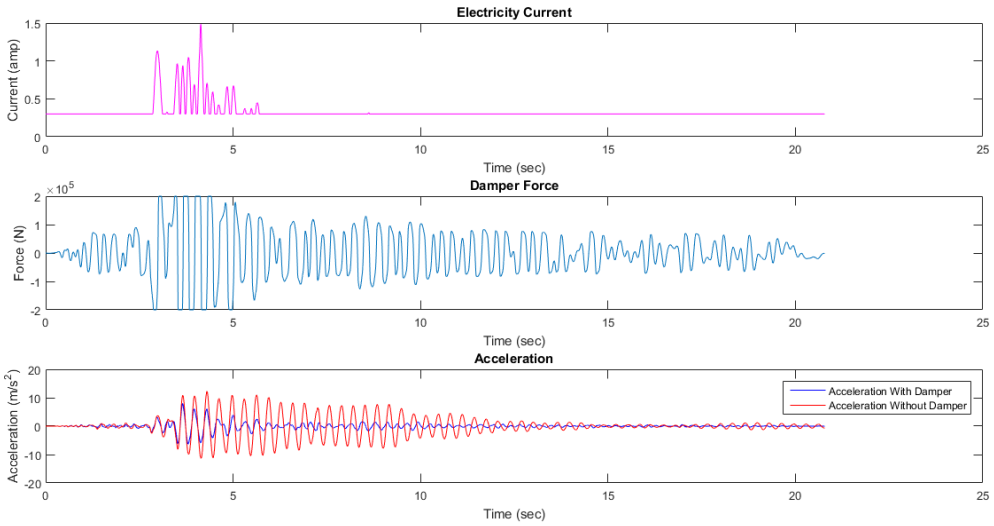

Figure 5-16: These graphs indicate the driven current to the damper by fuzzy controller, damper resistant force and the acceleration of the modeled structure vs Time, subjected to Erzican1992, near-field earthquake record

The Figure 5-21 and Figure 5-22 and analytical results in Table AI-3 to Table AI-9, subjected to the two suites of the 44 far-field and 91 near field pulse like earthquakes, illustrate that the MR damper which is controlled by the proposed fuzzy control system can properly reduce the displacement of the energy of the applied earthquake loads and it can improve the seismic demands of the model very well .

5-5- The efficiency of the Fuzzy controlled MR damper

The following graphs (Figure 5-17 and Figure 5-18) indicate that by less energy demand the adaptive MR damper controlled by the fuzzy controller has the performance almost similar to the MR damper working with the constant current 2A in reducing the seismic displacement of the structure. As an example, the results presented in Figure 5-17 and Figure 5-18, indicate that by using about 65% and 68% less total resistant force, the adaptive damper performed very similar to the damper working with 2A constant current in reducing the displacement of the structure subjected to Loma Prieta (121011) far-field and North Palm Spring near-field pulse like earthquake records, respectively.

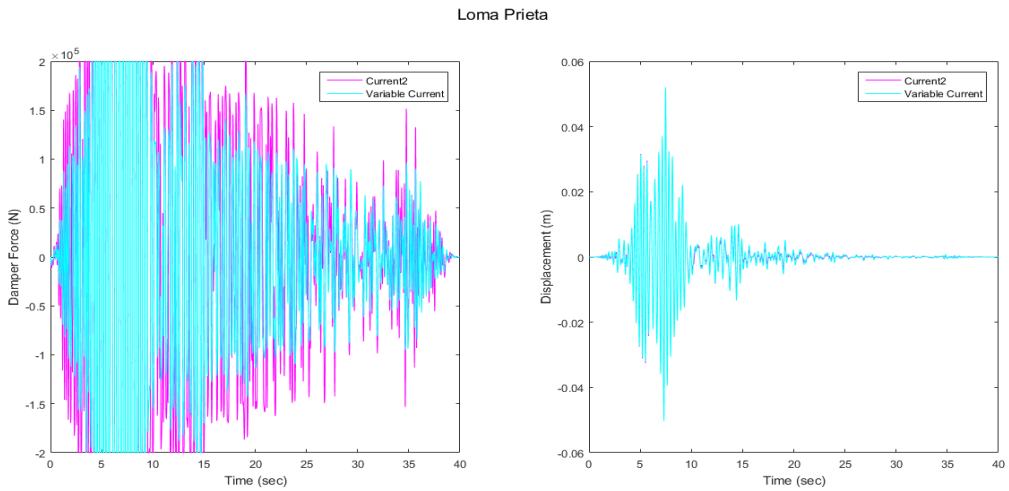

Figure 5-17: Left- comparison of damper force for adaptive and constant (2A) MR damper Right- comparison of seismic displacement of the structure using adaptive and constant (2A) MR damper subjected to Loma Prieta (121011) far-field record

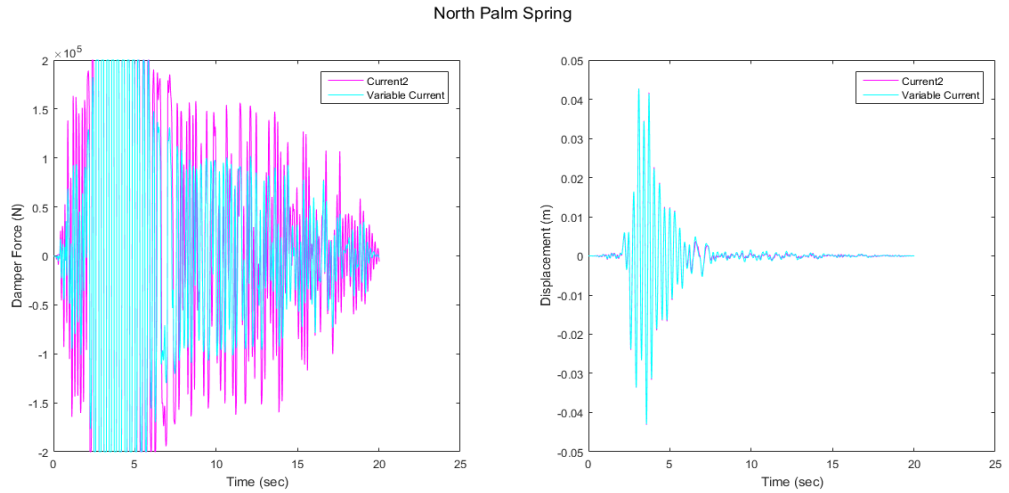

Figure 5-18: Left- comparison of damper force for adaptive and constant (2A) MR damper Right- comparison of seismic displacement of the structure using adaptive and constant (2A) MR damper subjected to North Palm Spring near-field pulse like record

In addition, the performance of the fuzzy control has been compared with an on/off control system in the MR damper utilized in this research. The graphs in Figure 5-19 and Figure 5-20 demonstrate that the fuzzy controlled MR damper reduces the maximum displacement and acceleration of the structure subjected to Northridge earthquake by 7% and 4.75%, more than the on/off controlled MR damper using the same amount of electricity.

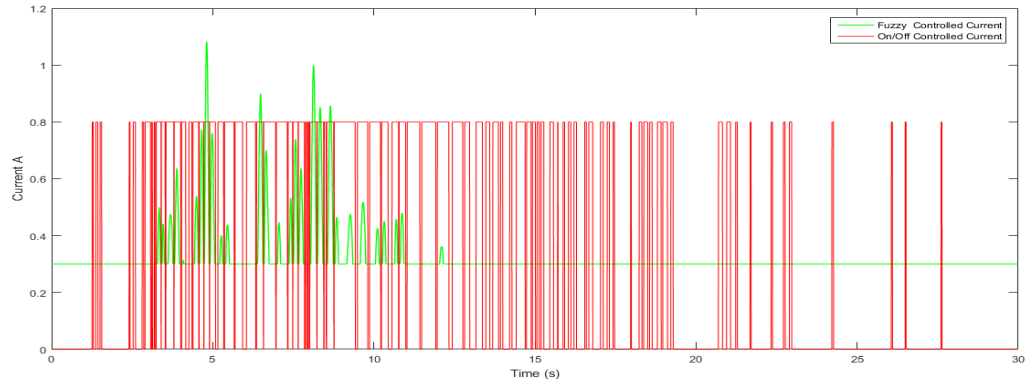

Figure 5-19: The comparison of the Electricity Current in On/Off and Fuzzy controllers subjected to Northridge 120111 Earthquake

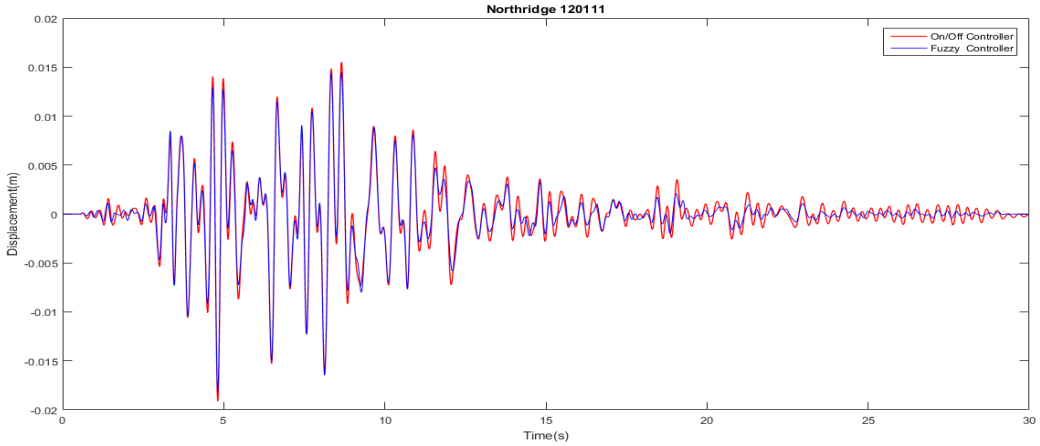

Figure 5-20: The comparison of the seismic displacement of the model with On/Off and Fuzzy controllers subjected to Northridge 120111 Earthquake

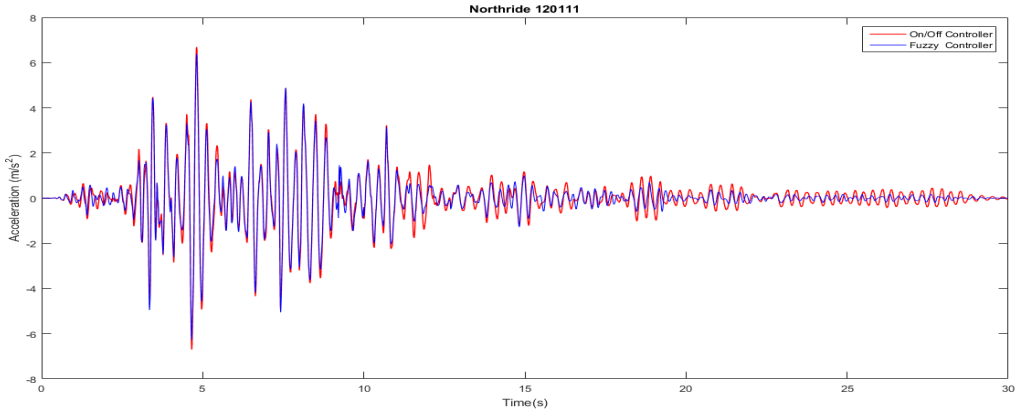

Figure 5-21: The comparison of the seismic acceleration of the model with On/Off and Fuzzy controllers subjected to Northridge 120111 Earthquake

5-6- Displacements Comparison:

The displacements are of the most important issues that must be controlled in a structure to provide it with sufficient level of safety.

Figure 5-21 and Figure 5-22 indicate that the proposed damping system can critically reduce the displacements of the modeled structure during the applied far-field and near field pulse like earthquakes. In the following, the bar charts in Figure 5-23 to Figure 5-26 compare the maximum displacements of the modeled structure in two conditions with and without the damper and it is seen that the proposed damping system decreases the maximum displacements of the structure significantly. The results Table AI-3 and Table AI-7, show that by using the proposed damping system the average maximum seismic displacements of the modeled structure have reduced by about 39% and 40% for the far-field and near-field pulse like records, respectively.

It should be noticed that the Figure 5-25 and Figure 5-26 illustrate that the corresponding displacements to the maximum displacements also decreased critically. And based on the results in Table AI-11 and Table AI-14, the average corresponding displacements to the average maximum displacements in the structure without the damper are decreased by about 55% for far-field and by slightly more than 53% for near-field pulse like records.

In the following to better show the performance of the proposed controllable damping system, the bar charts of the maximum displacements of the structure with and without the damper for the applied earthquake records are compared (Figure 5-23 and Figure 5-24). It is worth mentioning that the bar charts in Figure 5-25 and Figure 5-26 indicate that the displacements in the structure with the damper corresponding to its maximum displacements without the damper for the applied earthquake records.

The Simulink output graphs in Figure 5-27 , Figure 5-28 and the numerical data in Table AI-11 and Table AI-14, illustrate that by installing the controllable MR damper in the structure, it dissipates the effect of the Duzce earthquake and changes the pattern of vibration in the structure in a way that in the structure with the damper the corresponding displacement of the maximum displacement without the damper, occurring in 12.271s, is reduced by about 31% while, the maximum displacement of the structure with the damper, which occurs with a negligible time shift in 12.269 s, is also about 30.6% less than the maximum displacement of the structure without the damper.

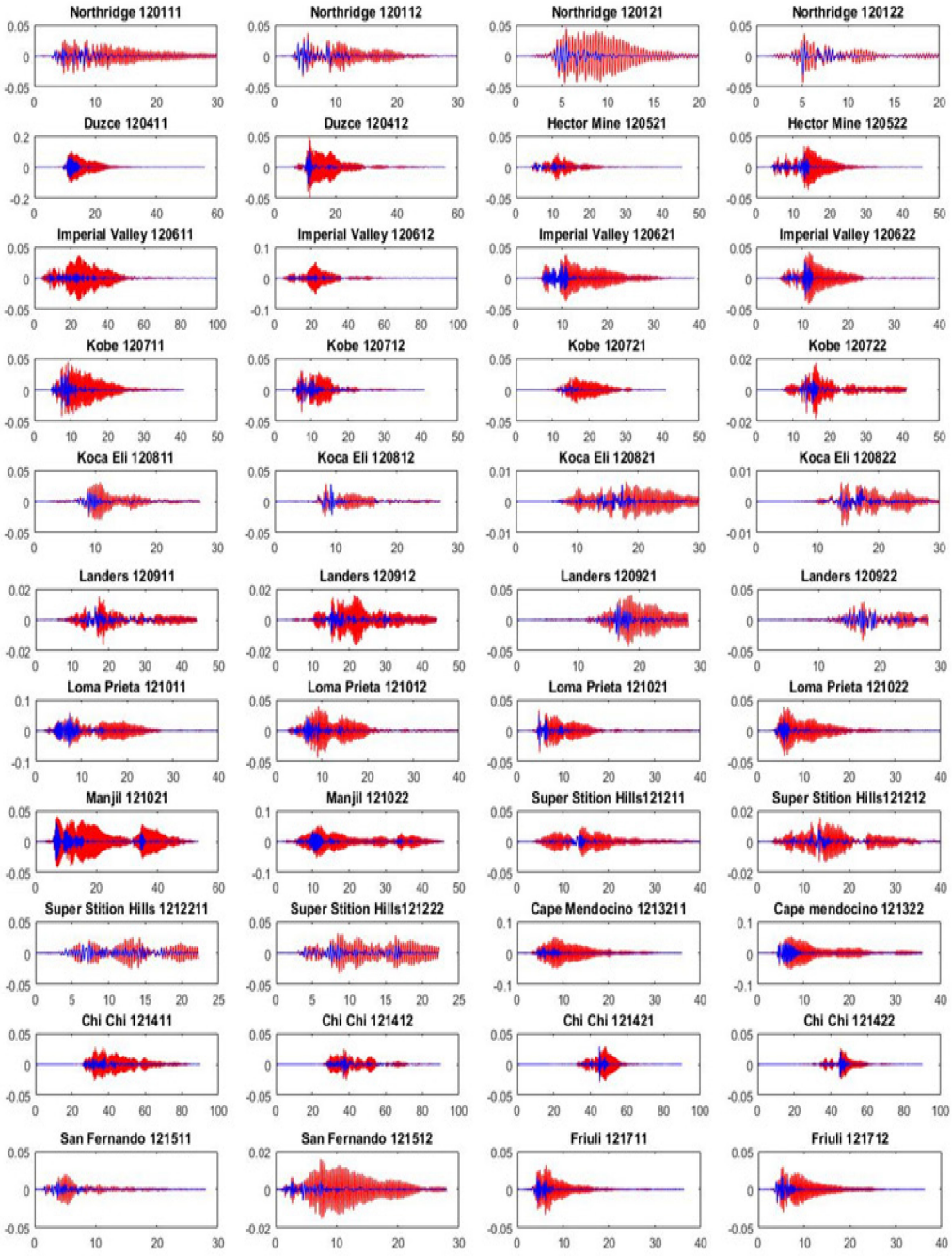

Figure 5-22 : These graphs indicate the reduction of structure displacement, due to the presence of smart MR damper, subjected to the 44 far-field earthquake records. The horizontal and vertical axes show displacement of the story in the model structure (m) and time of earthquake (s), respectively.

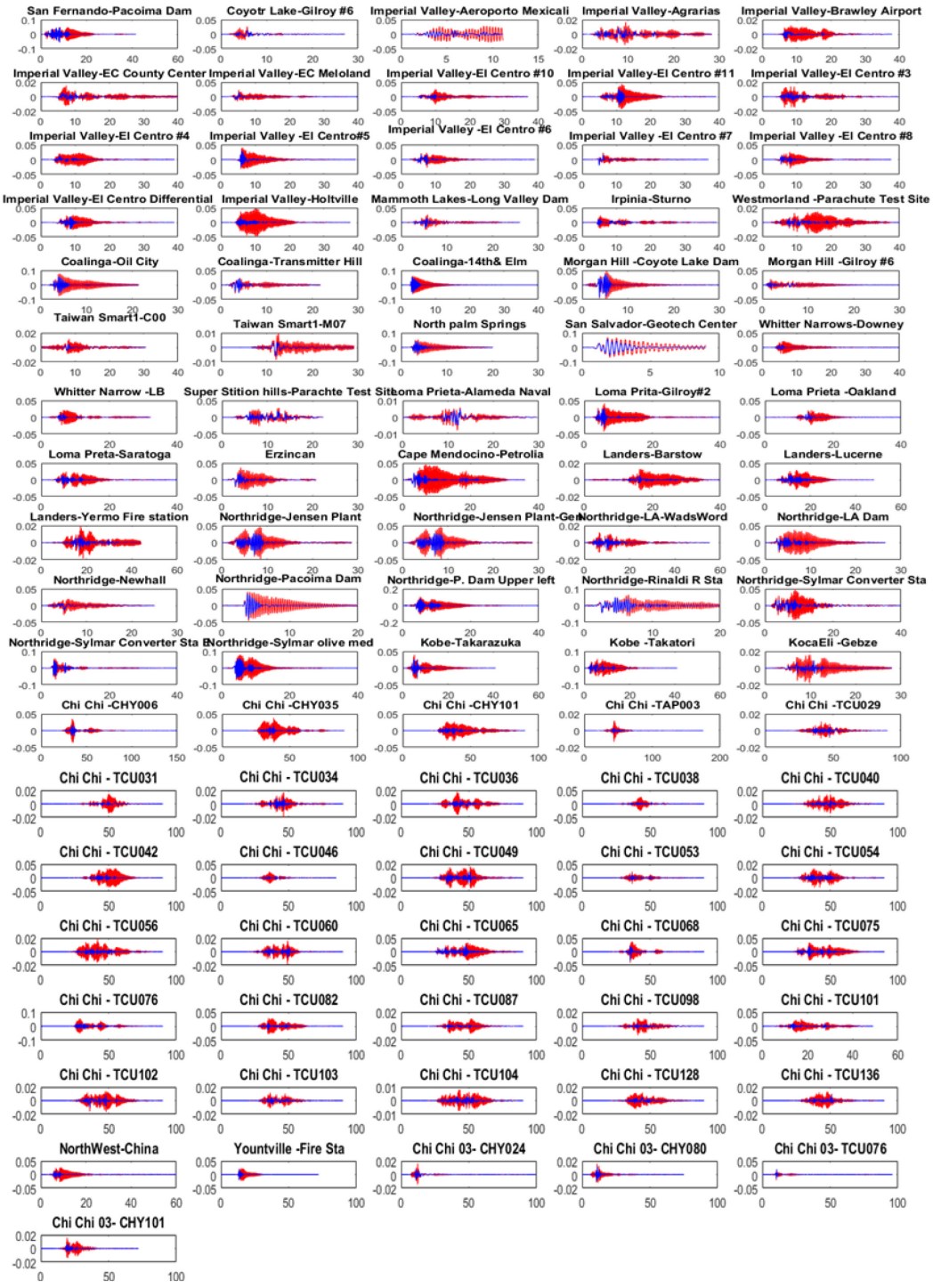

Figure 5-23 : These graphs indicate the reduction of structure displacement, due to the presence of smart MR damper, subjected to the 91 near-field (pulse like) earthquake records. The horizontal and vertical axes show displacement of the story in the model structure (m) and time of earthquake (s), respectively.

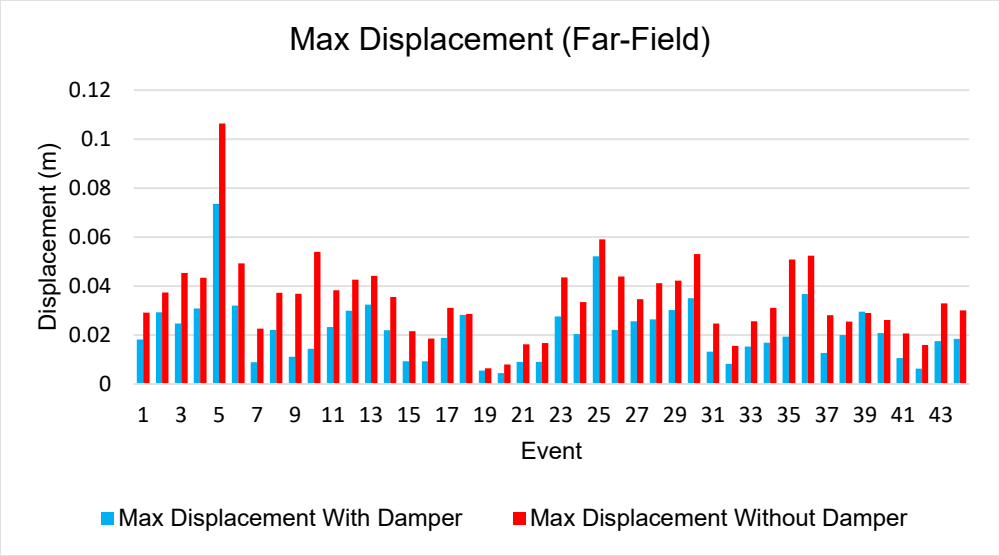

Figure 5-24 : The comparison between maximum displacements of the structure with damper and without damper subjected to 44 far-field earthquake records

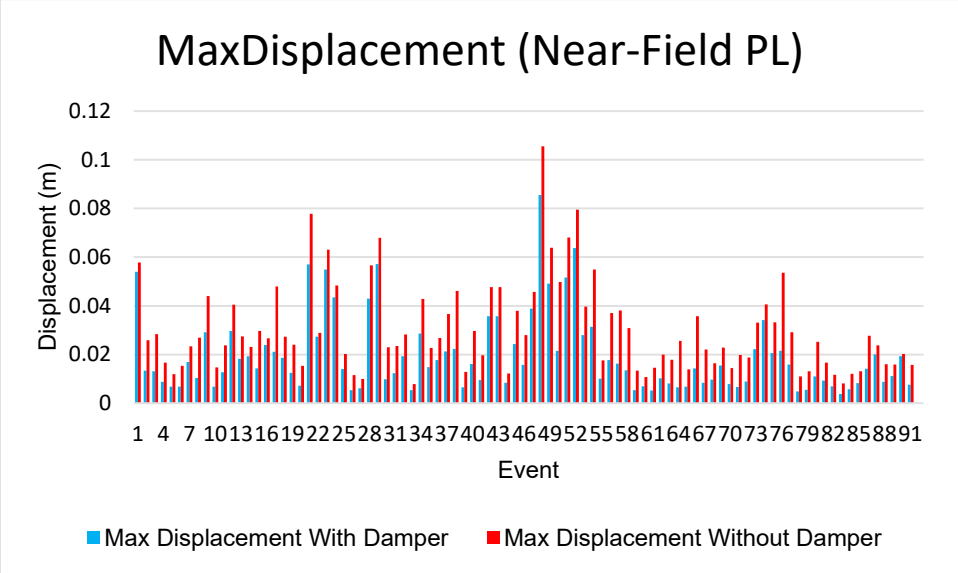

Figure 5-25 : The comparison between maximum displacements of the structure with damper and without damper subjected to 91 near-field pulse like earthquake records

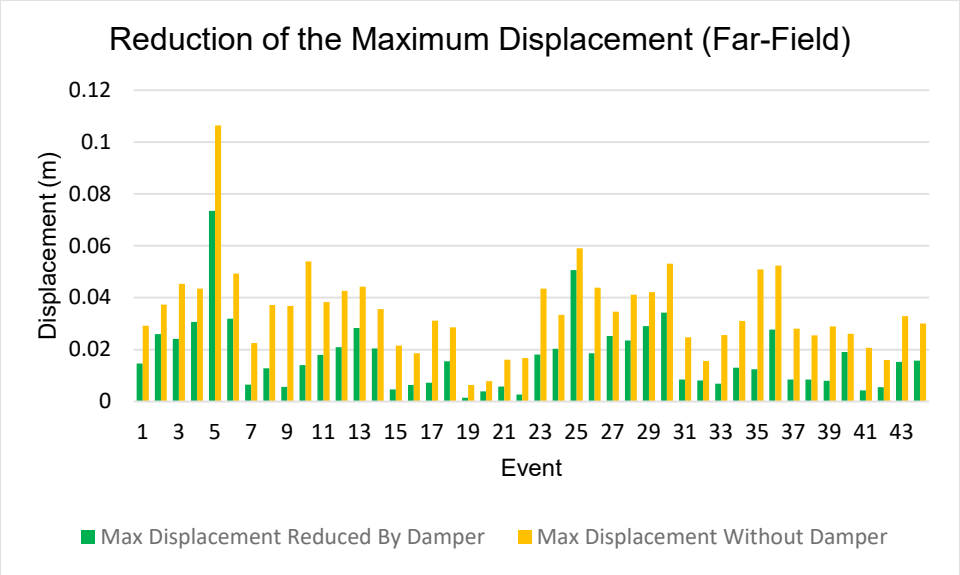

Figure 5-26 : The effect of the adaptive MR damper and the control unit in reducing the maximum displacements of the structure subjected to 44 far-field earthquake records

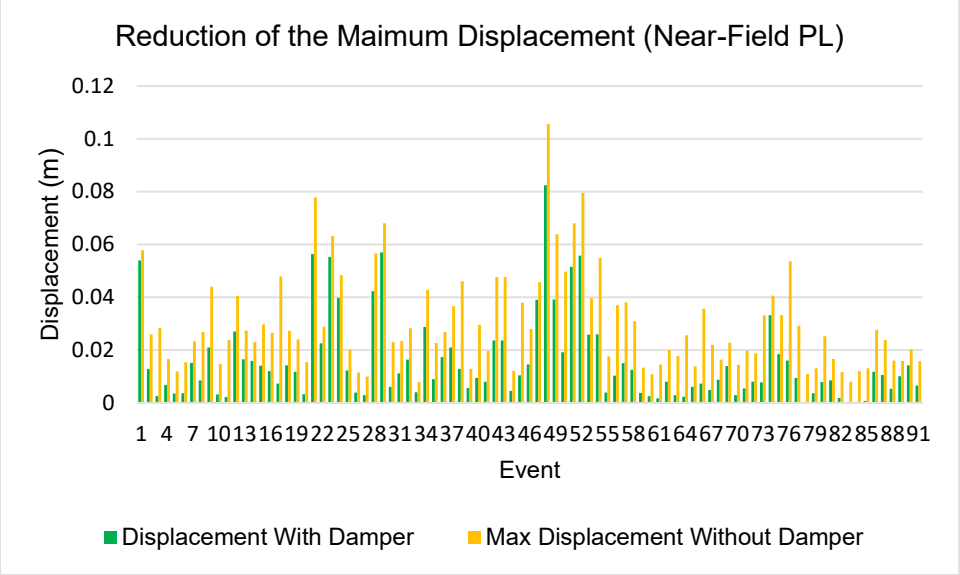

Figure 5-27 : The effect of the adaptive MR damper and the control unit in reducing the maximum displacements of the structure subjected to 91 near-field pulse like earthquake records

Based on Figure 5-23 and considering the numerical results in Table AI-3, it is observed that the Duzce-Turkey 1999 earthquake with the duration of 55.9 s causes the largest maximum displacement in the model without the damper, for the applied far-field records.

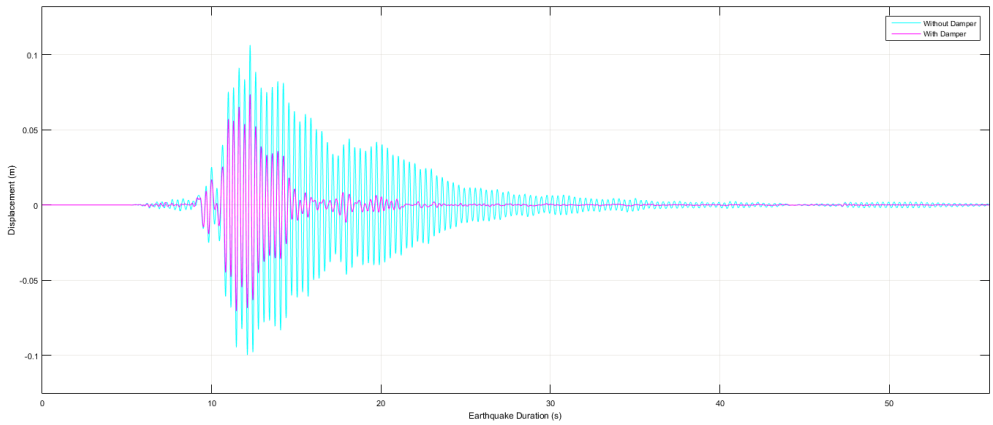

Figure 5-28 : The Displacement graphs of the modeled structure with and without damper subjected to Duzce- Turkey 1999 earthquake far-field records

The bar charts in Figure 5-24 and the numerical results in Table AI-11 illustrate that among the applied near-field pulse like records, Northridge 1994 earthquake recorded in Pacoima Dam caused the maximum displacement in the structure without the damper.

Based on the above mentioned numerical results and the visualization in Figure 5-28, it is seen that the maximum displacement occurs at 5.33 s, and by installing a damper in the model, the corresponding displacement reduces by about 21 %, while the damper also causes the maximum displacement to occur at a negligible time shift, at 5 s.

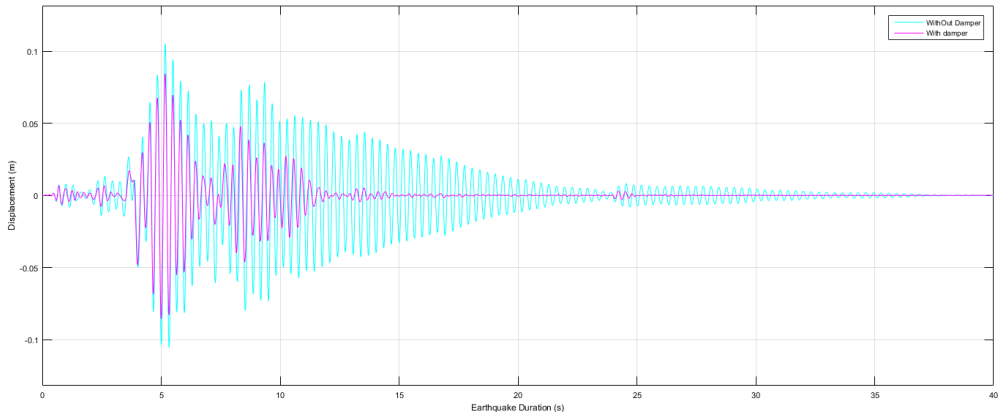

Figure 5-29 : The Displacement graphs of the modeled structure with and without damper subjected to Near-Field Pulse Like Northridge 1994 Earthquake Records

It should be noted that by comparing the results in Table AI-3, with Table AI-11, and Table AI-7 with Table AI-14, it is understood that the difference between the maximum displacement in the

structure with the damper and the displacement corresponding to the maximum displacement in the structure without the damper is very small and can be neglected.

5-7- Wave Energy

In this research considering the formula shown in Eq (5-1) , the energy of the earthquake waves in two different conditions including the structure with the damper and without the damper are compared. The results are drawn in the form of a bar chart in Figure 5-29.

$$E=\int_0^t |D(t)|^2 \, dt \quad \text{(Oppenheim et al. 1998)} \qquad \textbf{(5-1)}$$

Where E is the wave energy, D is the displacement of the structure and t is the earthquake time.

The bar chart in Figure 5-29 illustrate that the MR damper which is controlled with the proposed fuzzy control unit can dissipate the energy of earthquake waves significantly. The numerical results of the analyses (Table AI-6) indicate that the maximum energy dissipation is about 95% for the earthquake San Fernando (121512) in bar 42 and the smallest energy dissipation is about 63% for the earthquakes Koca Eli –Turkey (120812) and Landers (120922) in bars 18 and 24.

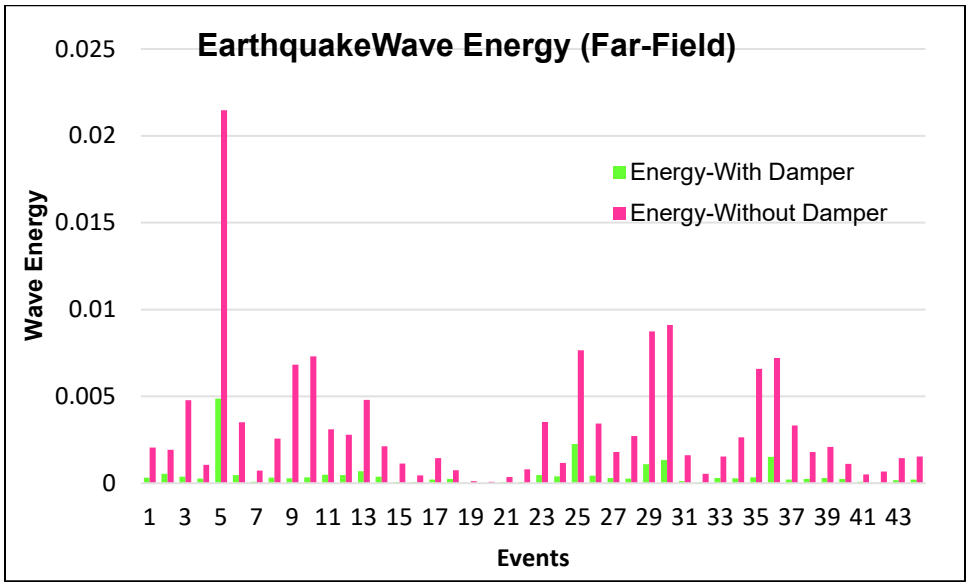

Figure 5-30 : The energy damping effect of the smart MR damper subjected to 44 far-field earthquake records

The highest bar in this bar chart belongs to the earthquake Duzce-Turkey (120411) and based on the analytical results in Table AI-6 the adaptive damper has dissipated its seismic energy by about

77%. The results also indicate that the average of energy dissipation for the 44 applied far-field records is about 84%.

The bar chart in Figure 5-30 indicates that the MR damper which is controlled with the proposed fuzzy control unit has critically dissipated the energy of the applied 91 near-field pulse like.

Based on the results in Table AI- 10 the maximum energy dissipation amounts are just above 93% for the Chi Chi–Taiwan earthquake (recorded in the station TCU042) and Imperial Valley earthquake (recorded in Holtville Post office) which are in the bars 66 and 17 in the bar chart.

The minimum energy dissipation is for the San Fernando earthquake (recorded in Pacoima Dam station) which is about 63% (bar 1).

In this figure the highest bar is the energy of the Northridge earthquake which is recorded in Pacoima Dam station and the results in Table AI- 10 illustrate that the fuzzy controller has commanded the MR damper in a way that it has dissipated about 71% of its seismic energy (bar 48).

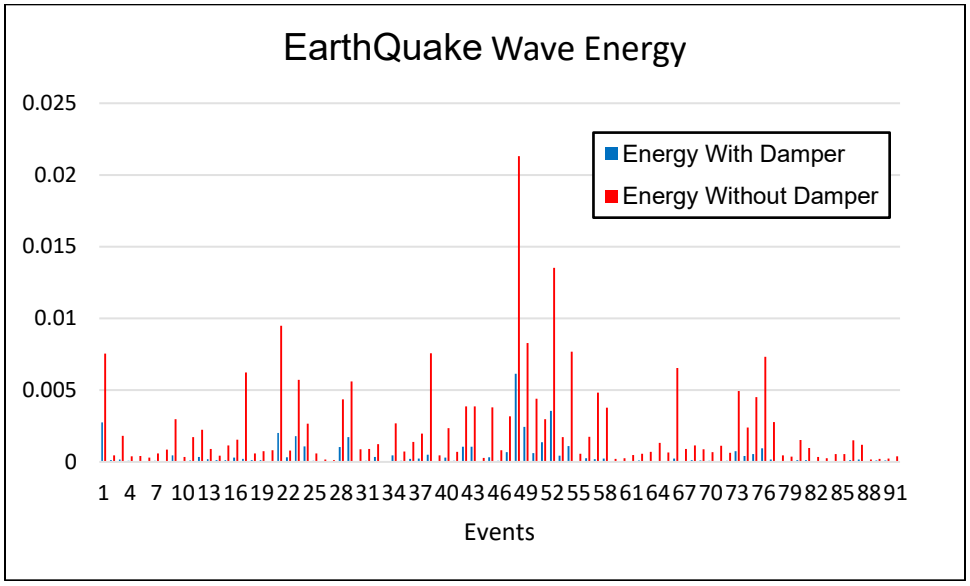

Figure 5-31 : The energy damping effect of the smart MR damper subjected to 91 near-field pulse-like earthquake records

5-8- Velocities Comparison:

Another important seismic demand that can show the behavior of the structure confronting the earthquakes is the velocity of the structure.

The bar charts in Figure 5-31 and Figure 5-32 and related results in Table AI-4 and Table AI-8, indicate that the average amounts of the maximum seismic velocities of the structure equipped with the proposed damping system is about 40% and 43% smaller than the average of the maximum seismic velocities of the structure without the damper subject to the far-field and near-field earthquake records, respectively.

It is also observed that the highest velocities of the structure are caused by the far-field record of Duzce –Turkey earthquake (120411) and the near-field pulse like record of Northridge earthquake (Pacoima Dam station) and the analytical results show that the MR damper adjusted with the fuzzy controller has decreased the maximum velocities of the mentioned earthquakes by about 31% and 20.5 %, respectively.

The bar charts in Figure 5-33 and Figure 5-34 compare the maximum seismic velocities of the structure without the damper and their corresponding seismic velocities in the structure with the damper for the applied far-field and near-field earthquake records.

Based on the analytical data indicated in the Table AI-12 and Table AI-15, in the structure with damper, the velocities are also about 31% and 20.5% smaller compared to the maximum seismic velocities in the structure without the damper subject to Duzce –Turkey (120411) and Northridge (Pacoima Dam station) earthquake loads.

It means that in these two mentioned cases, the maximum velocity in the structure with the damper and the maximum velocity in the structure without the damper almost occur in the same time.

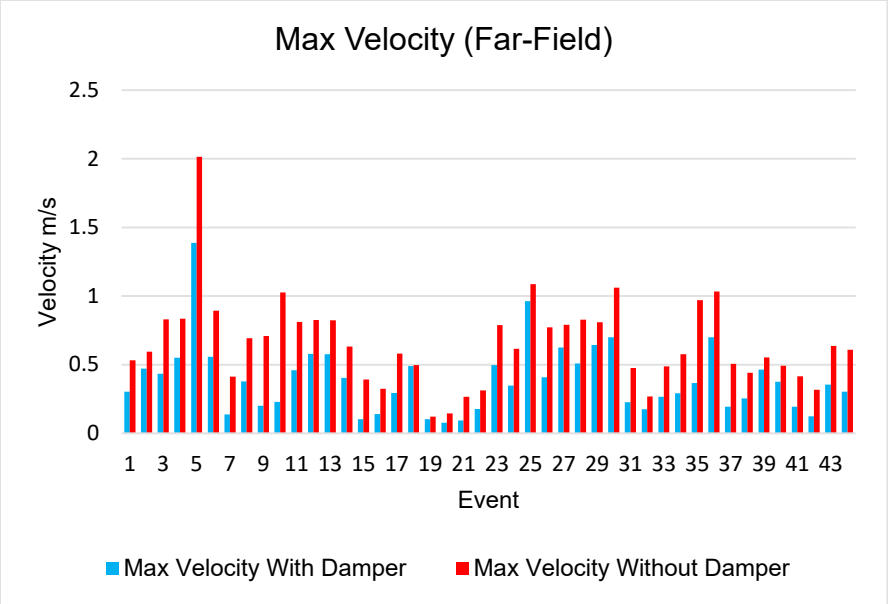

Figure 5-32 : The comparison between maximum velocities of the structure with damper and without damper subjected to 44 far-field earthquake records

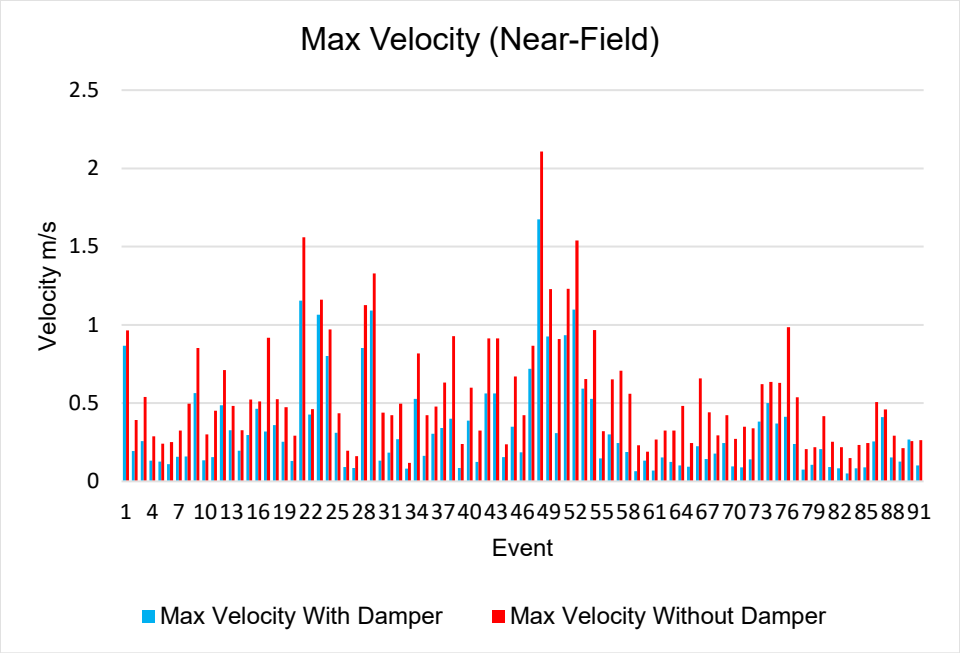

Figure 5-33 : The maximum velocities of the structure with damper and without damper subjected to 91 near-field pulse like earthquake records

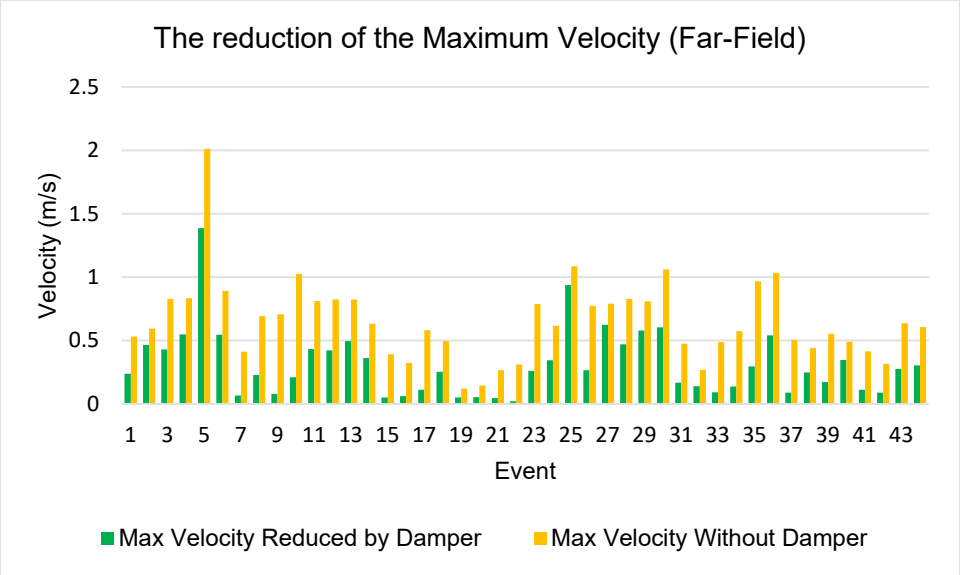

Figure 5-34 : The effect of the adaptive MR damper and the control unit in reducing the maximum velocities of the structure subjected to 44 far-field earthquake records

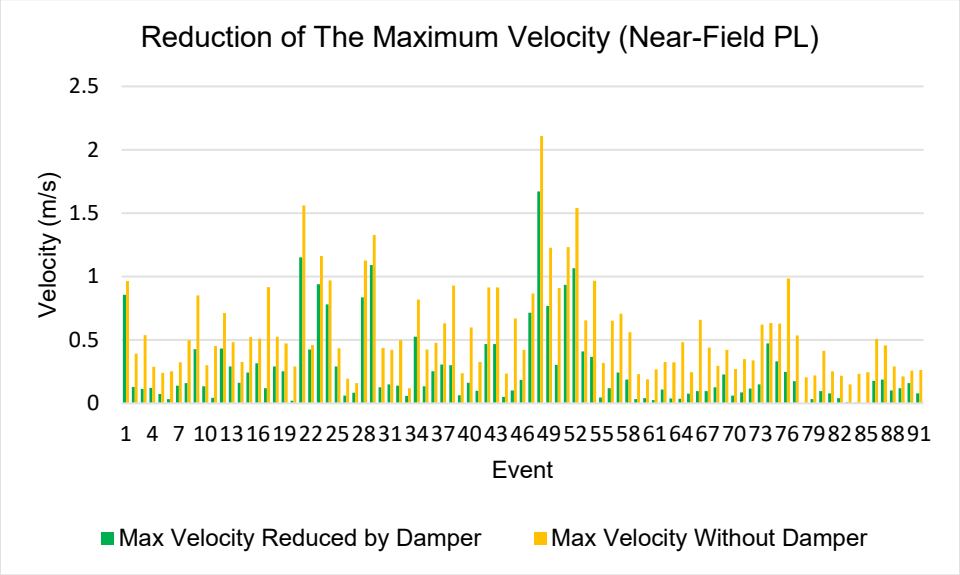

Figure 5-35 : The effect of the adaptive MR damper and the control unit in reducing the maximum velocities of the structure subjected to 91 near-field pulse-like earthquake records

5-9- Accelerations Comparison:

The seismic acceleration of the structure is a critical factor that should be considered in the analyses. The resulted data in Table AI-5 and Table AI-9 show that the MR damper which is adjusted with the fuzzy control unit decreases the seismic acceleration of the structure under the seismic loads of far-field and near-fields pulse like earthquake records.

The bar charts in Figure 5-35 and Figure 5-36 show the effects of the proposed damping system in reducing the maximum seismic acceleration of the modeled structure and the bar charts in Figure 5-37 and Figure 5-38 compare the maximum accelerations of the modeled structure without the damper and their corresponding accelerations reduced by the MR damper which is controlled by the fuzzy control unit.

The bar chart shown in Figure 5-35 illustrates that among the utilized far-field records, the record of Duzce–Turkey (120411) earthquake has caused the highest seismic acceleration in the structure.

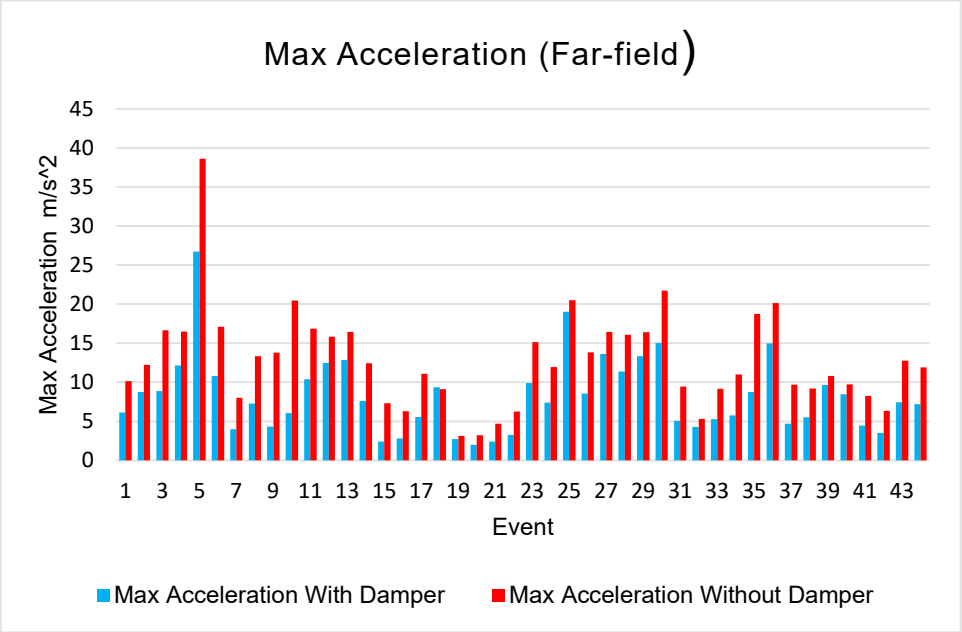

Figure 5-36 : The comparison between maximum acceleration with damper and the maximum acceleration without damper subjected to 44 far-field earthquake records

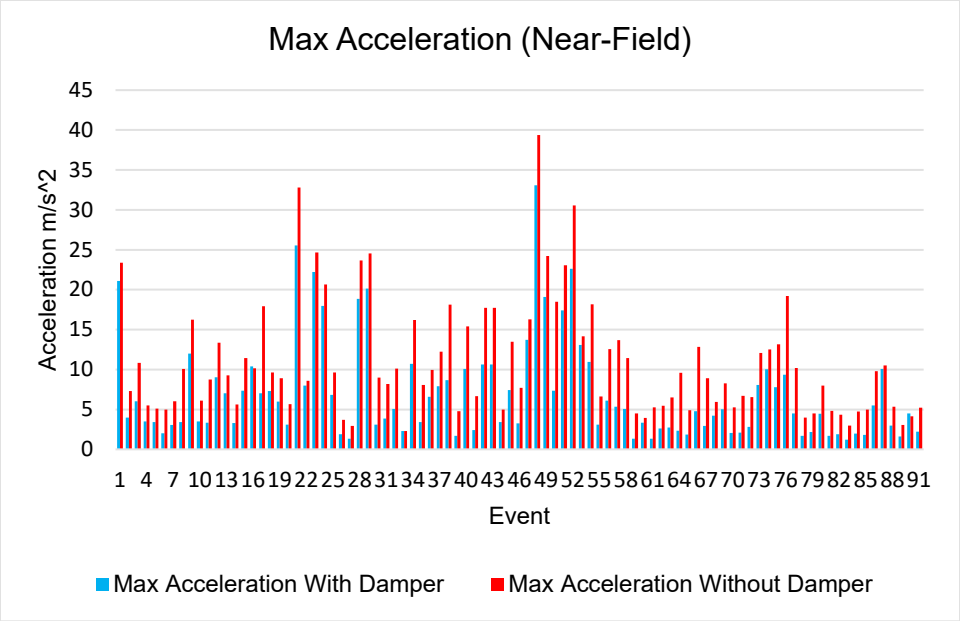

Figure 5-37 : The comparison between maximum accelerations of the structure with damper and without damper subjected to 91 near-field pulse-like earthquake records

The bar chart in Figure 5-35 and the results in Table AI-5, indicate that by applying the record of the Duzce –Turkey (120411) earthquake to the modeled structures with and without the damper, the highest seismic acceleration of the structure which is equipped with the proposed damping system is about 31% smaller than the largest seismic acceleration of the structure without the damper. The amounts of the seismic acceleration in Table AI-5, also indicate that the average of the maximum accelerations of the far-field records are reduced by about 38% due to the performance of the MR damper commanded by the proposed fuzzy controller.

The bar chart in Figure 5-37 and the related output data in Table AI-13, illustrate that the adjustable damping system has reduced the maximum acceleration of the structure subjected to the far-field record of the Duzce–Turkey (120411) earthquake by 31%. In this case the maximum acceleration in the structure with damper and the structure without the damper occurs almost at the same time during the earthquake.

Based on the bar charts in Figure 5-36 and considering Table AI-13, it is illustrated that by utilizing the damping system the average of the maximum acceleration of the structure can be reduced by about 36% and 40% for the far-field and near-field records, respectively. It is also understood that in the analyses with near-field pulse like records the damping system has such an effect that the maximum acceleration of the structure with the damper is 16% smaller than the maximum

acceleration of the structure without the damper and the corresponding acceleration to the highest acceleration in the model without damper is reduced by 17%.

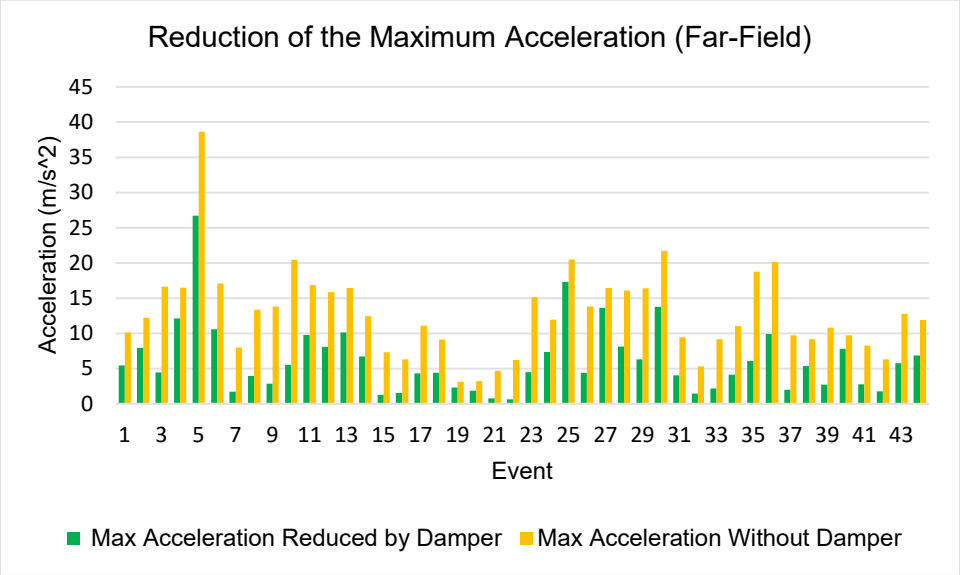

Figure 5-38 : The effect of the adaptive MR damper and the control unit in reducing the maximum accelerations of the structure subjected to 44 far-field earthquake records

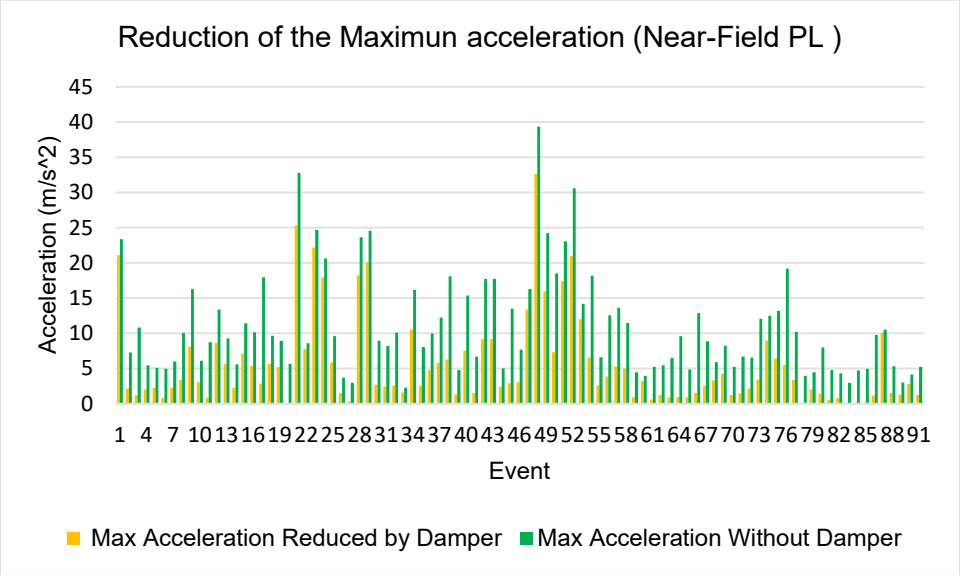

Figure 5-39 : The effect of the adaptive MR damper and the control unit in reducing the maximum accelerations of the structure subjected to 91 near-field pulse like earthquake records

5-10- Probability Curves for Displacements:

Another criterion that can be used to visualize the effect of the MR damper adjusted by the fuzzy controller in the system is the probability of exceedance of the median values of the dynamic response. By taking account of the results of the dynamic structural analysis; the probability curves for maximum displacement demand are drawn. The graphs in Figure 5-39 and Figure 5-40 show the maximum probability of displacement in two conditions with the damper and without the damper subjected to the two sets of earthquake records including 44 far-field records and 91 near-field pulse-like records. Hence, the standard normal cumulative distribution function (CDF) is fitted to the cumulative distribution of maximum displacement of the model for 44 selected far-field earthquakes (Baker 2015).

It can be observed that the medians of the data in the system with the damper are approximately 40% and 45% less than the system without the damper for the 44 far-field and 91 near-field pulse-like records respectively.

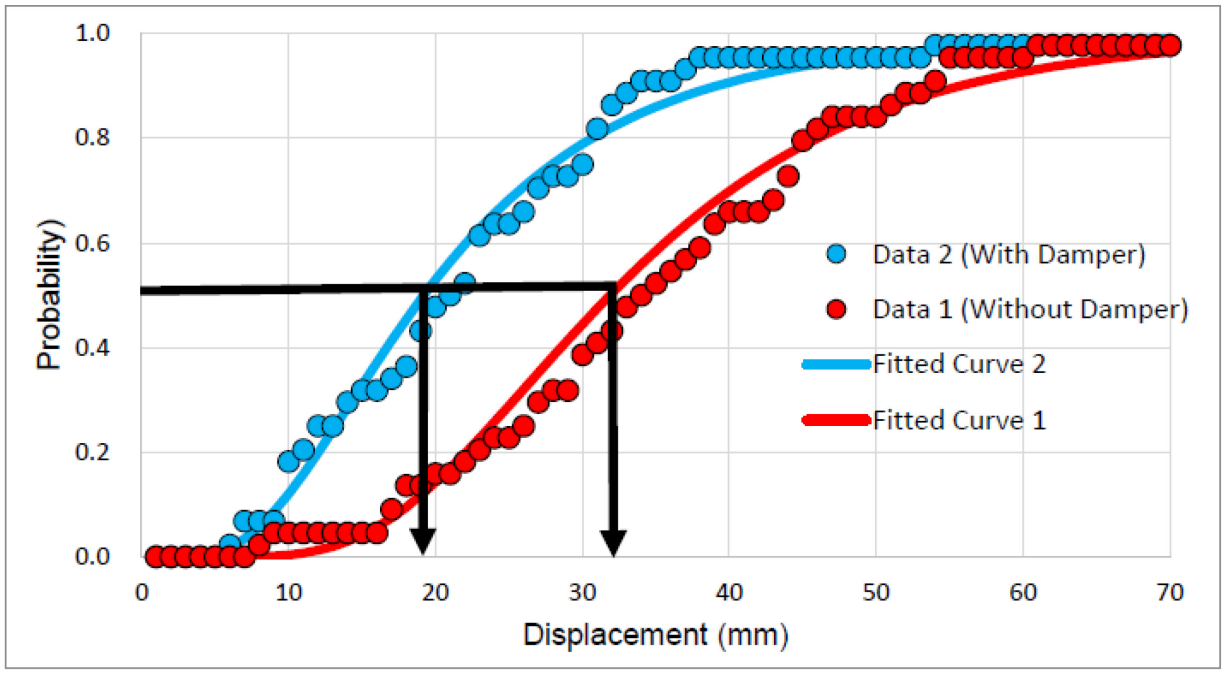

Figure 5-40: Median response of the system subjected to 44 far-field earthquake records

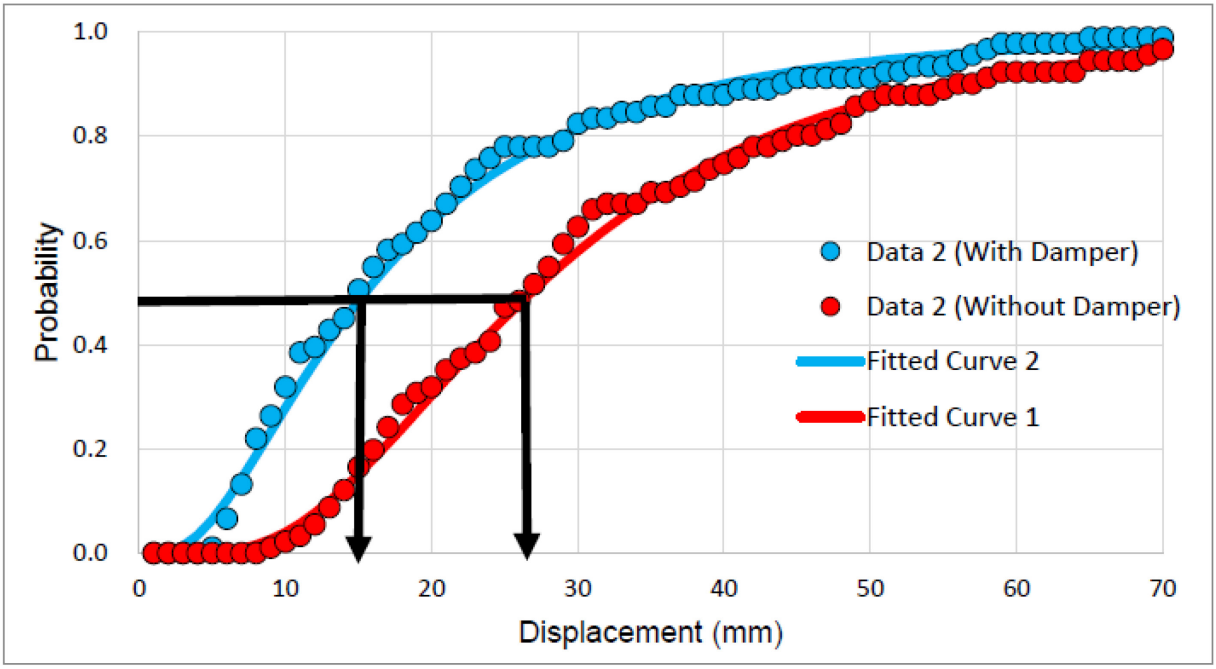

Figure 5-41: Median response of the system subjected to 91 near-field pulse like earthquake records

5-11- The Hysteresis loops of the System:

To show the effect of the proposed damping system on the hysteresis behavior of the Structure, the hysteresis-loops of the system subjected to 5 selected far-field and 5 near-field pulse-like earthquake records are drawn. The hysteresis-loops including Base-Shear versus displacement and Base-Shear versus Velocity illustrate that the damping system has improved the seismic behavior of the structure reducing Base-Shear force, displacement and the velocity.

5-11-1- Hysteresis loops of the structure for the selected far-field Earthquakes

In the following Figure 5-41 to Figure 5-45 illustrate the hysteresis loops for the structure with and without the damper for the 5 selected far-field earthquakes including Northridge (120111), Duzce (120411), Kobe 120711, Manjil 121111, and San Fernando 121511.

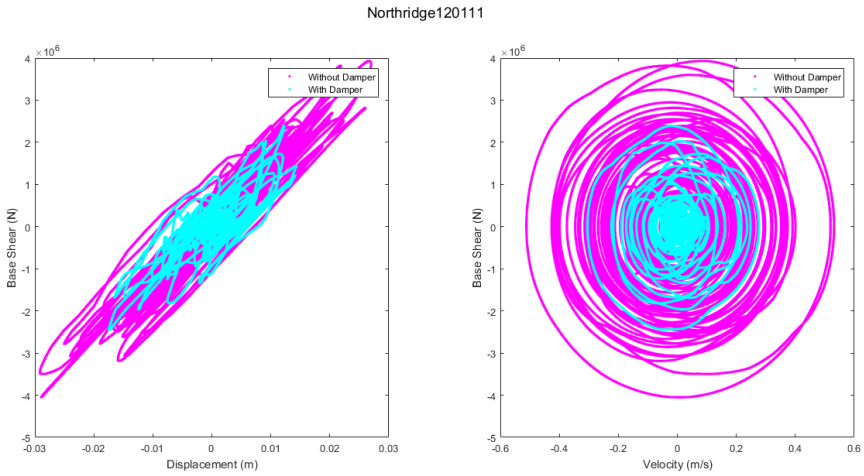

Figure 5-42 : Left –Base shear vs Displacement Right- Base shear vs Velocity for far-field Northridge (120111) earthquake

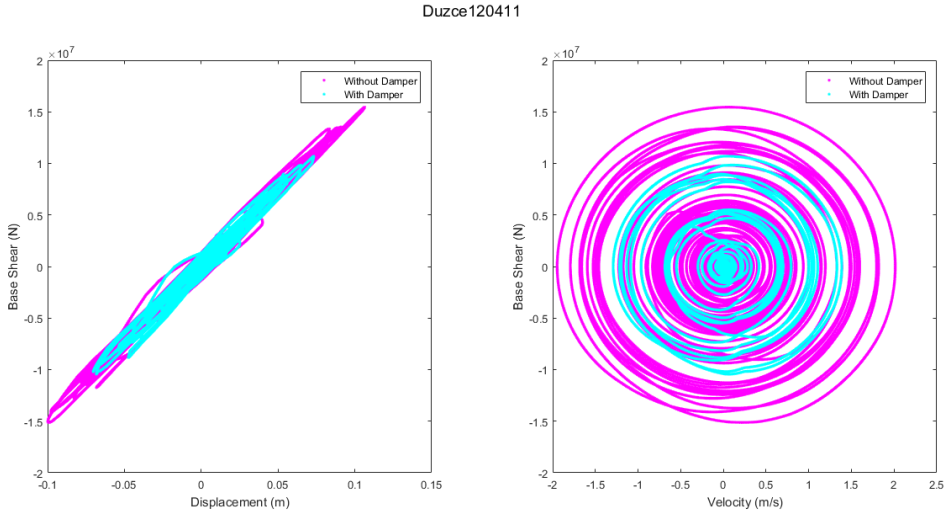

Figure 5-43 : Left –Base shear vs Displacement Right- Base shear vs Velocity for far-field Duzce (120411) earthquake

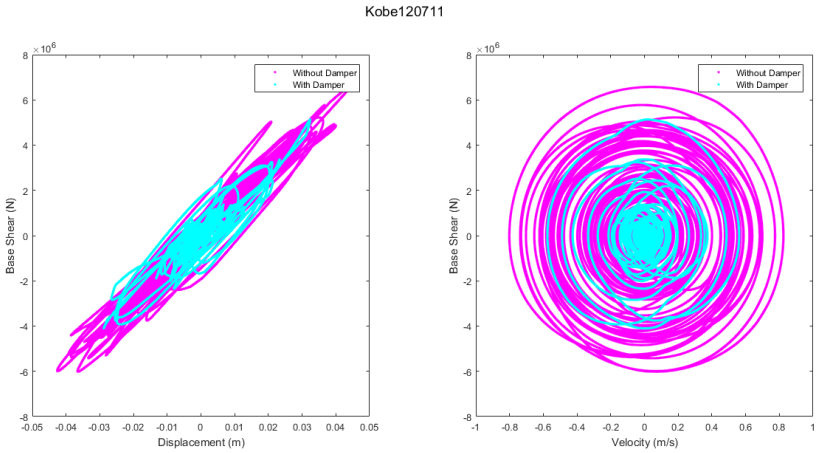

Figure 5-44 : Left –Base shear vs Displacement Right- Base shear vs Velocity for far-field Kobe (120711) earthquake

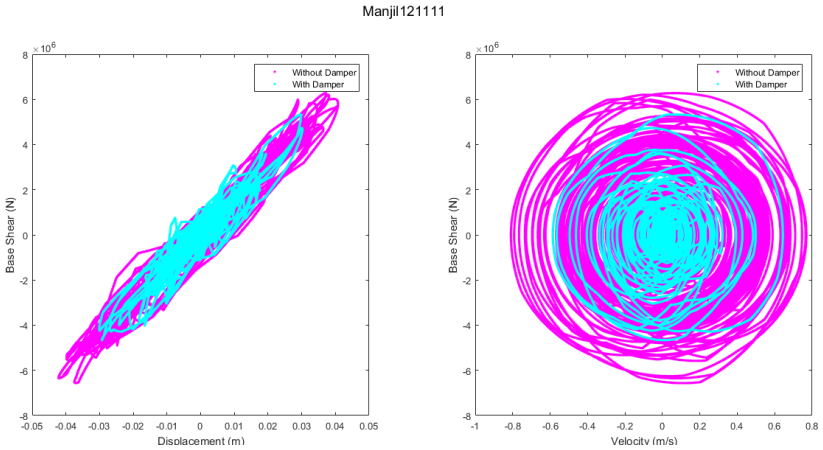

Figure 5-45 : Left –Base shear vs Displacement Right- Base shear vs Velocity for far-field Manjil (121111) earthquake

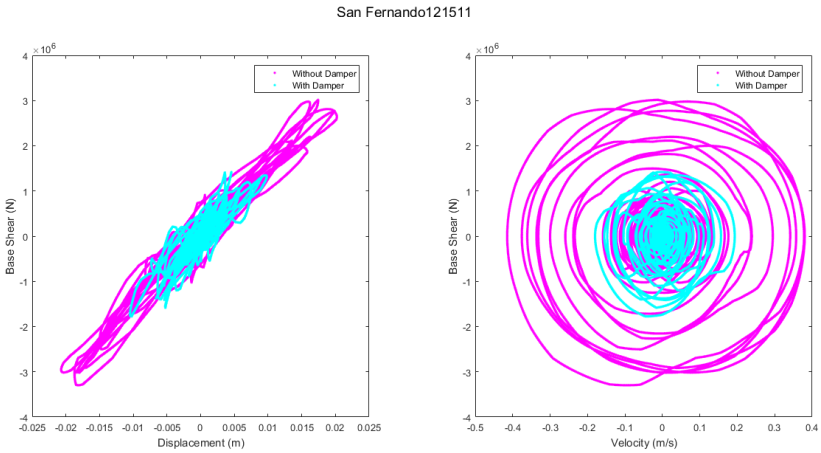

Figure 5-46 : Left –Base shear vs Displacement Right- Base shear vs Velocity for far-field san Fernando (121511) earthquake

5-11-2- Hysteresis loops of the structure for the selected near-Field Pulse Like Earthquakes

In the following the Figure 5-41 to Figure 5-45 illustrate the hysteresis loops for the structure with and without the damper for the 5 selected near-field pulse like earthquakes including Imperial Valley (06-Brawley Airport) , Coalinga (05-Oil City), Loma Prieta (Gilroy Allay #2), Northridge (Pacoima Dam) and Chi Chi-Taiwan (CHY006) .

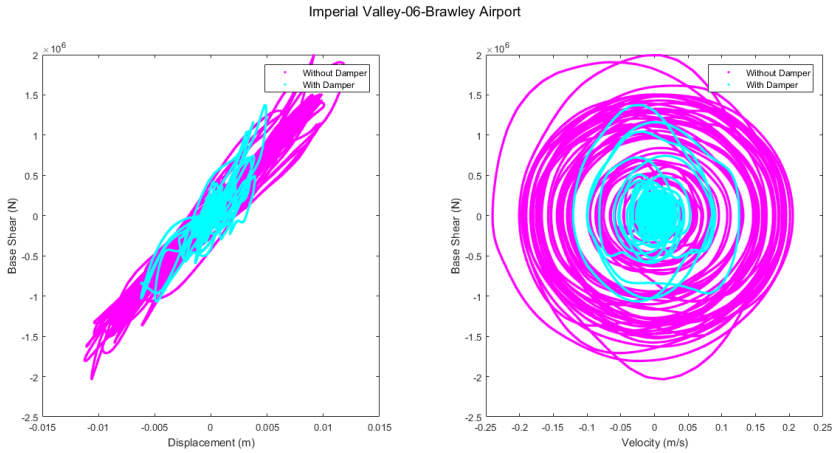

Figure 5-47 : Left –Base shear vs Displacement Right- Base shear vs Velocity for near-field pulse like Imperial Valley (06-Brawley Airport) earthquake

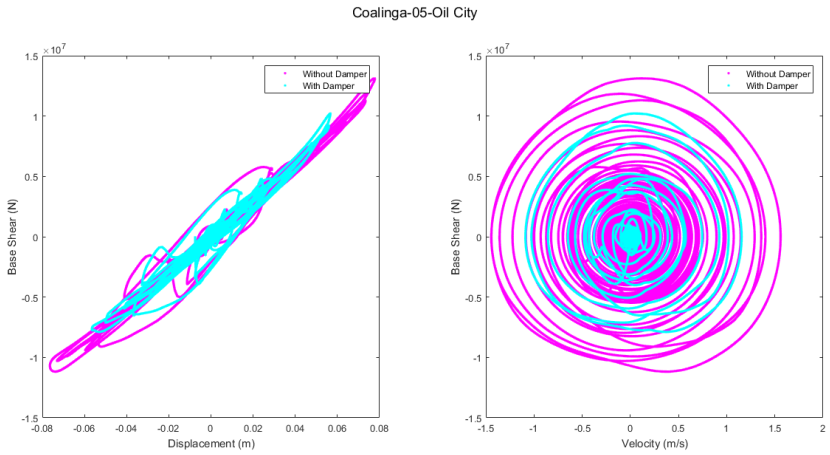

Figure 5-48 : Left –Base shear vs Displacement Right- Base shear vs Velocity for near-field pulse like Coalinga (05-Oil City) earthquake

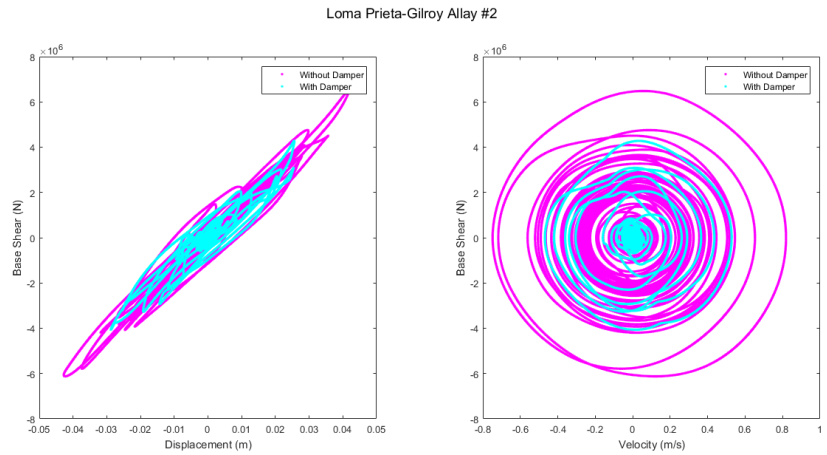

Figure 5-49: Left –Base shear vs Displacement Right- Base shear vs Velocity for near-field pulse like Loma Prieta (Gilroy Allay #2) earthquake

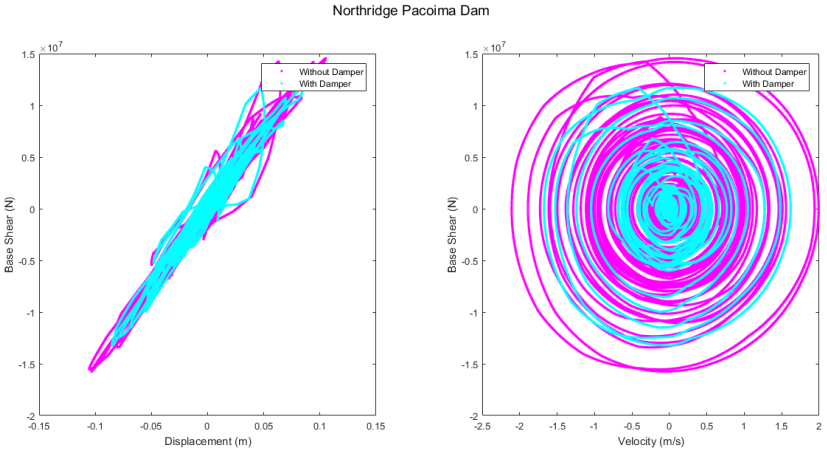

Figure 5-50: Left –Base shear vs Displacement Right- Base shear vs Velocity for near-field pulse like Northridge (Pacoima Dam) earthquake

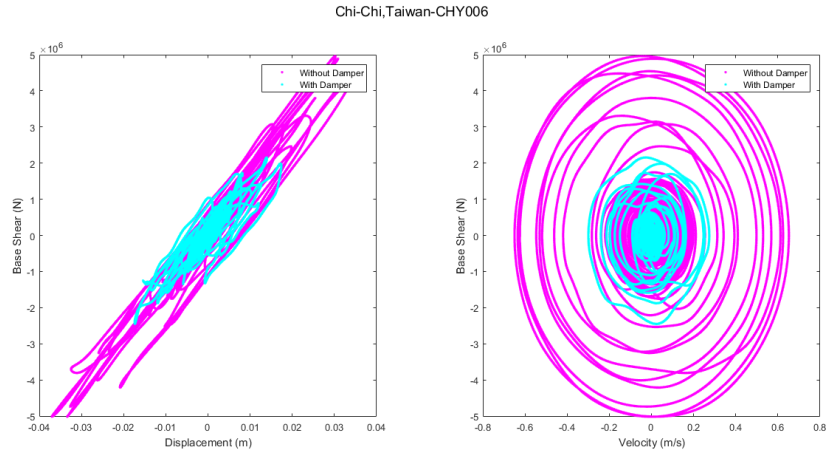

Figure 5-51: Left –Base shear vs Displacement Right- Base shear vs Velocity for near-field pulse like Chi Chi-Taiwan (CHY006) earthquake

5-12- Summary

In this chapter first, the seismic response of the modeled structure including displacement, velocity and acceleration subjected to Northridge and Manjil far-field earthquakes are discussed; and the performance of the damper, in different steps of the earthquake time, is investigated.

Then in a similar process, the functionality of the damper and seismic response of the structure subjected to Super Stition Hills and Erzincan far-field pulse like records are investigated.

In addition, the performance of the MR damper commanded by an On/Off control system and the proposed fuzzy control system is compared to show the efficiency of the fuzzy-controlled damper

Furthermore, the seismic response of the structure with and without fuzzy-controlled MR damper for the 44 far-field and 91 near-field pulse-like earthquakes are compared and summarized; and the probability curves for maximum seismic displacements of the structure for the two mentioned sets of the applied earthquakes, are drawn to illustrated the functionality level of the damper controlled by the proposed fuzzy system. Finally, the hysteresis loops of the structure with and without the damper subjected to five selected earthquakes are shown.

Chapter 6

Conclusion

6-1- Summary

In this research, by using the software Simulink and MATLAB, a dynamic system including a single degree of freedom 2D structure, a Magnetorheological damper and a fuzzy control unit are modeled. Then two sets of earthquake records including far-field and near-field pulse like earthquakes, are applied to the structure and the response of the structure in two conditions with the damper and without the damper were compared.

The applied earthquakes are of the most destructive ones which have occurred in different countries, mostly the US. As the main goal, the MR damper with the maximum 200 KN has been controlled by a fuzzy control unit which is designed based on Mamdani method using the expert knowledge.

The fuzzy controller utilizes the seismic displacement of the structure to adjust the viscosity of the MR damper to produce adaptive resistant force by driving the appropriate electricity current and producing an inductive electromagnetic field around the damper. It is also indicated that the proposed fuzzy control systems can be properly adapted with the MR damper and adjust it in the desired way to dissipate the energy of the applied earthquakes in the modeled structure, despite the fact that the system including the damper, the structure and the applied earthquake loads is so complex and non-linear.

It should be noticed that based on the characteristic of the magnetorheological fluid the damper can quickly response to the induced magnetic field and produce the desired resistant force. As mentioned before in this research in order to study the performance of the proposed damping system the effect of the 135 earthquake records including 44 far-field and 91 near-field pulse-like records on the modeled structure are investigated.

6-2- Conclusions

In this research a structure has been exposed to a variety of the most destructive earthquakes happened in the world since last 50 years.

The seismic behavior of the structure has been defined in two categories: equipped with a large-scale magnetorheological damper and without the damper.

Then the seismic demands of the both categories have been investigated in two phases:

First, against 44 far-field harsh earthquakes and second, against 91 near-field pulse-like strong earthquakes which are rarely investigated in previous researches.

In this study the behavior of the damper is simulated using the phenomenological spencer model.

Simulink and Matlab are the two main software used to simulate the studied dynamic system including the structure, damper and earthquakes. Furthermore, a fuzzy controller has been applied to the system to control the performance of the damper by adjusting the input electricity current to the damper.

An On/Off controller is designed and separately applied to the damper and its performance is investigated.

Based on the output of the Simulink model and comparative analyses the following results have been achieved.

- It is observed that the fuzzy controller has indicated better performance compared with the on/off controller; because the fuzzy controlled damper has dissipated the earthquake vibration better than the on/off controlled damper, using the same amount of energy.
- By comparing the fuzzy-controlled adaptive MR damper with a constant current driven MR damper with the same performance, it is observed that the fuzzy controlled one consumes less electricity energy therefore, it is more economic and reliable in harsh conditions.
- In the first phase, the fuzzy controlled damper has mitigated the average of maximum seismic demands of the structure including displacement, velocity, acceleration and vibration energy by energy by 38%, 40% ,36% and 83% respectively.
- In the second phase, the fuzzy controlled damper has dissipated the average of the maximum seismic demands including displacement, velocity, acceleration and vibration energy by 40%, 43% ,40% and 82% respectively.
- The results indicate that the control system designed by application of model-independent fuzzy method, can adjust the operation of the MR damper very well and improve the seismic response of the structure, despite the nonlinearity and complexity of the dynamic system including the structure, the MR damper and the applied earthquake forces.
- The output of the seismic demands including displacement, velocity and acceleration illustrate that although the fuzzy controller activates the damper since the start of earthquake, it takes the damper couple of seconds to reach its ideal and required performance which is called the response time of the MR damper.

- It is observed that utilizing state space method has simplified the complicated dynamic equation of the investigated dynamic system including the structure, the MR damper and the applied earthquake forces.
- The research has indicated that a large-scale 200 KN MR damper can be applicable in civil engineering structures to mitigate the seismic vibrations.
- The great number of the earthquakes with different characteristics utilized in this research has proofed the credibility of the designed adaptive MR damper theoretically. Considering the fact that the selected and investigated earthquakes are among the most destructive earthquakes that happened in the world, the results show that the fuzzy-controlled MR damper has efficiently dissipated the seismic vibrations of the structure and improved the seismic resilience of the structure.

6-3- Scope for future work

The following suggestions are proposed for the future studies and research.

- This system can be developed by improving the fuzzy control unit to a multi-input and single output system, in which the inputs are the displacement, velocity and acceleration, and the output is the electricity current used to control performance of the damper
- The fuzzy control system with different fuzzy rules can be defined and utilized to adjust the MR damper; then the performance of the adaptive damper can be compared in order to find the most effective fuzzy system.
- The performance of the adaptive semi active damping system can be investigated in multi-story structures.
- The research can be developed by studying the seismic demands of a multi-story structure equipped with several adaptive MR dampers and finding the best location for installing the dampers where they function more effectively.

References

Baker, J. W. "Quantitative classification of near-fault ground motions using wavelet analysis." *Bulletin of the Seismological Society of America* 97 (5):1486-1501. 2007.

Baker, J. W. "Efficient analytical fragility function fitting using dynamic structural analysis." *Earthquake Spectra* 31 (1):579-599. 2015.

BBC. "British Broadcasting Corporation (BBC)." www.bbc.com, June 2018.

Bertero, V. V., Mahin, S. A., and Herrera, R. A. "Aseismic design implications of near-fault San Fernando earthquake records." *Earthquake engineering & structural dynamics* 6 (1):31-42. 1978.

Bruneau, M., Uang, C.-M., and Whittaker, A. "Ductile Design of Steel Structures, MaGraw-Hill Companies." *Inc., NY, USA*. 1998.

Casciati, F., Magonette, G., and Marazzi, F. *Technology of semiactive devices and applications in vibration mitigation*: John Wiley & Sons.2006.

Chopra, A. K. "Dynamics of structures: Theory and applications." 2001.

Damptech. www.damptech.com, June 2018.

Dyke, S., Spencer Jr, B., Sain, M., and Carlson, J. "Modeling and control of magnetorheological dampers for seismic response reduction." *Smart materials and structures* 5 (5):565. 1996.

Esteki, K., Bagchi, A., and Sedaghati, R. "Semi-active control of seismic response of a building using MR fluid-based tuned mass damper." *Smart Structures and Systems* 16 (5):807-833. 2015.

FEMA. "National Earthquake Hazard Reduction Program (NEHRP) recommended provisions for seismic regulations for 348 new buildings and other structures—part 2: commentary (FEMA 450-2)." *Federal Emergency Management Agency, Washington, DC*. 2003.

FEMA, P. "695. Quantification of Building Seismic Performance Factors." *Federal Emergency Management Agency*. 2009.

Feng, M. Q., Shinozuka, M., and Fujii, S. "Friction-controllable sliding isolation system." *Journal of engineering mechanics* 119 (9):1845-1864. 1993.

Filiatrault, A., Robert, T., Constantin, C., and Didier, P. *Elements of earthquake engineering and structural dynamics*: Presses inter Polytechnique.2013.

Franklin, G. F., Powell, J. D., Emami-Naeini, A., and Powell, J. D. *Feedback control of dynamic systems*. Vol. 3: Addison-Wesley Reading, MA.1994.

Henrie, A. J. M., and Carlson, J. D. "Magnetorheological Fluids." *Encyclopedia of Smart Materials*. 2002.

Kurata, M., Leon, R., and DesRoches, R. "Rapid seismic rehabilitation strategy: concept and testing of cable bracing with couples resisting damper." *Journal of structural engineering* 138 (3):354-362. 2011.

Kwok, N., Ha, Q., Nguyen, M., Li, J., and Samali, B. "Bouc–Wen model parameter identification for a MR fluid damper using computationally efficient GA." *ISA transactions* 46 (2):167-179. 2007.

Lagaros, N. D., Plevris, V., and Mitropoulou, C. C. *Design optimization of active and passive structural control systems*: IGI Global.2012.

Lee, D., and Taylor, D. P. "Viscous damper development and future trends." *The Structural Design of Tall and Special Buildings* 10 (5):311-320. 2001.

Li, C. "Performance of multiple tuned mass dampers for attenuating undesirable oscillations of structures under the ground acceleration." *Earthquake Engineering & Structural Dynamics* 29 (9):1405-1421. 2000.

Lilly, J. H. *Fuzzy control and identification*: John Wiley & Sons.2011.

LORD. www.lord.com, June 2018.

Lu, L.-Y., Lin, C.-C., and Lin, G.-L. "Experimental evaluation of supplemental viscous damping for a sliding isolation system under pulse-like base excitations." *Journal of Sound and Vibration* 332 (8):1982-1999. 2013.

Mahin, S. A. "Lessons from damage to steel buildings during the Northridge earthquake." *Engineering structures* 20 (4-6):261-270. 1998.

Mamdani, E. H., and Gaines, B. R. *Fuzzy reasonings and its applications*: Academic Press, Inc.1981.

Naeim, F., and Kelly, J. M. *Design of seismic isolated structures: from theory to practice*: John Wiley & Sons.1999.

Narasimhan, S., and Nagarajaiah, S. "Smart base isolated buildings with variable friction systems: H∞ controller and SAIVF device." *Earthquake engineering & structural dynamics* 35 (8):921-942. 2006.

Nise, N. S. "Control system engineering, John Wiley & Sons." *Inc, New York*. 2011.

Ogata, K. "Modern control engineering." *Book Reviews* 35 (1181):1184. 1999.

Oppenheim, A. V., Willsky, A. S., and Nawab, S. H. *Señales y sistemas*: Pearson Educación.1998.

PEER. "Pacific Earthquake Engineering Research Center,." https://ngawest2.berkeley.edu, June 2018.

Pinkaew, T., and Fujino, Y. "Effectiveness of semi-active tuned mass dampers under harmonic excitation." *Engineering Structures* 23 (7):850-856. 2001.

QUAKETEK. www.quaketek.com, June 2018.

Robinson Seismic. www.rslir.com, June 2018.

Sapiński, B., and Filuś, J. "Analysis of parametric models of MR linear damper." *Journal of Theoretical and Applied Mechanics* 41 (2):215-240. 2003.

Sato, E., and Fujita, T. "Controllable friction damper using piezoelectric actuators for semi-active seismic isolation system." Proceedings of 13th world conference on earthquake engineering.2004.

Somerville, P. G., Smith, N. F., Graves, R. W., and Abrahamson, N. A. "Modification of empirical strong ground motion attenuation relations to include the amplitude and duration effects of rupture directivity." *Seismological Research Letters* 68 (1):199-222. 1997.

Soong, T. T., and Costantinou, M. C. *Passive and active structural vibration control in civil engineering*. Vol. 345: Springer.2014.

Spencer Jr, B., Dyke, S., Sain, M., and Carlson, J. "Phenomenological model for magnetorheological dampers." *Journal of engineering mechanics* 123 (3):230-238. 1997.

Tan, P., and Agrawal, A. K. "Benchmark structural control problem for a seismically excited highway bridge—part II: phase I sample control designs." *Structural Control and Health Monitoring* 16 (5):530-548. 2009.

Tena-Colunga, A. "Mathematical modelling of the ADAS energy dissipation device." *Engineering Structures* 19 (10):811-821. 1997.

TESoulution. www.tesolution.com, June 2018.

UNITED NATIONS. www.un.org/development/desa/en/. 2018.

Villarreal, K., Wilson, C., and Abdullah, M. "Effects of MR damper placement on structure vibration parameters." REUJAT Symposium, Tokyo, Japan.2004.

www.tesolution.com. "TESolution."

Yamamoto, Masashi, Sone, and Takayuki. "Behavior of active mass damper (AMD) installed in high-rise building during 2011 earthquake off Pacific coast of Tohoku and verification of regenerating system of AMD based on monitoring." *Structural Control and Health Monitoring* 21 (4):634-647. 2014.

Yang, D.-H., Shin, J.-H., Lee, H., Kim, S.-K., and Kwak, M. K. "Active vibration control of structure by active mass damper and multi-modal negative acceleration feedback control algorithm." *Journal of Sound and Vibration* 392:18-30. 2017.

Yang, G., Spencer Jr, B., Carlson, J., and Sain, M. "Large-scale MR fluid dampers: modeling and dynamic performance considerations." *Engineering structures* 24 (3):309-323. 2002.

Yang, G., Spencer Jr, B. F., Jung, H.-J., and Carlson, J. D. "Dynamic modeling of large-scale magnetorheological damper systems for civil engineering applications." *Journal of Engineering Mechanics* 130 (9):1107-1114. 2004.

Yoshioka, H., Ramallo, J., and Spencer Jr, B. ""Smart" base isolation strategies employing magnetorheological dampers." *Journal of engineering mechanics* 128 (5):540-551. 2002.

Appendix I
Analytical Results

Table AI- 1: List of assigned indexes to 44 far field earthquakes.

No.	Event name and index	Number	Event name and index
1	Northridge 120111	23	Northridge 120112
2	Northridge 120121	24	Northridge 120122
3	Duzce 120411	25	Duzce 120412
4	Hector Mine120521	26	Hector Mine120522
5	Imperial Valley 120611	27	Imperial Valley 120612
6	Imperial Valley 120621	28	Imperial Valley 120622
7	Kobe 120711	29	Kobe 120712
8	Kobe 120721	30	Kobe 120722
9	Koca Eli1 20811	31	Koca Eli1 20812
10	Koca Eli 120821	32	Kocaeli 120822
11	Landers 120911	33	Landers 120912
12	Landers 120921	34	Landers 120922
13	Loma Prieta 121011	35	Loma Prieta 121012
14	Loma Prieta 121021	36	Loma Prieta 121022
15	Manjil 121111	37	Manjil 121112
16	Super Stition Hills 121211	38	Super Stition Hills 121212
17	Super Stition Hills 121221	39	Super Stition Hills 121222
18	Cape Mendocino 121321	40	Cape Mendocino 121322
19	Chi Chi 121411	41	Chi Chi 121412
20	Chi Chi 121421	42	Chi Chi 121422
21	San Fernando121511	43	San Fernando121512
22	Friuli 121711	44	Friuli 121712

Table AI- 2: List of assigned indexes to 91 near field earthquakes.

No.	Event name	Station	No.	Event name	Station	No.	Event name	Station
1	San Fernando	Pacoima Dam (upper lef abut)	31	Superstition Hills-02	Parachute Test Site	62	Chi-Chi, Taiwan	TCU034
2	Coyote Lake	Gilroy Array #6	32	Loma Prieta	Alameda Naval Air Stn Hanger	63	Chi-Chi, Taiwan	TCU036
3	Imperial Valley-06	Aeropuerto Mexicali	33	Loma Prieta	Gilroy Array #2	64	Chi-Chi, Taiwan	TCU038
4	Imperial Valley-06	Agrarias	34	Loma Prieta	Oakland - Outer Harbor Wharf	65	Chi-Chi, Taiwan	TCU040
5	Imperial Valley-06	Brawley Airport	35	Loma Prieta	Saratoga - Aloha Ave	66	Chi-Chi, Taiwan	TCU042
6	Imperial Valley-06	EC County Center FF	36	Erzican, Turkey	Erzincan	67	Chi-Chi, Taiwan	TCU046
7	Imperial Valley-06	EC Meloland Overpass FF	37	Cape Mendocino	Petrolia	68	Chi-Chi, Taiwan	TCU049
8	Imperial Valley-06	El Centro Array #10	38	Landers	Barstow	69	Chi-Chi, Taiwan	TCU053
9	Imperial Valley-06	El Centro Array #11	39	Landers	Lucerne	70	Chi-Chi, Taiwan	TCU054
10	Imperial Valley-06	El Centro Array #3	40	Landers	Yermo Fire Station	71	Chi-Chi, Taiwan	TCU056
11	Imperial Valley-06	El Centro Array #4	41	Northridge-01	Jensen Filter Plant	72	Chi-Chi, Taiwan	TCU060
12	Imperial Valley-06	El Centro Array #5	42	Northridge-01	Jensen Filter Plant Generator	73	Chi-Chi, Taiwan	TCU065
13	Imperial Valley-06	El Centro Array #6	43	Northridge-01	LA - Wadsworth VA Hospital North	74	Chi-Chi, Taiwan	TCU068
14	Imperial Valley-06	El Centro Array #7	44	Northridge-01	LA Dam	75	Chi-Chi, Taiwan	TCU075
15	Imperial Valley-06	El Centro Array #8	45	Northridge-01	Newhall - W Pico Canyon Rd.	76	Chi-Chi, Taiwan	TCU076
16	Imperial Valley-06	El Centro Differential Array	46	Northridge-01	Pacoima Dam (downstr)	77	Chi-Chi, Taiwan	TCU082
17	Imperial Valley-06	Holtville Post Office	47	Northridge-01	Pacoima Dam (upper left)	78	Chi-Chi, Taiwan	TCU087
18	Mammoth Lakes-06	Long Valley Dam (Upr L Abut)	48	Northridge-01	Rinaldi Receiving Sta	79	Chi-Chi, Taiwan	TCU098
19	Irpinia, Italy-01	Sturno	49	Northridge-01	Sylmar - Converter Sta	80	Chi-Chi, Taiwan	TCU101
20	Westmorland	Parachute Test Site	50	Northridge-01	Sylmar - Converter Sta East	81	Chi-Chi, Taiwan	TCU102
21	Coalinga-05	Oil City	51	Northridge-01	Sylmar - Olive View Med FF	82	Chi-Chi, Taiwan	TCU103
22	Coalinga-05	Transmitter Hill	52	Kobe, Japan	Takarazuka	83	Chi-Chi, Taiwan	TCU104
23	Coalinga-07	Coalinga-14th & Elm (Old CHP)	53	Kobe, Japan	Takatori	84	Chi-Chi, Taiwan	TCU128
24	Morgan Hill	Coyote Lake Dam (SW Abut)	54	Kocaeli, Turkey	Gebze	85	Chi-Chi, Taiwan	TCU136
25	Morgan Hill	Gilroy Array #6	55	Chi-Chi, Taiwan	CHY006	86	Northwest China-03	Jiashi
26	Taiwan SMART1(40)	SMART1 C00	56	Chi-Chi, Taiwan	CHY035	87	Yountville	Napa Fire Station #3
27	Taiwan SMART1(40)	SMART1 M07	57	Chi-Chi, Taiwan	CHY101	88	Chi-Chi, Taiwan-03	CHY024
28	N. Palm Springs	North Palm Springs	58	Chi-Chi, Taiwan	TAP003	89	Chi-Chi, Taiwan-03	CHY080
29	San Salvador	Geotech Investig Center	59	Chi-Chi, Taiwan	TCU029	90	Chi-Chi, Taiwan-03	TCU076
30	Whittier Narrows-01	Downey - Co Maint Bldg	60	Chi-Chi, Taiwan	TCU031	91	Chi-Chi, Taiwan-06	CHY101
31	Whittier Narrows-01	LB - Orange Ave	61	Chi-Chi, Taiwan	TCU034			

Table AI-3 :Maximum displacements of the model with and without damper subjected to 44 far-field earthquake records

Event	Max Displacement Without Damper(m)	Max Displacement With Damper(m)	Displacement Dissipation %
1	0.02915066	0.018135768	37.78607922
2	0.037314738	0.029256361	21.5956944
3	0.045353731	0.024670444	45.60437802
4	0.043450851	0.030892205	28.90310788
5	0.106425416	0.073535688	30.90401652
6	0.049283	0.032003581	35.06162139
7	0.022608018	0.008851544	60.84776696
8	0.037253785	0.022046204	40.82157336
9	0.036867876	0.011152019	69.75139215
10	0.053963226	0.014433991	73.25217167
11	0.038348315	0.023230091	39.42343841
12	0.042653608	0.029920998	29.85119124
13	0.044202945	0.032473971	26.53437208
14	0.035582801	0.021989267	38.20254034
15	0.021568183	0.009324447	56.76758499
16	0.018550183	0.009312203	49.79994003
17	0.031133206	0.018840242	39.48505601
18	0.028618201	0.028213072	1.4156338
19	0.006388517	0.00554378	13.22274572
20	0.007927367	0.004425779	44.17087628
21	0.016186626	0.009001136	44.3915247
22	0.016741098	0.009011806	46.16956154
23	0.043513948	0.027552277	36.68173485
24	0.033403233	0.0203339	39.12595369
25	0.059084694	0.05209177	11.83542382
26	0.043920373	0.022088502	49.70784414
27	0.034576433	0.025656085	25.79892692
28	0.041119354	0.026340595	35.94112691
29	0.042200238	0.030241672	28.33767529
30	0.053111047	0.034994708	34.11030277
31	0.024706146	0.013227612	46.46023513
32	0.015614952	0.00819355	47.52753713
33	0.025646351	0.015235888	40.59237425
34	0.031084751	0.01687516	45.71241616
35	0.050894379	0.01937505	61.9308649
36	0.052400849	0.036704857	29.95369786
37	0.028154485	0.012743386	54.73763255
38	0.025535953	0.019997874	21.68738079
39	0.028994681	0.029510754	-1.779889101
40	0.026133524	0.020732247	20.66800032
41	0.020708674	0.010628099	48.67803255
42	0.015985702	0.006216637	61.11126821
43	0.032952645	0.017510788	46.86074899
44	0.030063372	0.018377211	38.87175742
			Average= 38.6%

Table AI-4 :Maximum velocities of the model with and without damper subjected to 44 far-field earthquake records

Event	Max Velocity Without Damper	Max Velocity With Damper	Velocity Dissipation %
1	0.531382941	0.317992842	40.15749883
2	0.59486827	0.471076953	20.80987055
3	0.830380759	0.441274551	46.85876978
4	0.834841808	0.564143057	32.42515506
5	2.013836283	1.391564857	30.89980209
6	0.892292074	0.5612881	37.0959222
7	0.413117289	0.166326463	59.73868268
8	0.69270206	0.38786664	44.00671482
9	0.70866537	0.223554526	68.45414837
10	1.026242474	0.258270145	74.83341888
11	0.812135901	0.470435428	42.0742973
12	0.825241983	0.583705894	29.26851679
13	0.824017381	0.577572619	29.907714
14	0.632517809	0.411310706	34.97247022
15	0.39202706	0.111538032	71.5483844
16	0.323407427	0.146676842	54.64642123
17	0.581133536	0.299459418	48.46977517
18	0.496598536	0.487929835	1.745615534
19	0.122758623	0.104243137	15.08283926
20	0.145522192	0.083549206	42.58662212
21	0.267200043	0.119453496	55.2943577
22	0.311730152	0.188310338	39.59187553
23	0.789380678	0.508875957	35.53478429
24	0.616594596	0.345763994	43.92360933
25	1.087320603	0.964950527	11.25427737
26	0.772666348	0.407031293	47.32120868
27	0.791505729	0.630931443	20.28719185
28	0.828866388	0.519907472	37.27487573
29	0.809252215	0.643879134	20.43529543
30	1.060915688	0.693518642	34.63018313
31	0.475070717	0.238614843	49.77277393
32	0.268491584	0.169982598	36.68978528
33	0.488814929	0.269800479	44.80518836
34	0.575436594	0.304296465	47.11902794
35	0.969092782	0.380623594	60.72372005
36	1.034188763	0.697124997	32.59209319
37	0.505426015	0.205908241	59.26045856
38	0.441798293	0.263953684	40.25470718
39	0.554058835	0.471735879	14.85816132
40	0.491203442	0.363023514	26.09507933
41	0.414607417	0.195330006	52.88796143
42	0.316465004	0.136568733	56.84554969
43	0.636823985	0.357466161	43.86735279
44	0.608226703	0.313002572	48.53850206
			Average= 40.57%

Table AI-5 :Maximum acceleratins of the model with and without damper subjected to 44 far-field earthquake records

Event	Max Acceleration Without Damper	Max Acceleration With Damper	Acceleration Dissipation %
1	10.12807068	6.372055101	37.08520308
2	12.22110149	8.666392018	29.08665374
3	16.64494708	8.99767144	45.94352631
4	16.49078428	12.34638692	25.13159644
5	38.63308807	26.81322854	30.59517146
6	17.09112017	10.84485063	36.5468704
7	7.992623299	3.873480143	51.53681091
8	13.34513722	7.47850369	43.96083335
9	13.78797666	4.747734253	65.56612788
10	20.45108965	6.599847584	67.72862622
11	16.85522602	10.55118559	37.40110293
12	15.83050245	12.57484425	20.56572883
13	16.43678342	12.88188207	21.62771908
14	12.4550461	7.861146579	36.88384199
15	7.324273315	2.315130252	68.39099044
16	6.31121953	3.123629914	50.50671428
17	11.10332069	5.642103205	49.18544313
18	9.131627935	9.348714873	-2.377308182
19	3.141889432	2.716628564	13.53519521
20	3.237687518	2.141739158	33.84972621
21	4.685438008	2.691676455	42.55229818
22	6.238159523	3.449293484	44.70655213
23	15.14216867	10.12944927	33.10436905
24	11.96038389	7.35339539	38.51873436
25	20.49491705	19.04888898	7.055544851
26	13.82330305	8.547707681	38.16450636
27	16.46390479	13.76555145	16.38951007
28	16.06269707	11.57150947	27.960358
29	16.40996885	13.39270372	18.38678157
30	21.72934641	14.91732588	31.3494037
31	9.456332738	5.32279679	43.71182849
32	5.298208579	4.077135438	23.04690581
33	9.155492459	5.210980723	43.08355617
34	11.01279133	6.033506752	45.21364683
35	18.75620212	9.002342762	52.00338159
36	20.12069283	14.92265548	25.8342861
37	9.704571457	4.88788883	49.63313062
38	9.188787732	5.678980386	38.19663103
39	10.79298837	9.807015502	9.135309287
40	9.7208275	8.163558652	16.01992062
41	8.242252683	4.524763442	45.10283031
42	6.331896016	3.546119377	43.99593159
43	12.76109589	7.523193018	41.04587035
44	11.90552957	7.384599811	37.97336131
			Average= 35.79%

Table AI-6: Comparison of the seismic energy of the model with and without damper subjected to 44 far-field earthquake records

Event	AUC-With	AUC-Without	Energy-Dissipation %
1	0.000329237	0.002057071	83.99488611
2	0.000565653	0.001917084	70.49408718
3	0.000400056	0.004778119	91.62733261
4	0.000295572	0.001063938	72.21901693
5	0.004934845	0.021469389	77.01450604
6	0.000495132	0.003504538	85.87170135
7	9.73711E-05	0.000728423	86.63262161
8	0.000357354	0.002564507	86.0654062
9	0.000366532	0.006822341	94.62747103
10	0.000433242	0.007297687	94.06330385
11	0.000515921	0.003111418	83.41847003
12	0.000479197	0.002784572	82.79100016
13	0.000720005	0.004801579	85.00483706
14	0.000404584	0.002120603	80.9212968
15	7.35085E-05	0.001131105	93.50117795
16	7.87511E-05	0.000448146	82.42735503
17	0.000229302	0.001452695	84.2154376
18	0.000268167	0.000737541	63.64039882
19	1.44466E-05	0.000117579	87.71325948
20	1.58363E-05	8.56671E-05	81.51410426
21	7.76758E-05	0.000354951	78.11646225
22	8.09492E-05	0.000807261	89.97237049
23	0.000513506	0.00353352	85.46758356
24	0.000422552	0.001162401	63.64836461
25	0.002302078	0.007661043	69.95085238
26	0.000464611	0.00343895	86.48973666
27	0.000323142	0.001789773	81.94508676
28	0.000306795	0.002720097	88.72117225
29	0.001124733	0.008743144	87.13582838
30	0.001370457	0.00910324	84.94539217
31	0.000141583	0.00160928	91.20209634
32	5.71773E-05	0.000549789	89.60013323
33	0.000335048	0.00154253	78.27935395
34	0.000331786	0.00264656	87.46350515
35	0.000393151	0.006578753	94.02393123
36	0.00152564	0.007220907	78.87190909
37	0.000281753	0.00332155	91.51743953
38	0.000292234	0.001789491	83.66944107
39	0.000331119	0.002090552	84.16118714
40	0.000242356	0.001112481	78.21479026
40	9.81671E-05	0.000509962	80.75013019
41	3.12364E-05	0.000677445	95.38908236
42	0.000195868	0.001453071	86.52041341
43	0.000238303	0.001543059	84.55648421
44	0.000329237	0.002057071	83.99488611
			Average=83.83%

Table AI-7: Maximum displacements of the model with and without damper subjected to 91 near-field pulse-like earthquake records

Event	Max Displacement Without Damper	Max Displacement With Damper	Displacement Dissipation %
1	0.057843487	0.053987503	6.66623793
2	0.025918716	0.013381842	48.36996687
3	0.028387641	0.013058654	53.99880347
4	0.016680738	0.008748841	47.55123778
5	0.011896167	0.006834088	42.55218258
6	0.015390136	0.006761103	56.06859762
7	0.023346201	0.016867764	27.74942857
8	0.026895982	0.010399143	61.3356987
9	0.043984716	0.029160696	33.70266311
10	0.01470515	0.006864903	53.3163367
11	0.023731978	0.012735109	46.33776709
12	0.040464495	0.02970585	26.58786496
13	0.027474591	0.018297451	33.40227986
14	0.023103812	0.019299823	16.46476935
15	0.029668317	0.014344231	51.65134876
16	0.026625301	0.023928738	10.12781865
17	0.047916653	0.021161975	55.83586672
18	0.027348783	0.018599095	31.99296913
19	0.024042049	0.012500627	48.00515301
20	0.015384011	0.007134177	53.62603066
21	0.077782228	0.057027274	26.68341324
22	0.028851307	0.027375985	5.113536321
23	0.063105725	0.05498576	12.8672409
24	0.048412501	0.043508292	10.13004704
25	0.020274224	0.01400647	30.91489023
26	0.011582776	0.005403696	53.34714076
27	0.009968072	0.006100973	38.79485107
28	0.056656014	0.04302148	24.06546644
29	0.067977264	0.057142018	15.9395146
30	0.023040088	0.009859549	57.206982
31	0.023471729	0.012271866	47.71639267

Event	Max Displacement Without Damper	Max Displacement With Damper	Displacement Dissipation %
32	0.02821649	0.019274732	31.68983258
33	0.007855288	0.00537239	31.60797581
34	0.042770785	0.028638101	33.04284394
35	0.022662366	0.014823688	34.58896656
36	0.026841127	0.017762359	33.82409319
37	0.036641607	0.021249332	42.00764234
38	0.046073347	0.022339872	51.51237393
39	0.012894334	0.006545613	49.23651854
40	0.02964512	0.016096599	45.70236491
41	0.019655784	0.009619247	51.06149257
42	0.047686243	0.035707946	25.118978
43	0.047691338	0.035709679	25.12334328
44	0.012142275	0.008422268	30.63682361
45	0.03797671	0.024289719	36.04048588
46	0.027975571	0.015780221	43.59285386
47	0.045715581	0.038904036	14.89983294
48	0.105521951	0.085569046	18.90877226
49	0.063915468	0.04912792	23.13610199
50	0.049745608	0.021510344	56.75931128
51	0.068005662	0.05165765	24.03919301
52	0.079503087	0.063685269	19.89585336
53	0.03961389	0.027941263	29.46599603
54	0.054862838	0.031356737	42.84521434
55	0.017621634	0.010063644	42.8904044
56	0.037027108	0.017711836	52.16521786
57	0.038092292	0.016257214	57.32151333
58	0.030907456	0.013471024	56.41496915
59	0.013328087	0.005377723	59.65120026
60	0.010780304	0.006974555	35.30279506

Event	Max Displacement Without Damper	Max Displacement With Damper	Displacement Dissipation %
61	0.014541497	0.005199709	64.24226988
62	0.019970579	0.010172025	49.06494632
63	0.017787613	0.008156119	54.1471966
64	0.025646826	0.006600773	74.26280673
65	0.013860223	0.006802654	50.91959473
66	0.035665934	0.014253564	60.03591499
67	0.021992388	0.00840987	61.7600893
68	0.016403783	0.009639075	41.23870618
69	0.022850227	0.015538316	31.99929363
70	0.014400984	0.007824437	45.66734837
71	0.019838422	0.006626904	66.59560821
72	0.018768013	0.008959852	52.25998282
73	0.033108014	0.022185091	32.99177778
74	0.040654788	0.034134596	16.03794499
75	0.033194722	0.02058484	37.98761128
76	0.05363786	0.021507258	59.90284101
77	0.029208077	0.01581189	45.86466668
78	0.010973408	0.004838084	55.91083353
79	0.013098299	0.005494441	58.05225575
80	0.025197791	0.010979775	56.42564621
81	0.01666651	0.009358314	43.8495907
82	0.011654284	0.006993049	39.99589088
83	0.008060247	0.003746795	53.51513809
84	0.012070111	0.005709459	52.69754467
85	0.013150682	0.008202422	37.62740418
86	0.02766611	0.014112757	48.9890109
87	0.023801576	0.020026264	15.86160404
88	0.016057782	0.008830898	45.00549529
89	0.015902266	0.011181661	29.68511388
90	0.02024602	0.019234767	4.994826513
91	0.015790927	0.007653567	51.53186598
			Average=40.28%

Table AI-8: Maximum velocitiesof the model with and without damper subjected to 91 near-field pulse-like earthquake records

Event	Max Velocity Without Damper	Max Velocity With Damper	Velocity Dissipation %
1	0.964961622	0.864334131	10.42813394
2	0.391360057	0.194562112	50.28564906
3	0.538299117	0.249023156	53.73888825
4	0.288728279	0.155816496	46.03351743
5	0.24000906	0.135824394	43.40863876
6	0.251723145	0.119371082	52.57842404
7	0.324360265	0.171335984	47.17725874
8	0.49653381	0.183838097	62.9757142
9	0.851709673	0.569598913	33.12287854
10	0.300696189	0.155010767	48.44937419
11	0.452279768	0.145870679	67.74768851
12	0.711103001	0.493831925	30.55409358
13	0.482403614	0.330702571	31.44691266
14	0.327195228	0.189264258	42.15555687
15	0.523717609	0.291693635	44.30325993
16	0.509727142	0.46423412	8.924975418
17	0.917908888	0.333834849	63.63093842
18	0.525360341	0.362886588	30.92615485
19	0.473196947	0.264503141	44.10294865
20	0.291894471	0.140766494	51.77486792
21	1.55936345	1.161037589	25.54413222
22	0.461005995	0.425883077	7.618755247
23	1.161232365	1.057731519	8.913017676
24	0.970048522	0.800679085	17.4598933
25	0.434379523	0.325518549	25.06125834
26	0.195120049	0.097326331	50.11976939
27	0.160661936	0.090256753	43.8219437
28	1.126068992	0.85199053	24.33940225
29	1.327622836	1.094024079	17.59526503
30	0.438220714	0.152533783	65.19247526
31	0.423265454	0.194939484	53.94391823

Event	Max Velocity Without Damper	Max Velocity With Damper	Velocity Dissipation %
32	0.496625678	0.275564217	44.51269253
33	0.118636521	0.084039968	29.16180639
34	0.818329783	0.524249975	35.93658864
35	0.423513449	0.17373197	58.97840547
36	0.478053199	0.306568559	35.87145549
37	0.630774245	0.344140934	45.44150518
38	0.928612717	0.403147938	56.58599859
39	0.238917376	0.101035548	57.71109245
40	0.598452511	0.389621491	34.89516975
41	0.324949593	0.13288382	59.10632816
42	0.91358135	0.557497295	38.97672109
43	0.913648736	0.557496963	38.98125822
44	0.235657783	0.162391072	31.09029951
45	0.669465893	0.35800917	46.5231651
46	0.422867563	0.209311596	50.50185589
47	0.86603302	0.711537913	17.83940141
48	2.108444695	1.679003748	20.36766473
49	1.227821145	0.926450627	24.54514813
50	0.909695144	0.317572868	65.09018764
51	1.231457829	0.935616322	24.02368153
52	1.539882891	1.100110492	28.55882101
53	0.654517274	0.58887156	10.02963809
54	0.966110983	0.526311372	45.52268
55	0.319500605	0.155811233	51.2328834
56	0.651971724	0.305552125	53.13414466
57	0.707526192	0.267582441	62.18056044
58	0.559993494	0.203323542	63.69180287
59	0.229864439	0.088071612	61.68541224
60	0.189220403	0.13664759	27.78390295

Event	Max Velocity Without Damper	Max Velocity With Damper	Velocity Dissipation %
61	0.268005879	0.077478117	71.09088885
62	0.324915765	0.160325988	50.65613766
63	0.323739356	0.142609724	55.94921606
64	0.481605399	0.127359451	73.55522771
65	0.244212321	0.104425031	57.24006465
66	0.658292202	0.241312124	63.34270358
67	0.440534035	0.157132532	64.33135256
68	0.294607698	0.19019415	35.44155463
69	0.422887638	0.25705659	39.21397387
70	0.270594966	0.104447641	61.40074513
71	0.349452422	0.105911409	69.69218053
72	0.33804864	0.158553837	53.0973302
73	0.621894364	0.372165368	40.15617619
74	0.63525545	0.507138532	20.16777935
75	0.63010971	0.370468646	41.20569167
76	0.985430475	0.410631095	58.32977513
77	0.536766914	0.239959015	55.29549064
78	0.206099214	0.089888034	56.38603765
79	0.219121253	0.118474354	45.93205689
80	0.415581509	0.212340555	48.9051966
81	0.252410853	0.096952379	61.5894572
82	0.218782999	0.09725916	55.54537579
83	0.149044419	0.060138352	59.65071845
84	0.233128593	0.101326909	56.53604407
85	0.245684327	0.095903828	60.9646129
86	0.506906959	0.26504674	47.71294112
87	0.45851414	0.407101126	11.21296149
88	0.291775801	0.165095327	43.4170597
89	0.212075538	0.130961524	38.247699
90	0.2579963	0.26230885	-1.67155514
91	0.264093984	0.116077763	56.04679784
91			Average=43.67%

Table AI-9: Maximum acceleratins of the model with and without damper subjected to 91 near-field pulse-like earthquake records

Event	Max Acceleration Without Damper	Max Acceleration With Damper	Acceleration Dissipation %
1	23.38802196	21.06692204	9.924310487
2	7.304744866	4.001616714	45.21893937
3	10.82582464	5.815038292	46.28549338
4	5.49079356	3.509225747	36.08891486
5	5.082776547	3.704227973	27.12195906
6	4.961331909	2.234544271	54.96079859
7	6.024706058	3.356090186	44.29454063
8	10.06388193	3.918621494	61.06252518
9	16.26390506	12.13398677	25.39315295
10	6.088498238	3.621858078	40.51311281
11	8.7559993	3.735310438	57.33998702
12	13.35602499	9.153247177	31.46728026
13	9.281552321	7.095453478	23.55315973
14	5.606793563	3.200633676	42.91507901
15	11.4187554	7.381492541	35.35641771
16	10.16218949	10.45756391	-2.906602214
17	17.94526024	7.37450362	58.90556323
18	9.639315875	7.25769732	24.70734008
19	8.927728015	6.153974742	31.0689715
20	5.652738117	3.390852702	40.0139785
21	32.79408109	25.65277245	21.77621207
22	8.602999921	7.984971398	7.183872241
23	24.66529562	22.11271377	10.34888
24	20.65021066	17.98196433	12.9211579
25	9.621657857	7.042474565	26.80601754
26	3.705651386	2.035971206	45.05767021
27	2.948029793	1.434171556	51.35152434
28	23.65680402	18.86460659	20.25716331
29	24.56073076	20.18134904	17.83082827
30	8.979227372	3.51843213	60.81586996

Event	Max Acceleration Without Damper	Max Acceleration With Damper	Acceleration Dissipation %
31	8.186327921	4.05190101	50.50404713
32	10.11375855	5.272282133	47.87019971
33	2.306501656	2.281230036	1.095668874
34	16.19853151	10.64746741	34.26893422
35	8.051227651	3.838624262	52.32249754
36	9.94631754	6.665946235	32.98076189
37	12.225784	7.970346091	34.80707586
38	18.11882465	8.703725249	51.9630803
39	4.77700014	2.015774572	57.80250131
40	15.39235415	10.28206338	33.20018965
41	6.673364617	2.616347959	60.79417042
42	17.73250184	10.57709816	40.35191282
43	17.73376642	10.57710792	40.35611123
44	4.998201816	3.232139732	35.33394906
45	13.49795264	7.691850815	43.01468513
46	7.686957209	3.731941371	51.45099329
47	16.28409345	13.59903352	16.48885116
48	39.37438148	33.14005254	15.83346507
49	24.21988639	19.10696596	21.11042285
50	18.50774734	7.566993051	59.1144567
51	23.05346383	17.46425256	24.24456173
52	30.574746	22.62953078	25.98620187
53	14.17671375	12.96599801	8.540172048
54	18.17272827	10.95751045	39.7035476
55	6.624297277	3.458223721	47.79485919
56	12.54262825	6.264215905	50.05659276
57	13.66172038	5.805375294	57.50626471
58	11.4536621	5.397843833	52.87233213
59	4.481141576	1.771725876	60.46262217
60	3.952466507	3.225300938	18.39776674

Event	Max Acceleration Without Damper	Max Acceleration With Damper	Acceleration Dissipation %
61	5.254656191	1.484260058	71.75343155
62	5.460963435	2.885362027	47.16386475
63	6.501185232	3.12469648	51.93651053
64	9.588601545	2.787398879	70.93007915
65	4.896887269	1.932328726	60.53965265
66	12.85694665	5.090929794	60.40327511
67	8.890002225	3.239934079	63.55530632
68	5.944804843	4.391479213	26.12912738
69	8.257616707	5.226590788	36.70581993
70	5.260886408	2.185083567	58.46548665
71	6.692097447	2.337534222	65.07023036
72	6.561481877	3.190025197	51.3825496
73	12.05616356	7.79061797	35.38062147
74	12.53261845	10.13743129	19.11162598
75	13.17081141	7.742083875	41.21786704
76	19.20247087	9.292355399	51.60854318
77	10.18930454	4.500784924	55.82834031
78	3.987471093	1.921610408	51.80879401
79	4.483304372	2.505337889	44.11849652
80	7.991126478	4.569534154	42.81739668
81	4.803407576	1.796711255	62.59506971
82	4.330498601	2.046859069	52.73387069
83	2.962418	1.297591692	56.19822414
84	4.744055351	2.237531213	52.83505255
85	4.977275995	1.98522144	60.11429862
86	9.797091402	5.704687993	41.7716161
87	10.53140798	10.02316428	4.825980461
88	5.334306799	3.264700183	38.79804243
89	3.03587536	1.697887981	44.07253988
90	4.142240606	4.457703539	-7.615755902
91	5.221395384	2.33752294	55.23183425
			Average=40 %

Table AI- 10: Comparison of the seismic energy of the model with and without damper subjected to 91 near-field pulse-like earthquake records

Event	AUC-With	AUC-Without	Energy-Dissipation
1	0.002791427	0.007558941	63.0711956
2	0.000139499	0.000463058	69.87443173
3	0.000202457	0.001819319	88.87184412
4	8.88235E-05	0.000380953	76.68384695
5	3.12129E-05	0.000408814	92.36502527
6	5.01941E-05	0.000310527	83.83581655
7	9.93576E-05	0.000584948	83.01427846
8	8.48276E-05	0.000860161	90.13816782
9	0.000479261	0.002988856	83.96507412
10	5.2311E-05	0.000343883	84.78811273
11	0.000116373	0.001724125	93.25028868
12	0.000377102	0.002251021	83.24749852
13	0.000197513	0.000910106	78.29775491
14	0.000122755	0.000429267	71.40369917
15	0.000140557	0.001139103	87.66069558
16	0.000317466	0.001546944	79.47786735
17	0.000287673	0.006229529	95.38210617
18	0.000142019	0.000595862	76.16577113
19	0.00013766	0.000749595	81.6354523
21	5.47421E-05	0.000809371	93.23646513
22	0.002054096	0.009493513	78.36316537
23	0.00032242	0.000798099	59.60154793
24	0.001762698	0.005725314	69.21219803
25	0.001094602	0.002661661	58.87524902
26	8.76184E-05	0.000582232	84.95129287
27	2.06004E-05	0.000172297	88.04366297
28	1.99049E-05	0.000115472	82.76219795
29	0.001040775	0.0043582	76.11916085
30	0.001752028	0.005608728	68.76247166

Event	AUC-Structure With Damper	AUC-Structure Without Damper	Energy-Dissipation %
31	8.97665E-05	0.000894923	89.96936356
32	0.000381876	0.001228517	68.91571799
33	2.59673E-05	6.13671E-05	57.6852925
34	0.000469243	0.002693532	82.57890332
35	9.83951E-05	0.000717177	86.28021369
36	0.000232513	0.001403089	83.42848857
37	0.000262336	0.001978997	86.74397874
38	0.000546104	0.007583823	92.79909225
39	2.70649E-05	0.000448371	93.96371203
40	0.000346207	0.002350605	85.27158031
41	8.98766E-05	0.000710269	87.34612664
42	0.001052543	0.003866786	72.77991659
43	0.001052546	0.00386807	72.78886782
44	7.0331E-05	0.000286895	75.48546882
45	0.000372553	0.003803059	90.20385952
46	9.96151E-05	0.00082125	87.87031167
47	0.000674392	0.003181829	78.80487705
48	0.006199356	0.021303078	70.89924544
49	0.002482623	0.008284985	70.03466527
50	0.000650151	0.004414299	85.2717005
51	0.001394289	0.00298603	53.30626308
52	0.00361415	0.013522947	73.27394572
53	0.00044609	0.001720346	74.06975029
54	0.00114565	0.007680741	85.08412471
55	6.50195E-05	0.000562749	88.44608788
56	0.000284569	0.00174893	83.72899381
57	0.000242069	0.004830253	94.98848725
58	0.000291186	0.003790217	92.31742196
59	2.35476E-05	0.000201817	88.33220589
60	5.29461E-05	0.000259524	79.59875867

Event	AUC-Structure With Damper	AUC-Structure Without Damper	Energy-Dissipation %
61	3.36585E-05	0.000489801	93.12811869
62	0.000116723	0.000564246	79.31350919
63	7.69012E-05	0.000708851	89.15128156
64	8.75876E-05	0.001321968	93.3744541
65	6.54156E-05	0.000650974	89.95112507
66	0.000285839	0.00653831	95.62824505
67	6.31053E-05	0.000907706	93.04783392
68	0.000151305	0.001156033	86.91166444
69	0.000130945	0.000882725	85.16585946
70	0.000106042	0.00069047	84.64210874
71	8.80324E-05	0.001122998	92.16094253
72	9.75096E-05	0.000630868	84.54357781
73	0.000817097	0.004939143	83.45671035
74	0.000439365	0.002388513	81.60507062
75	0.000620675	0.00451524	86.25376839
76	0.001034684	0.007332234	85.88856144
77	0.000210212	0.002768403	92.40675211
78	3.18026E-05	0.00046685	93.18784282
79	3.27227E-05	0.000367844	91.10417428
80	0.000154046	0.001531211	89.93960125
81	0.000130237	0.0009652	86.50672727
82	5.98167E-05	0.000343764	82.59946093
83	3.20082E-05	0.000254892	87.44247944
84	6.29838E-05	0.000548271	88.5123015
85	5.84789E-05	0.000547115	89.31139922
86	0.000151869	0.001506962	89.92220194
87	0.000183856	0.001188125	84.52551588
88	4.45271E-05	0.00015814	71.84318733
89	9.87572E-05	0.000215395	54.15065141
90	0.000102352	0.00023293	56.05893432
91	4.65528E-05	0.000394139	88.18873967
			Average = 82.4%

Table AI-11:comparion of maximum displacements of the model with damper and the corresponding displacements of the model without damper subjected to 44 far-field earthquake records

Event	Max Displacement Without Damper	Corresponding Reduced Displacement	Displacement Dissipation %
1	0.02915066	0.014629018	49.81582436
2	0.037314738	0.025940758	30.48120161
3	0.045353731	0.024106559	46.84768324
4	0.043450851	0.030719696	29.30012866
5	0.106425416	0.073468766	30.96689815
6	0.049283	0.031912016	35.24741574
7	0.022608018	0.006560955	70.9795229
8	0.037253785	0.012804525	65.62892944
9	0.036867876	0.005647292	84.68235105
10	0.053963226	0.014078682	73.91059967
11	0.038348315	0.018012695	53.0287176
12	0.042653608	0.020919039	50.95599086
13	0.044202945	0.028365783	35.82829583
14	0.035582801	0.020437826	42.56262618
15	0.021568183	0.004628996	78.53785006
16	0.018550183	0.006414348	65.42164577
17	0.031133206	0.007225269	76.79240372
18	0.028618201	0.015477061	45.91882157
19	0.006388517	0.001418745	77.79226402
20	0.007927367	0.003912725	50.64281051
21	0.016186626	0.005786276	64.25273309
22	0.016741098	0.002636234	84.25291747
23	0.043513948	0.018069391	58.47448552
24	0.033403233	0.020327198	39.14601558
25	0.059084694	0.050670083	14.24161013
26	0.043920373	0.018611493	57.62446454
27	0.034576433	0.025240751	27.00013001
28	0.041119354	0.023586191	42.63968387
29	0.042200238	0.029093015	31.05959419
30	0.053111047	0.034240977	35.52946401
31	0.024706146	0.008514124	65.53843596
32	0.015614952	0.008166619	47.70000749
33	0.025646351	0.006868261	73.21934267
34	0.031084751	0.013037457	58.0583505
35	0.050894379	0.012479854	75.47891561
36	0.052400849	0.027696843	47.14428461
37	0.028154485	0.008428756	70.0624756
38	0.025535953	0.00849882	66.71821954
39	0.028994681	0.007959996	72.54670351
40	0.026133524	0.019095856	26.92965601
41	0.020708674	0.004286143	79.30267054
42	0.015985702	0.005531306	65.3984172
43	0.032952645	0.015323255	53.49916585
44	0.030063372	0.015808742	47.41527409
			Average= 54.51%

Table AI-12: Comparion of maximum velocities of the model with damper and the corresponding velocities of the model without damper subjected to 44 far-field earthquake records

Event	Max Velocity Without Damper	Max Velocity Reduced by Damper	Velocity Dissipation %
1	0.531382941	0.241844385	54.48774017
2	0.59486827	0.466643961	21.5550762
3	0.830380759	0.437532043	47.3094676
4	0.834841808	0.564059073	32.43521491
5	2.013836283	1.390803578	30.93760452
6	0.892292074	0.551282801	38.21722538
7	0.413117289	0.093818111	77.29019982
8	0.69270206	0.236134858	65.91105019
9	0.70866537	0.11060752	84.39213708
10	1.026242474	0.238747489	76.73576226
11	0.812135901	0.443092512	45.44108792
12	0.825241983	0.425836071	48.39864189
13	0.824017381	0.497887167	39.57807466
14	0.632517809	0.372713045	41.07469549
15	0.39202706	0.073236908	81.31840492
16	0.323407427	0.085398068	73.59427733
17	0.581133536	0.129231667	77.76213915
18	0.496598536	0.26430986	46.77594863
19	0.122758623	0.060666963	50.58028373
20	0.145522192	0.061748603	57.56756961
21	0.267200043	0.057193611	78.59520905
22	0.311730152	0.044263814	85.800599
23	0.789380678	0.273767043	65.31875545
24	0.616594596	0.343057818	44.36250011
25	1.087320603	0.939174526	13.62487534
26	0.772666348	0.279610792	63.81222077
27	0.791505729	0.630885147	20.29304097
28	0.828866388	0.486176099	41.34445484
29	0.809252215	0.580015607	28.32696698
30	1.060915688	0.600720943	43.37712696
31	0.475070717	0.177137893	62.71336323
32	0.268491584	0.141746963	47.20618019
33	0.488814929	0.121579208	75.12776291
34	0.575436594	0.156592849	72.78712364
35	0.969092782	0.320878873	66.88873558
36	1.034188763	0.539656181	47.81840607
37	0.505426015	0.113868162	77.47085454
38	0.441798293	0.257336608	41.75246659
39	0.554058835	0.192467891	65.26219261
40	0.491203442	0.334769259	31.84712679
41	0.414607417	0.137280608	66.88901291
42	0.316465004	0.103908331	67.165933
43	0.636823985	0.282341588	55.66410888
44	0.608226703	0.31286951	48.56037923
			Average=54.62%

Table AI-13: Comparion of maximum accelerations of the model with damper and the corresponding accelerations of the model without damper subjected to 44 far-field earthquake records

Event	Max Acceleration Without Damper	Max Acceleration Reduced by Damper	Acceleration Dissipation %
1	10.12807068	5.73450339	43.380101
2	12.22110149	7.999591111	34.54279783
3	16.64494708	4.936601766	70.3417395
4	16.49078428	12.34269603	25.15397796
5	38.63308807	26.77893895	30.68392849
6	17.09112017	10.6776233	37.52531614
7	7.992623299	2.170730452	72.84082621
8	13.34513722	4.106255857	69.23032122
9	13.78797666	3.373247323	75.53486342
10	20.45108965	6.15691626	69.89443416
11	16.85522602	9.965318419	40.87698137
12	15.83050245	8.147465688	48.53312009
13	16.43678342	10.15268937	38.23189666
14	12.4550461	6.941876003	44.26454993
15	7.324273315	1.684152337	77.00587807
16	6.31121953	1.997153368	68.35550786
17	11.10332069	4.325966235	61.03898684
18	9.131627935	4.593781226	49.69373196
19	3.141889432	2.449614587	22.03371124
20	3.237687518	2.003133366	38.13073824
21	4.685438008	0.87654476	81.29214902
22	6.238159523	1.148248696	81.59314952
23	15.14216867	4.709304706	68.89940399
24	11.96038389	7.298124539	38.98085039
25	20.49491705	17.33380789	15.423869
26	13.82330305	4.655302114	66.32279495
27	16.46390479	13.76555145	16.38951007
28	16.06269707	8.448918107	47.40037698
29	16.40996885	6.546839643	60.10449684
30	21.72934641	13.67144342	37.08304355
31	9.456332738	4.199347271	55.59222177
32	5.298208579	1.845196204	65.17320568
33	9.155492459	2.751614885	69.9457468
34	11.01279133	4.49589354	59.17571299
35	18.75620212	6.59108126	64.85919049
36	20.12069283	9.834573858	51.12209136
37	9.704571457	2.362075585	75.66017629
38	9.188787732	5.46716891	40.50173897
39	10.79298837	3.06404016	71.61082682
40	9.7208275	7.548192179	22.35031247
41	8.242252683	3.356382261	59.27833822
42	6.331896016	2.078443214	67.17502611
43	12.76109589	5.894109796	53.81188383
44	11.90552957	7.010290597	41.11735597
			Average=52.91%

Table AI-14: Comparion of maximum displacements of the model with damper and the corresponding displacements of the model without damper subjected to 91 near-field pulse-like records

Event	Max Displacement Without Damper	Max Displacement Reduced by Damper	Displacement dissipation %
1	0.057843487	0.053905634	6.807774038
2	0.025918716	0.012944119	50.05879718
3	0.028387641	0.004195472	85.22078025
4	0.016680738	0.008123487	51.3001965
5	0.011896167	0.00393858	66.89202515
6	0.015390136	0.004621012	69.97419816
7	0.023346201	0.015845238	32.12926634
8	0.026895982	0.009753136	63.73757363
9	0.043984716	0.021225882	51.74259692
10	0.01470515	0.004280287	70.89260028
11	0.023731978	0.003616505	84.76104829
12	0.040464495	0.027440951	32.18511595
13	0.027474591	0.016804689	38.83552519
14	0.023103812	0.016070642	30.44160051
15	0.029668317	0.014180405	52.20354183
16	0.026625301	0.012177766	54.26242939
17	0.047916653	0.008848718	81.53310491
18	0.027348783	0.014401816	47.34019561
19	0.024042049	0.012332393	48.70490244
20	0.015384011	0.004598157	70.11080602
21	0.077782228	0.056667239	27.14628903
22	0.028851307	0.0225998	21.66801916
23	0.063105725	0.054960735	12.90689651
24	0.048412501	0.039885039	17.61417422
25	0.020274224	0.013322707	34.28746364
26	0.011582776	0.004921946	57.5063317
27	0.009968072	0.00376377	62.24174666
28	0.056656014	0.042390997	25.17829201
29	0.067977264	0.057078743	16.03259752
30	0.023040088	0.007062535	69.34675348
31	0.023471729	0.012228673	47.90041456
32	0.02821649	0.016799006	40.46387219
33	0.007855288	0.004563054	41.91104883
34	0.042770785	0.028529066	33.29777342
35	0.022662366	0.010088016	55.48559999
36	0.026841127	0.017571368	34.53565757
37	0.036641607	0.021209564	42.11617424
38	0.046073347	0.013578895	70.52765766
39	0.012894334	0.006511773	49.49895896
40	0.02964512	0.010334193	65.14032348
41	0.019655784	0.009135345	53.5233749
42	0.047686243	0.023481549	50.75823256
43	0.047691338	0.023483154	50.76012782
44	0.012142275	0.005369995	55.7743908
45	0.03797671	0.010910108	71.27158194
46	0.027975571	0.015644409	44.07831988
47	0.045715581	0.038713196	15.31728396
48	0.105521951	0.082635449	21.68885409
49	0.063915468	0.039235293	38.61377584

50	0.049745608	0.019664894	60.46908583
51	0.068005662	0.051651411	24.04836638
52	0.079503087	0.055877649	29.71637827
53	0.03961389	0.025908984	34.59621301
54	0.054862838	0.026285272	52.08911325
55	0.017621634	0.004785438	72.84339283
56	0.037027108	0.011068485	70.10707749
57	0.038092292	0.016256491	57.32341167
58	0.030907456	0.013151827	57.44772241
59	0.013328087	0.005157657	61.30234722
60	0.010780304	0.003377377	68.67085703
61	0.014541497	0.002721739	81.28295057
62	0.019970579	0.009208848	53.88792483
63	0.017787613	0.00411502	76.86581011
64	0.025646826	0.003751964	85.37064842
65	0.013860223	0.006781265	51.07391261
66	0.035665934	0.008582345	75.93685496
67	0.021992388	0.006186263	71.87089201
68	0.016403783	0.009584001	41.57444881
69	0.022850227	0.014530494	36.40984809
70	0.014400984	0.003931311	72.70109644
71	0.019838422	0.006616702	66.64703292
72	0.018768013	0.008939881	52.36639246
73	0.033108014	0.008239544	75.11314268
74	0.040654788	0.033396431	17.85363396
75	0.033194722	0.018647049	43.82526038
76	0.05363786	0.016701094	68.86323581
77	0.029208077	0.009969093	65.86871309
78	0.010973408	0.000587841	94.64303643
79	0.013098299	0.00475536	63.69482655
80	0.025197791	0.00865775	65.64083897
81	0.01666651	0.008616327	48.30155352
82	0.011654284	0.002767713	76.25153542
83	0.008060247	0.000483402	94.00264179
84	0.012070111	0.001270888	89.47078411
85	0.013150682	0.001705226	87.03317662
86	0.02766611	0.012412577	55.13436186
87	0.023801576	0.01153149	51.55157064
88	0.016057782	0.006407906	60.09470064
89	0.015902266	0.010362138	34.83860669
90	0.02024602	0.014854035	26.63232144
91	0.015790927	0.007616847	51.76440685
			Average=53.19%

Table AI-15: Comparion of maximum velocities of the model with damper and the corresponding velocities of the model without damper subjected to 91 near-field pulse-like earthquake records

Event	Max Velocity Without Damper	Max Velocity Reduced by Damper	Velocity Dissipation %
1	0.964961622	0.854868216	11.4090968
2	0.391360057	0.158608663	59.47244488
3	0.538299117	0.140361962	73.92491322
4	0.288728279	0.144418724	49.98109477
5	0.24000906	0.082282567	65.71689127
6	0.251723145	0.047435215	81.1557992
7	0.324360265	0.153733712	52.60402442
8	0.49653381	0.18383764	62.97580611
9	0.851709673	0.431838382	49.29746652
10	0.300696189	0.154660403	48.56589181
11	0.452279768	0.069052037	84.73245054
12	0.711103001	0.439281625	38.22531693
13	0.482403614	0.29746028	38.33788331
14	0.327195228	0.164461481	49.73597806
15	0.523717609	0.242786237	53.64176548
16	0.509727142	0.318659381	37.48432163
17	0.917908888	0.15122109	83.52547932
18	0.525360341	0.294126985	44.01423887
19	0.473196947	0.264241535	44.15823342
20	0.291894471	0.024716046	91.5325404
21	1.55936345	1.157822315	25.75032367
22	0.461005995	0.423303384	8.178334154
23	1.161232365	0.93497269	19.48444441
24	0.970048522	0.781585294	19.42822695
25	0.434379523	0.30829173	29.02710328
26	0.195120049	0.078029146	60.00967261
27	0.160661936	0.088947503	44.6368533
28	1.126068992	0.83640424	25.72353504
29	1.327622836	1.093237068	17.65454476
30	0.438220714	0.143524726	67.24830161
31	0.423265454	0.161745982	61.78616042
32	0.496625678	0.160362949	67.70949309
33	0.118636521	0.066459801	43.98031836
34	0.818329783	0.521802314	36.23569309
35	0.423513449	0.156605789	63.02223956
36	0.478053199	0.253790433	46.91167568
37	0.630774245	0.310793845	50.72819668
38	0.928612717	0.313914222	66.1953561
39	0.238917376	0.086196657	63.92198093
40	0.598452511	0.178218272	70.22014802
41	0.324949593	0.116796349	64.05708729
42	0.91358135	0.464667599	49.13779721
43	0.913648736	0.464665811	49.14174424
44	0.235657783	0.072836408	69.0922967
45	0.669465893	0.117975074	82.377732
46	0.422867563	0.206113496	51.25814454
47	0.86603302	0.709276264	18.10055184
48	2.108444695	1.674694527	20.57204387
49	1.227821145	0.768464848	37.41231358

50	0.909695144	0.31373855	65.51168248
51	1.231457829	0.935611662	24.02405991
52	1.539882891	1.06628044	30.75574474
53	0.654517274	0.411189761	37.17663732
54	0.966110983	0.380014062	60.66558922
55	0.319500605	0.062696092	80.37684721
56	0.651971724	0.135234517	79.25761013
57	0.707526192	0.267217936	62.23207861
58	0.559993494	0.199986094	64.2877825
59	0.229864439	0.060617168	73.6291669
60	0.189220403	0.055881789	70.46735538
61	0.268005879	0.044712903	83.31644703
62	0.324915765	0.128079297	60.58076871
63	0.323739356	0.064642397	80.03257997
64	0.481605399	0.062344757	87.05480531
65	0.244212321	0.090319078	63.01616649
66	0.658292202	0.12164904	81.5205102
67	0.440534035	0.123947569	71.86424664
68	0.294607698	0.144728145	50.87428258
69	0.422887638	0.237354632	43.87288472
70	0.270594966	0.075495597	72.10014714
71	0.349452422	0.105655048	69.76554129
72	0.33804864	0.134036928	60.34980994
73	0.621894364	0.153786098	75.27134723
74	0.63525545	0.47761289	24.815617
75	0.63010971	0.334301974	46.94543366
76	0.985430475	0.2596558	73.65052058
77	0.536766914	0.182998126	65.90733867
78	0.206099214	0.008726722	95.76576664
79	0.219121253	0.051376795	76.55325814
80	0.415581509	0.109015104	73.7680571
81	0.252410853	0.082196077	67.43560119
82	0.218782999	0.054878933	74.91627165
83	0.149044419	0.028374964	80.96207539
84	0.233128593	0.026255697	88.7376762
85	0.245684327	0.024666124	89.96023689
86	0.506906959	0.18653413	63.20150545
87	0.45851414	0.204319149	55.4388554
88	0.291775801	0.119772965	58.95034325
89	0.212075538	0.124497272	41.29578843
90	0.2579963	0.173842057	32.61839131
91	0.264093984	0.09648448	63.46585461
			Average=56.83%

Table AI-16: Comparion of maximum accelerations of the model with damper and the corresponding accelerations of the model without damper subjected to 91 near-field pulse-like records

Event	Max Acceleration Without Damper	Max Acceleration Reduced by Damper	Acceleration Dissipation %
1	23.38802196	21.06393063	9.937100861
2	7.304744866	2.737265618	62.52756712
3	10.82582464	1.752140085	83.81518135
4	5.49079356	2.530306925	53.91728177
5	5.082776547	2.758880767	45.72099046
6	4.961331909	1.14453655	76.93086109
7	6.024706058	2.510594004	58.32835695
8	10.06388193	3.914828285	61.10021648
9	16.26390506	8.203050382	49.56284882
10	6.088498238	3.444164303	43.43162849
11	8.7559993	1.315211706	84.97930778
12	13.35602499	8.761169847	34.40286424
13	9.281552321	5.777716908	37.75053237
14	5.606793563	2.322421941	58.57842964
15	11.4187554	7.149397062	37.38899894
16	10.16218949	5.458336933	46.28778632
17	17.94526024	3.412822679	80.98203852
18	9.639315875	5.815724705	39.66662385
19	8.927728015	5.428962713	39.18987335
20	5.652738117	0.367524983	93.49828392
21	32.79408109	25.4323429	22.44837467
22	8.602999921	7.805445734	9.270652026
23	24.66529562	22.05267824	10.59228083
24	20.65021066	17.97205804	12.96912977
25	9.621657857	6.278941801	34.74158098
26	3.705651386	1.789707645	51.70329158
27	2.948029793	0.697787362	76.33038297
28	23.65680402	18.29616627	22.66002516
29	24.56073076	20.16107786	17.91336318
30	8.979227372	3.02538844	66.30680665
31	8.186327921	2.737269424	66.56291501
32	10.11375855	3.01440843	70.19497336
33	2.306501656	1.619082736	29.80353032
34	16.19853151	10.51532843	35.08468086
35	8.051227651	2.969823712	63.1134053
36	9.94631754	4.876947931	50.9673011
37	12.225784	5.927579663	51.51575015
38	18.11882465	6.559427725	63.79771949
39	4.77700014	1.73925676	63.59102555
40	15.39235415	8.058587821	47.64551452
41	6.673364617	2.068797328	68.99918637
42	17.73250184	9.122705442	48.55376006
43	17.73376642	9.122680242	48.55757075
44	4.998201816	2.6457907	47.06514869
45	13.49795264	3.291810426	75.61252056
46	7.686957209	3.474276527	54.80296777
47	16.28409345	13.3005484	18.32183693
48	39.37438148	32.69373603	16.96698514
49	24.21988639	15.94584903	34.16216424

50	18.50774734	7.542791643	59.24522036
51	23.05346383	17.45213616	24.29711957
52	30.574746	21.01727771	31.25935467
53	14.17671375	12.00527793	15.31691943
54	18.17272827	6.853167444	62.2887255
55	6.624297277	3.052311936	53.92247949
56	12.54262825	4.097779179	67.32918255
57	13.66172038	5.787233606	57.63905683
58	11.4536621	5.349943489	53.29054199
59	4.481141576	1.440203846	67.86078232
60	3.952466507	3.148349729	20.34468291
61	5.254656191	1.098692302	79.09107157
62	5.460963435	1.679199789	69.2508509
63	6.501185232	1.435070153	77.9260227
64	9.588601545	1.407686377	85.31916912
65	4.896887269	1.144014473	76.63792507
66	12.85694665	2.083993154	83.790917
67	8.890002225	3.072104914	65.44314798
68	5.944804843	3.680701422	38.08541205
69	8.257616707	4.459314192	45.99756382
70	5.260886408	1.516397144	71.17601433
71	6.692097447	1.91827426	71.33523122
72	6.561481877	2.49178708	62.02401947
73	12.05616356	3.454251733	71.34866565
74	12.53261845	9.02566493	27.98260821
75	13.17081141	6.393899532	51.45401955
76	19.20247087	5.758822531	70.0099921
77	10.18930454	3.5049354	65.60181916
78	3.987471093	0.21954216	94.49420059
79	4.483304372	2.43895928	45.59906984
80	7.991126478	1.888444701	76.36822911
81	4.803407576	0.895712502	81.35256092
82	4.330498601	1.094528681	74.72511178
83	2.962418	0.515162824	82.61005623
84	4.744055351	0.456272569	90.38222502
85	4.977275995	0.606205169	87.82054341
86	9.797091402	1.743243942	82.20651548
87	10.53140798	10.0188013	4.867408812
88	5.334306799	1.940139948	63.62901458
89	3.03587536	1.32621917	56.31509821
90	4.142240606	2.912568039	29.68616947
91	5.221395384	1.581043734	69.71990019
			Average=54.32%

Appendix II
Design Procedure

The design procedure of a typical SDOF moderately ductile (MD) steel frame

The national building code of Canada (NBCC 2010) presents technical specifications and requirements which covers common design standards and regulations to make sure that structures will be safe due to the different loads they experience in their service life. Based on the NBCC code the structures should be designed to have sufficient structural capacity and they should efficiently sustain all expected loads regarding the service provided by them.

In this way, the seismic provision of NBCC code provides designers with the minimum requirements for seismic resisting design of structures.

In this provision the minimum lateral loads and the allowable drift limits are defined. In this way the following items and criteria are considered:

- Site specific seismic hazard spectra
- Characteristics of the site and soil type
- Probability of occurrence of the design earthquake
- Type of the structures and foundations
- Sustainable damage level
- Allowable material stresses

In the following considering the national building code of Canada (NBCC 2010) and Canadian Steel Association code CSA-S16-09, the design procedure of a typical low-rise moderately ductile (MD) moment resisting SDOF steel frame, by an example, is briefly explained:

Demonstrative example

In this example a SDOF steel moment frame with the following specifications is designed.

Frame type: MD (laterally supported)

Height =3 m

Length =5 m

Specified Loads:

The specified dead and live loads according to NBCC is explained in the following:

Dead and Live Loads:

Dead Loads including membrane, insulation, steel deck, mechanical, …	3 KPa
Live load (typical roof):	2 KPa

Snow load: Calculated for a typical building in east Montreal (NBCC 2010):

S_s=2.7 KPa

S_r=0.4 KPa

I_s=1.0 normal importance

C_b=0.8 basic factor for small roof

C_w=1.0 building not exposed

C_s=1.0 flat roof

C_a=1.0 flat roof (no accumulation)

SL =$I_s(S_s(C_bC_wC_sC_a) + S_r)$ = 2.56 KPa

Load Combination:

1.25 DL+1.5 LL+0.5 SL +E

Minimum Earthquake design load according to NBCC 2010:

The NBCC allows to use the equivalent static force procedure for design of members in the structures with the total height of less than 60 m.

The structure is considered in the category of high importance and located on a Class C site in Montreal. Therefore, the site coefficients are F_a =F_v =1 and the importance factor is I_E=1.3

For a steel moment resisting frame with a height h_n=3 m the design period T_a is given by:

$T_a = 0.085\ {h_n}^{0.75}$= 0.2 s

For this structure which has a period T_a less than 1s the higher mode factor is M_v=1.

In the following the design spectrum for Montreal is utilized to calculate spectral acceleration; in this spectrum the specified spectral ordinates correspond to 2% probability of exceedance in 50 years uniform hazard spectrum (UHS) values with 5% damping.

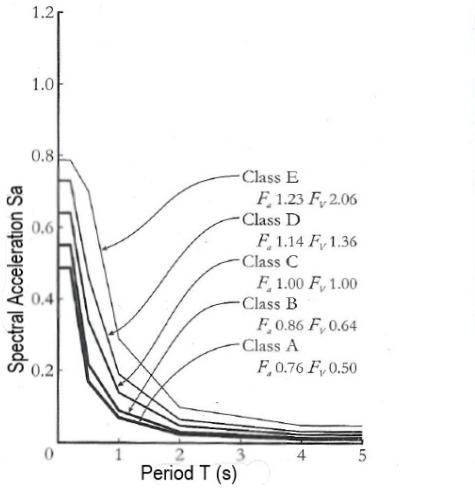

Figure AII- 1: Designed spectra foe eastern Canada (Filiatrault et al. 2013).

Table AII- 1: Design spectral accelertion for Montreal,QC (Filiatrault et al. 2013).

T_a(s)	0.2	0.5	1	2
S_a	0.64g	0.34g	0.14	0.048

S(T_a=0.2s) = 0.64

The steel frame is considered MD category therefore, R_d=3.5 and R_0=1.5

where

R_d is ductility -related force modification factor and R_0 is over-strength force modification factor

Base Shear calculation (V):

According to NBCC the minimum seismic base shear (V) is defined as bellow:

$$V = \frac{S(T_a)\, M_v\, I_E\, W}{R_d\, R_0}$$

The boundaries for minimum seismic base shear are:

$$\frac{S(T_a)\, M_v\, I_E\, W}{R_d\, R_0} \leq V \leq \frac{S(0.2\ s)\, M_v\, I_E\, W}{R_d\, R_0}$$

In this example:

W= DL+0.25 SL =91 KPa

V = $\frac{S(T_a)\, M_v\, I_E\, W}{R_d\, R_0}$ =$\frac{0.64*1*1.3*91}{3.5*1.5}$ = 14.3 KN

V≤2/3 V(0.2s) = $\frac{2}{3} * \frac{0.64*1*1.3*91}{3.5*1.5}$ = 9.6 KN

V≥V(2s) = $\frac{0.048*1*1.3*91}{3.5*1.5}$ = 1.04 KN

And $F_x = (V - F_t)\frac{W_i h_i}{\sum W_i h_i}$

where

F_t is a concentrated load added at the top of the structure to reproduce the effect of higher modes.

(Here F_t=0)

then

F_x =V

Capacity design procedure according to CSA-S16-09:

- The preliminary elements size including beams and columns considering combined gravity and seismic loads should be selected
- The selected elements should meet the requirements of the code to satisfy the concept of strong column – weak beam.
- Strength control and verification
- Determination of the column web panel zone
- Drift verification

This procedure is briefly explained as following:

Based on CSA-S16-09, in moderately ductile(MD) steel moment resisting frames beams and columns shall be Class 1 or 2.
Clause 27.2.3.1

By considering the maximum factored bending moment M_f a section (class1 or 2) with resistant moment M_r=ϕ Z f_y , should be assigned to the beam element.

Where ϕ =0.9, Z is the plastic section modulus and f_y is the yield stress of steel ($f_y = 345$ MPa for ASTM A99, A572 Grade 50)

Furthermore, the columns factored resistance decreases due to axial loads therefore according to the code CSA-S16-09, the following equations should be satisfied:

$$\sum M'_{rc} \geq M_c$$

Where:

$M_c = \sum \left[1.1\, R_y M_{pb} + V_h \left(x + \frac{d_c}{2}\right)\right]$ Clause 27.2.3.2

$M'_{rc} = 1.18\, \phi M_{pc} \left[1 - \frac{C_f}{\phi\, C_y}\right] \leq \phi\, M_{pc}$; $M_{pc} = Z\, f_y$

M_{pc} is the plastic moment capacity of the column.

C_f and C_y are axial load and axial yield stress of the column, respectively.

$C_y = A\, f_y$ (A is the section area of column).

M_{pb} is nominal plastic moment resistance of the beam.

V_h is shear acting at that beam plastic hinge location due to gravity loads on the beam plus moments.

equal to 1.1RyMpb at beam hinge locations

x is the distance from the center of a beam plastic hinge to the column face.

The predicted mechanism in this design is the plastic hinged form in beams outside the connections (panel zones). In this design the criteria of strong column-weak beam is considered and according to the above-mentioned equations, the column is designed to efficiently sustain, the bending moments developed in columns due to the plastic hinging occurred in the beams, the conducted axial force and the axial force caused by the load combination of 1DL+0.5LL+0.25SL.

The designed elements for this case, which are verified by the software SAP 2000, are summarized in the following table:

Table AII- 2: The sections used for the case study

Elements	Section	$Z\ (mm^3)$	$M_r = \phi\, Z\, f_y$ (KN-m)
Beam	W200x27	279000	86.6
column	W250x39	513000	159

Drift control:

In moment resisting frames the lateral deflection is so important therefore the drift control is one of the major requirements in designing these frames.

According to the CSA-S16-09 the drift for the building in high importance category, should be limited to 2%.

In this case the drift is less than 1% which satisfies the code requirement.